

---

# A Quantum Mechanical Toy Model for Black Holes

---



*A dissertation submitted in the fulfilment of  
the requirement for the Master of Science in  
the school of physics*

---

Author: Regan W. Cannell  
Supervisor: Prof. Vishnu Jejjala

---

# Declaration

I, Regan Cannell, hereby declare that this dissertation has been written by me, under the supervision of Professor Vishnu Jejjala, at the University of the Witwatersrand in Johannesburg, South Africa. The work done is my own original work. For sections that are based on the work of others, I have ensured that references are accurately given. This work has not been submitted before for any other degree, nor has it been published or sent for publication.

AUTHOR'S SIGNATURE:  .....

DATE: 09 July 2018 .....

# Abstract

The main aim of this dissertation is to investigate properties of the entropy of black holes. Our primary goal is to investigate the microstates of black holes. Our secondary goal is to study decoherence within the context of black holes. The methodology employed is to study simple, exactly solvable quantum models. These quantum models should serve as toy models for black holes.

We consider exactly solvable quantum systems which have a non-degenerate energy spectrum. The energy levels of these quantum systems should not be equally spaced. By choosing an appropriate class of observables, we calculate the expectation values of these observables for different states within a suitably chosen ensemble. This is where the notion of quantum typicality arises. By comparing the expectation values of the chosen observable for several states within the ensemble, we discover that it is not always possible to distinguish among the several states. These findings are then generalised to the microstates of black holes, i.e. no measurement can distinguish black hole microstates.

We then study the coherent and squeezed states of a simple quantum system. We deduce that even for such states, distinguishability is not possible. Finally, we study decoherence within the context of black holes. We find a simple quantum model that exhibits decoherence. We conclude that spacetime fluctuations can cause decoherence in quantum systems. Furthermore, by treating Hawking radiation as an effect of decoherence, we conclude that no information is lost in a black hole.

## Acknowledgements

I would like to thank my supervisor, Professor Vishnu Jejjala, from whom I have learned a great deal through our weekly discussions. He often gave me interesting ideas, as well as different perspectives on how to approach certain topics. He has also been patient enough to proof-read and provide corrections for the earlier drafts of this dissertation. In both 2016 and 2017, Professor Jejjala gave a series of lectures on the AdS/CFT correspondence. These lectures were excellently structured, and provided us with valuable information and tools that will be of great use for any future work in the field. In addition to the lectures given by my supervisor, I would also like to thank Professor Robert de Mello Koch for the many lectures he gave on advanced quantum field theory, conformal field theory, and several mathematical topics.

I am also grateful for the funding I received from the National Institute for Theoretical Physics (NITheP), and from my supervisor's SARCHI grant. The funding greatly aided me in the duration of my studies.

I'd also like to thank my family and friends for all their support and encouragement. Finally, I'd like to express my gratitude to the University of the Witwatersrand, which has provided me with all the resources I needed to complete this dissertation.

# Contents

List of Figures	iii
<b>1 Introduction</b>	<b>1</b>
<b>2 Gravity and Thermodynamics</b>	<b>3</b>
2.1 Black Holes	3
2.1.1 Semi-classical Black Hole Thermodynamics	5
2.1.2 Entropy and Information	7
2.2 Hawking Radiation	8
2.2.1 Stellar Collapse	8
2.2.2 Quantum Fields in a Schwarzschild Background	12
2.3 Schwarzschild Black Hole in Anti-de Sitter Spacetime	18
2.3.1 Anti-de Sitter Spacetime	18
2.3.2 Temperature of the Schwarzschild-AdS Black Hole	22
2.3.3 The Eternal Black Hole	25
<b>3 Quantum Information and Black Holes</b>	<b>28</b>
3.1 Measurements in Quantum Physics	28
3.1.1 POVM Formalism	28
3.1.2 Density Operators	29
3.1.3 Classical and Quantum Entropy	32
3.2 Information and Distinguishability	34
3.2.1 Distance Measures	35
3.2.2 Quantum Entanglement	35
3.2.3 Quantum Xerox Machine	39
3.3 Black Holes and Information	40
3.3.1 Black Hole Information Paradox	40
3.3.2 Information Recovery from a Black Hole	44
3.4 Quantum Typicality	46
3.4.1 Typicality in an Intuitive Sense	46
3.4.2 Levy's Lemma	47
<b>4 Quantum Typicality in Simple Quantum Systems</b>	<b>51</b>
4.1 Quantum Models	54
4.1.1 Infinite Potential Well	55
4.1.2 Finite Potential Well	63
4.1.3 The Morse Potential	69
4.2 Distinguishing Microstates	70
4.2.1 Distance Measures in Quantum Information	71
4.2.2 Making A Measurement	72
4.3 Typicality on Quantum Models in the Canonical Formalism	73

4.3.1	Simple Quantum Models in the Canonical Ensemble . . . . .	73
4.3.2	Composite System and the Canonical Ensemble . . . . .	77
<b>5</b>	<b>Decoherence and Black Holes</b>	<b>80</b>
5.1	Coherent States and Squeezed States . . . . .	80
5.1.1	Definitions . . . . .	80
5.1.2	Ladder Operators for a Particle in an Infinite Potential Square Well .	83
5.1.3	Coherent States for the Infinite Square Well . . . . .	86
5.1.4	Entropy of a Squeezed Vacuum . . . . .	90
5.2	Decoherence in Quantum Systems . . . . .	93
5.2.1	A Simple Decoherence Quantum Model . . . . .	94
5.2.2	Hawking Radiation from Decoherence . . . . .	97
<b>6</b>	<b>Conclusion</b>	<b>101</b>
<b>A</b>	<b>The Morse Potential</b>	<b>103</b>
A.1	The Energy Levels . . . . .	103
A.2	The Wave Function . . . . .	106
<b>B</b>	<b>The Wigner Distribution</b>	<b>109</b>

# List of Figures

1	A Penrose diagram for the collapsing star. The curve labelled $B$ represents the outer boundary of the star as it collapses. $C$ represents the ray of an incoming null geodesic, $v = v_1$ , that enters the black hole through the event horizon, labelled $H$ . . . . .	11
2	Two sketches of the contours drawn in the complex plane. Sketch (a) corresponds to equation (2.66), while sketch (b) corresponds to equation (2.67). . . . .	15
3	A sketch of $\text{AdS}_{d+1}$ as it is embedded in $\mathbb{R}^{2,d}$ . . . . .	20
4	Poincaré coordinates covering only half of AdS space. The shaded region is known as the Poincaré patch. . . . .	22
5	Both figures show the relationship between the temperature and the mass of a Schwarzschild black hole. Figure (a) is for a black hole in Minkowski space, while figure (b) corresponds to a black hole in AdS space. . . . .	24
6	A sketch of how the Hawking radiation “bounces” off from the boundaries of the AdS cylinder, and makes its way back to the black hole. . . . .	24
7	A sketch showing the state-operator map. States live in the cylinder, and can be mapped to operators in the complex plane. . . . .	26
8	This is an entropy Venn diagram. It provides a graphical representation of the different entropy measures discussed above. . . . .	33
9	A simple drawing of the hypothetical Quantum Xerox Machine. . . . .	40
10	A simple sketch depicting the creation of particle/anti-particle pairs on the horizon of a black hole. . . . .	41
11	A diagram depicting the creation of particle pairs, labelled $b_i$ and $c_i$ respectively, due to the “stretching” of spacelike slices. This figure is taken directly from [28]. . . . .	42
12	A sketch of a sphere with a spherical cap of radius $r$ . . . . .	49
13	A plot showing the difference between raw moments and standardised moments for the third state and fourth moment, with $L = 10$ . . . . .	59
14	A plot demonstrating the values of the fourth standardised moments for all the states in the ensemble. . . . .	67
15	A plot demonstrating the values of the fifth standardised moments for all the states in the ensemble. . . . .	67
16	A plot demonstrating the deviation of the expectation value of a given state from the ensemble average. The observable is $A = x^4$ in this case. . . . .	68
17	A plot demonstrating the deviation of the expectation value of a given state from the ensemble average. The observable is $A = x^5$ in this case. . . . .	68
18	Two sketches comparing a coherent state to a squeezed state, as represented in phase space. . . . .	88
19	A simple sketch of the infinite potential well of length $L$ . The grey regions illustrate how the length of well fluctuates. . . . .	95

# 1 Introduction

In 1915, the world first learned about general relativity, the theory which describes the force of gravity. Gravity acts on masses through the curvature of spacetime, which consequently is caused by the masses themselves. This relationship between spacetime curvature and mass is expressed through the Einstein equations,

$$R_{\mu\nu} - \frac{1}{2}Rg_{\mu\nu} = 8\pi G_N T_{\mu\nu}. \quad (1.1)$$

Our main aim in this dissertation is to investigate the entropy of black holes. Our primary goal is to study properties of the microstates of black holes. As a secondary goal, we study the effects of decoherence within the context of black holes.

The second section discusses the relationship between gravity and thermodynamics. Black holes are the common factor between these two seemingly different theories. We begin the discussion of black holes within the context of a collapsing star. We restrict ourselves to the Kerr-Newman family of black holes. The important definitions and results pertaining to this family of black holes are discussed, with the main goal of illustrating the thermodynamic properties of these black holes. The black hole entropy is of the most interest to us. In statistical physics, we understand that the entropy of a system depends on the number of underlying microstates of the system. When it comes to investigating the microstates of a black hole, we are faced with a problem: we cannot probe beyond the event horizon. We then move on to the derivation of Hawking radiation. The derivation is strongly based on Hawking's original calculation, and it is also within the context of a collapsing star. We then move on to discuss the Schwarzschild black hole in anti-de Sitter (AdS) space. These black holes are eternal, i.e. they never evaporate away. A black hole in AdS is in equilibrium with its Hawking radiation.

In the third section, we introduce important concepts pertaining to the theory of quantum information. We look at what it means to distinguish between two quantum states, and how entropy is a measure of uncertainty. Interesting phenomena, like entanglement and quantum cloning, are also briefly discussed. All these discussions ultimately lead us to the black hole information paradox, whereby we learn that quantum mechanics and general relativity do not get along very well with each other. We go through some of the important details about the information paradox, and even briefly summarise an interesting paper [1] in which the authors propose that information recovery from a black hole is theoretically possible, but physically impractical. We conclude the section by discussing quantum typicality. At first, we speak about typicality in a very conceptual way. We then move on to introduce Levy's lemma, which provides a mathematical framework for quantum typicality. Levy's lemma is important for the work done in the fourth section.

The fourth section begins with a brief introduction of the necessary mathematical tools that will be needed for the rest of the section. We then move on to discuss simple quantum models that we will use to investigate quantum typicality in the microcanonical formalism. We work

through three examples, and briefly mention other quantum models that were investigated, but not included in this work. Our results lead us to conclude that it is not physically possible to distinguish among the microstates of a black hole. Using important results from [2], we further verify the impossibility of distinguishing black hole microstates. The last part of this section extends these ideas to the canonical formalism. By looking at two weakly interacting systems, we show that the density matrix of the weakly interacting composite system is indistinguishable from the thermal density matrix. By applying this idea to black holes, we show that a distant observer would not be able to distinguish between black body radiation and Hawking radiation.

The fifth section looks at decoherence within a gravitational context. We also study decoherence in a simple quantum system, and try to find analogies between the quantum toy model and black holes. We also discuss coherent and squeezed states, with the intention of finding aspects within simple quantum models that can be generalised to black holes.

## 2 Gravity and Thermodynamics

When discussing the thermodynamics of self-gravitating systems, it is difficult to describe the concept of equilibrium. This is because self-gravitating systems, such as stars and black holes, have a negative heat capacity. By giving off heat energy, they become hotter. This is very different from the behaviour of physical systems in the laboratory. For instance, a cup of coffee gets colder (much to our displeasure) as it loses heat energy to the environment.

Despite these differences between gravitational physics and thermodynamics, black holes obey physical laws that are analogous to the laws of thermodynamics. In this chapter, we shall discuss black holes and the laws of thermodynamics which they obey. We shall see that black holes radiate energy. This emitted radiation is known as Hawking radiation. We shall see that in an asymptotically flat spacetime, black holes eventually evaporate away completely. However, in the interesting case of the AdS spacetime, black holes reach thermal equilibrium with their surroundings, so complete evaporation does not occur.

### 2.1 Black Holes

Let us begin our discussion of black holes within the context of stellar collapse. Over a long period of time, stars begin to shrink as they radiate energy. Since a star is a self-gravitating system [3], as it gets smaller, its own gravitational pull gets stronger. For an uncharged, spherical star, the critical radius is

$$r_c = \frac{2G_N M}{c^2}, \quad (2.1)$$

where  $M$  is the star's mass;  $G_N$  is Newton's constant; and  $c$  is the speed of light. Classically, this is the radius at which the escape velocity exceeds that of light. When the star reaches this critical radius, an outside observer will not be able to observe any light coming from the star, i.e. the star is black. Since no light can be observed from outside, we call this region a black hole. If light cannot resist being "sucked" inward, then certainly ordinary matter, which follow timelike paths, will have to be sucked inward as well. The centre of a black hole, or the point to which everything gets "sucked", is known as the singularity.

In general relativity, black holes are solutions to Einstein-Maxwell theory. In  $(3+1)$  dimensions, the most general of these solutions belong to the Kerr-Newman family, which describes black holes that rotate and carry electric charge. The spacetime representing these black holes is axisymmetric and free of matter. The simplest example, which has no charge and angular momentum, is the Schwarzschild black hole, whose metric is given by

$$ds^2 = - \left( 1 - \frac{2G_N M}{rc^2} \right) dt^2 + \left( 1 - \frac{2G_N M}{rc^2} \right)^{-1} dr^2 + r^2 d\theta^2 + r^2 \sin^2 \theta d\varphi^2. \quad (2.2)$$

The spherical surface,  $r_c = \frac{2GM}{c^2}$ , acts as an event horizon: it separates the events from outside the critical radius to those of inside the critical radius. When an observer crosses the event horizon, an interesting phenomenon occurs: radial motion and time exchange roles. This can be seen by studying the metric. Within the event horizon,  $1 - \frac{2G_N M}{rc^2} < 0$ . The  $dt^2$  term becomes positive, while the  $dr^2$  term becomes negative. Radial motion, described by the  $r$ -coordinate, behaves like time. In our every day lives, we cannot control the direction of time. It is a one-way street. We are constantly moving towards the future, i.e. forward in time. We cannot move backwards in time nor can we “stop” time for our convenience. Now for the observer across the horizon, his/her radial motion moves in only one direction: towards the black hole singularity. The observer’s motion cannot be stopped or redirected outward. Once the event horizon has been crossed, there is only one destination for the observer: the singularity.

These black hole solutions are characterised by a set of three parameters, namely the mass ( $M$ ), the angular momentum ( $J$ ), and the electric charge ( $Q$ ). If two black holes have the same  $M$ ,  $J$ , and  $Q$ , then we would not be able to tell the difference between the two black holes.

These three parameters can be measured. The constituents of the imploding star do not matter, only  $M$ ,  $J$ , and  $Q$  are used to identify the black hole. This means that a macrostate ( $M, J, Q$ ) can be realised by a very large number of internal microstates. In statistical mechanics, the entropy of a system is related to its number of microstates. Since there is generally a large number of microstates that could describe a given macrostate ( $M, J, Q$ ), black holes have a large entropy.

If an observer wishes to measure the electric field at neighbouring regions of the star’s surface, to determine the charge difference, the lines of force will appear to approach a purely radial configuration, due to the increased curvature of spacetime. This bending of the force lines causes the charge distribution to appear uniform. As far as the distant observer is concerned, a type of coarse-graining is imposed. As equilibrium is approached exponentially, all information about the star, such as temperature, charge distributions, density distributions, etc., becomes impossible to measure from outside the black hole.

The formation of a black hole due to stellar collapse is a process in which a system originally in a structured, ordered state changes to one which is disordered and described by few parameters. The final state of the system contains no observable memory of the system’s initial state. There are many different possible initial states that could give rise to a particular final state. Our inability to track how the final state evolved from the initial state is attributed to what we call “information loss”. The number of internal microstates that can produce a given black hole is dependent on how much information was lost during the black hole’s formation. This suggests that the entropy is related to the size of the black hole.

### 2.1.1 Semi-classical Black Hole Thermodynamics

The event horizon acts as a one-way surface: objects can fall into the black hole, but nothing can come out of it. When objects fall into the black hole, the black hole gets bigger. Since nothing can escape from the black hole, this means that the black hole can never get smaller. The size of the black hole can only ever increase or stay the same, it never decreases. This should remind us of the second law of thermodynamics, in which the entropy can only ever increase or remain the same.

The total surface area of the horizon is given by [4]

$$A = \frac{4\pi G_N}{c^4} \left( 2G_N M^2 - \frac{Q^2}{4\pi\epsilon_0} + 2M \sqrt{G_N^2 M^2 - \frac{G_N Q^2}{4\pi\epsilon_0} - \frac{c^2 J^2}{M^2}} \right), \quad (2.3)$$

where  $G_N^2 M^2 - \frac{G_N Q^2}{4\pi\epsilon_0} - \frac{c^2 J^2}{M^2} \geq 0$ .

Hawking showed that as long as no negative energy is involved, the area can never decrease [5]. Thus, the Hawking area theorem is

$$dA \geq 0. \quad (2.4)$$

For reversible processes,  $dA = 0$ .

From equation (2.3), we see that  $A = A(M, Q, J)$ , and

$$dA = \left( \frac{\partial A}{\partial M} \right)_{Q,J} dM + \left( \frac{\partial A}{\partial Q} \right)_{M,J} dQ + \left( \frac{\partial A}{\partial J} \right)_{M,Q} dJ. \quad (2.5)$$

An explicit calculation yields

$$\left( \frac{\partial A}{\partial M} \right)_{Q,J} = \frac{8\pi G_N}{c^4} \frac{2G_N M \sqrt{G_N^2 M^2 - \frac{G_N Q^2}{4\pi\epsilon_0} - \frac{c^2 J^2}{M^2}} + 2G_N M^2 - \frac{G_N Q^2}{4\pi\epsilon_0}}{\sqrt{G_N^2 M^2 - \frac{G_N Q^2}{4\pi\epsilon_0} - \frac{c^2 J^2}{M^2}}}, \quad (2.6)$$

$$\left( \frac{\partial A}{\partial Q} \right)_{M,J} = -\frac{8\pi G_N}{c^4} \frac{Q}{4\pi\epsilon_0} \left( 1 + \frac{G_N M}{\sqrt{G_N^2 M^2 - \frac{G_N Q^2}{4\pi\epsilon_0} - \frac{c^2 J^2}{M^2}}} \right), \quad (2.7)$$

$$\left( \frac{\partial A}{\partial J} \right)_{M,Q} = \frac{-8\pi G_N}{M c^2} \frac{J}{\sqrt{G_N^2 M^2 - \frac{G_N Q^2}{4\pi\epsilon_0} - \frac{c^2 J^2}{M^2}}}. \quad (2.8)$$

By manipulating equation (2.5), we have

$$dM = \left( \frac{\partial M}{\partial A} \right)_{Q,J} dA - \left( \frac{\partial M}{\partial A} \right)_{Q,J} \left( \frac{\partial A}{\partial Q} \right)_{M,J} dQ - \left( \frac{\partial M}{\partial A} \right)_{Q,J} \left( \frac{\partial A}{\partial J} \right)_{M,Q} dJ. \quad (2.9)$$

Finally, we have

$$dM = \frac{\kappa}{8\pi}dA + \Phi dQ + \Omega dJ, \quad (2.10)$$

where

$$\kappa = \frac{c^4}{8\pi G_N} \frac{\sqrt{G_N^2 M^2 - \frac{G_N Q^2}{4\pi\epsilon_0} - \frac{c^2 J^2}{M^2}}}{2G_N M \left( G_N M + \sqrt{G_N^2 M^2 - \frac{G_N Q^2}{4\pi\epsilon_0} - \frac{c^2 J^2}{M^2}} \right) - \frac{G_N Q^2}{4\pi\epsilon_0}} \quad (\text{surface gravity}), \quad (2.11)$$

$$\Phi = \frac{Q \left( G_N M + \sqrt{G_N^2 M^2 - \frac{G_N Q^2}{4\pi\epsilon_0} - \frac{c^2 J^2}{M^2}} \right)}{8\pi G_N M \epsilon_0 \left( G_N M \sqrt{G_N^2 M^2 - \frac{G_N Q^2}{4\pi\epsilon_0} - \frac{c^2 J^2}{M^2}} - G_N Q^2 \right)} \quad (\text{electric potential}), \quad (2.12)$$

$$\Omega = \frac{Jc^2}{2G_N M^2 \left( G_N M \sqrt{G_N^2 M^2 - \frac{G_N Q^2}{4\pi\epsilon_0} - \frac{c^2 J^2}{M^2}} - \frac{G_N Q^2}{4\pi\epsilon_0} \right)} \quad (\text{angular velocity}). \quad (2.13)$$

If  $J^2$  or  $Q^2$  becomes so large that

$$G_N^2 M^2 - \frac{G_N Q^2}{4\pi\epsilon_0} - \frac{c^2 J^2}{M^2} = 0, \quad (2.14)$$

then  $\kappa$  will vanish. In such a case, we say that the black hole is an extreme Kerr-Newman black hole. The surface gravity of a star, for instance, can be described as the acceleration due to gravity that a test particle would experience near the surface of the star. This description of surface gravity holds for objects, like stars and planets, which can be studied within the Newtonian framework. Black holes, however, cannot be discussed within the Newtonian framework. The surface gravity of a Kerr-Newman black hole can be described as the acceleration that a test particle would need to exert in order to stay at the horizon. It is important to note that even though the surface gravity vanishes, the area does not.

If the discriminant in equation (2.3) is negative, then the event horizon would disappear and a naked singularity would exist, i.e. the outside universe would be able to see the singularity. The cosmic censorship conjecture says that no naked singularities can form from gravitational collapse [6].

We can rearrange the expression for the area, equation (2.3), to get

$$M^2 = \frac{\pi c^4}{AG_N^4} \left( \frac{A}{4\pi} + \frac{G_N^2 Q^2}{4\pi\epsilon_0 c^4} \right)^2 + \frac{4\pi J^2}{Ac^2}. \quad (2.15)$$

The mathematical expression,

$$dM = \frac{\kappa}{8\pi}dA + \Omega dJ + \Phi dQ, \quad (2.16)$$

corresponds to the first law of thermodynamics and the conservation of mass-energy. From this expression,  $\kappa dA \sim TdS$ . This suggests that  $\kappa$  plays the role of temperature. It can

be shown that  $\kappa$  remains constant across the surface of the event horizon, just as the temperature of a system in thermal equilibrium is constant throughout the entire system. This corresponds to the zeroth law of thermodynamics. This is unlike Earth, for which acceleration due to gravity depends on location.

Finally, the cosmic censorship conjecture prevents the situation in which  $\kappa \rightarrow 0$  (i.e. absolute zero). It plays the role of the third law of thermodynamics. In summary, we have

Law	Thermodynamics	Black Holes
Zeroth	Thermal equilibrium $\Rightarrow$ constant $T$	Stationary black hole $\Rightarrow$ constant $\kappa$
First	$dE = TdS + pdV + \mu dN$	$dE = \frac{\kappa}{8\pi}dA + \Omega dJ + \Phi dQ$
Second	$dS \geq 0$	$dA \geq 0$
Third	$T \rightarrow 0$ impossible in a finite process	$\kappa \rightarrow 0$ impossible to achieve

Table 1: A table summarising the laws of black hole thermodynamics.

It is important to note that the third law of thermodynamics is a “rule of thumb”. There exist systems in which the third law does not hold [7]. However, it holds in most cases.

## 2.1.2 Entropy and Information

For a Schwarzschild black hole ( $J = Q = 0$ ), we have

$$A = \frac{16\pi G_N^2 M^2}{c^4} \quad (2.17)$$

$$\kappa = 8\pi \frac{\partial M}{\partial A} = \frac{c^4}{4G_N M}. \quad (2.18)$$

From a strictly classical perspective, black holes should have zero temperature. If  $\kappa$  is to play the role of temperature, then  $\kappa \rightarrow 0 \Rightarrow M \rightarrow \infty \Rightarrow A \rightarrow \infty$ . This is quite absurd!

Since the energy  $M$  is finite, zero temperature implies infinite entropy, which is also nonsensical. By manipulating the expression for the area, i.e.  $A = \frac{16\pi G_N^2 M^2}{c^4}$ , we have

$$M = \frac{A\kappa}{4\pi G_N}. \quad (2.19)$$

This demonstrates that both  $A$  and  $\kappa$  are finite quantities. In the next chapter, we shall discuss the relationship between entropy and information. For now, we merely need to know that a loss in information corresponds to a gain in entropy, and vice versa.

From our earlier discussion, a black hole that forms from gravitational collapse “swallows” up a lot of information. If we assign one bit of information to every degree of freedom of

the black hole, then classical physics suggests that the entropy of a black hole is unbounded. It is unbounded because particles of arbitrarily small mass can be thrown into the black hole. However, quantum theory forbids particles of arbitrarily small mass to be part of a black hole because of de Broglie's relation between energy and wavelength:  $E = \frac{2\pi\hbar}{\lambda}$ . The wavelength of the particle,  $\lambda$ , must be smaller than the black hole. By choosing  $\lambda \approx \frac{2G_N M}{c^2}$ , we have a minimum particle energy (or mass) of the order  $\frac{\hbar}{M}$ .

Since  $S \sim A \sim M^2$ , an estimate of the entropy is

$$S \sim \left(\frac{k_B}{\hbar}\right) \left(\frac{Ac^3}{G_N}\right), \quad (2.20)$$

where  $k_B$  is Boltzmann's constant. In the classical limit, where  $\hbar \rightarrow 0$ , the entropy  $S$  diverges. Furthermore, using the thermodynamic relation  $E = 2TS$ , (the factor of 2 appears because the entropy is proportional to the square of the mass), we have

$$T = \frac{E}{2S} = \frac{Mc^2}{2S} \sim \left(\frac{Mc^2}{2}\right) \left(\frac{\hbar G_N}{k_B Ac^3}\right), \quad (2.21)$$

and using equation (2.17),

$$T \sim \left(\frac{\hbar c^3}{8\pi G_N M k_B}\right) \quad (\text{temperature of the Schwarzschild black hole}). \quad (2.22)$$

A black hole is completely black ( $T = 0$ ) only in the classical limit ( $\hbar \rightarrow 0$ ). Otherwise, using equation (2.19),

$$T \sim \left(\frac{4\pi\hbar}{k_B}\right) \kappa, \quad (2.23)$$

which is proportional to  $\kappa$ . When temperature is involved, the notion of thermal equilibrium enters the picture. For the black hole to have temperature  $T$ , it must be capable of being in equilibrium with a surrounding heat bath at the same temperature  $T$ . In this subsection, our discussion was highly conceptual, and lacked any serious mathematical treatment. In the next section, we shall go through the derivation of Hawking radiation.

## 2.2 Hawking Radiation

In this subsection, and for the subsections still to come, we shall set  $\hbar = c = \frac{1}{4\pi\epsilon_0} = 1$ .

### 2.2.1 Stellar Collapse

One of the interesting phenomena that we learn from semi-classical physics is that it is possible to disturb the vacuum (excite modes) without having any source present. In the

case of a black hole formed by the implosion of a star, the changing geometry of the spacetime “twists” the modes geometrically. The background motion excites the modes of the quantum field.

Let us attempt to derive the Hawking radiation for a Schwarzschild black hole. We shall present the derivation as found in [8]. Recall the metric for a Schwarzschild black hole,

$$ds^2 = - \left(1 - \frac{2G_N M}{r}\right) dt^2 + \left(1 - \frac{2G_N M}{r}\right)^{-1} dr^2 + r^2 d\theta^2 + r^2 \sin^2 \theta d\varphi^2 \quad (2.24)$$

For a classical particle with coordinates  $x^\mu$  and velocities  $\frac{dx^\mu}{d\tau}$ , the Lagrangian is given by

$$\mathcal{L} = \frac{1}{2} g_{\mu\nu} \frac{dx^\mu}{d\tau} \frac{dx^\nu}{d\tau}. \quad (2.25)$$

By extremising  $\int_b^a \mathcal{L} dt$ , we can find the particle’s geodesics. From the Euler-Lagrange equations, we know that if  $g_{\mu\nu}$  (and consequently  $\mathcal{L}$ ) is independent of  $x^\mu$ , then the conjugate momentum,

$$p^\mu \equiv \frac{\partial \mathcal{L}}{\partial (dx^\mu/d\tau)} = g_{\mu\nu} \frac{dx^\nu}{d\tau}, \quad (2.26)$$

is constant along the geodesic. In the Schwarzschild case, the metric is independent of  $t$  and  $\varphi$ . This means that translations in  $t$  and  $\varphi$  shall leave the metric invariant. We call any transformation that leaves the metric invariant a *symmetry*. Noether’s theorem teaches us that behind every continuous, global symmetry within a system, there exists some conservation law. This is an appropriate place for us to introduce Killing vectors [9]. In the case where  $\partial_\alpha g_{\mu\nu} = 0$ , i.e. the metric is independent of  $x^\alpha$ , then the corresponding Killing vector is  $\xi^\mu = \delta^\mu_\alpha$ . This allows us to express the symmetry in the form of the following equation,

$$\partial_\alpha g_{\mu\nu} \xi^\alpha = 0. \quad (2.27)$$

This equation may only hold in a suitably chosen coordinate system. It is not a tensor equation. The covariant form, which holds in any coordinate system, is

$$\nabla_\mu \xi_\nu + \nabla_\nu \xi_\mu = 0. \quad (2.28)$$

This is known as Killing’s equation [9].

Continuing with our derivation, we let the plane lie at  $\theta = \frac{\pi}{2}$ , then

$$p_t = g_{tt} \frac{dt}{d\tau} = - \left(1 - \frac{2G_N M}{r}\right) \frac{dt}{d\tau} = E, \quad \text{and} \quad (2.29)$$

$$p_\varphi = g_{\varphi\varphi} \frac{d\varphi}{d\tau} = r^2 \sin^2(\pi/2) \frac{d\varphi}{d\tau} = L. \quad (2.30)$$

Thus, we have the following expressions,

$$\left(1 - \frac{2G_N M}{r}\right) \frac{dt}{d\tau} = -E, \quad (2.31)$$

and

$$r^2 \frac{d\varphi}{d\tau} = L. \quad (2.32)$$

Along null geodesics, the expression for  $\mathcal{L}$  (equation (2.25)) disappears, i.e.

$$-\left(1 - \frac{2G_N M}{r}\right) \left(\frac{dt}{d\tau}\right)^2 + \left(1 - \frac{2G_N M}{r}\right)^{-1} \left(\frac{dr}{d\tau}\right)^2 + r^2 \left(\frac{d\varphi}{d\tau}\right)^2 = 0. \quad (2.33)$$

Using equations (2.31) and (2.32), we have

$$\left(\frac{dr}{d\tau}\right)^2 + \left(1 - \frac{2G_N M}{r}\right) \frac{L^2}{r^2} = E^2. \quad (2.34)$$

For radial null geodesics,  $L = 0$ . Thus,  $\frac{dr}{d\tau} = \pm E$ , where  $+$  corresponds to outgoing geodesics, and  $-$  corresponds to incoming ones. From equations (2.31) and (2.33), we have

$$\frac{dt}{d\tau} \mp \left(1 - \frac{2G_N M}{r}\right)^{-1} \frac{dr}{d\tau} = 0. \quad (2.35)$$

We define the tortoise coordinate  $r^*$  such that

$$\frac{dr^*}{dr} = \left(1 - \frac{2G_N M}{r}\right)^{-1}, \quad (2.36)$$

where  $-\infty < r^* < \infty$ ,  $r^* \rightarrow -\infty$  as  $r \rightarrow 2G_N M$ , and  $r^* \rightarrow r$  as  $r \rightarrow \infty$ .

Using the tortoise coordinate in equation (2.35), we now have

$$\frac{dt}{d\tau} \mp \frac{dr^*}{dr} \frac{dr}{d\tau} = \frac{d}{d\tau} (t \mp r^*) = 0. \quad (2.37)$$

We define the tortoise lightcone coordinates  $u$  and  $v$ , where

$$u \equiv t - r^* \quad (2.38)$$

is constant along outgoing radial null geodesics; and

$$v \equiv t + r^* \quad (2.39)$$

is constant along incoming radial null geodesics.

Let us define  $C$ , an incoming radial null geodesic, by  $v = v_1$  for some  $v_1$  that passes through the event horizon. The null coordinate  $u$  is a function of  $\tau$  along this geodesic  $C$ , i.e.



From an inspection of the Penrose diagram (figure 1 above), we see that  $v - v_0$  must be related to the affine parameter  $\tau$  between  $u(v)$  and  $u(v_0)$  on  $\mathcal{I}^+$ , i.e.

$$v_0 - v = K_2\tau, \quad \text{where } K_2 < 0. \quad (2.46)$$

For  $u(v)$ , we have

$$u(v) = -4G_N M \ln \left( \frac{\tau}{K_1} \right) \quad (2.47)$$

$$= -4G_N M \ln \left( \frac{v_0 - v}{K_1 K_2} \right), \quad (2.48)$$

thus

$$u(v) = -4G_N M \ln \left( \frac{v_0 - v}{K} \right), \quad (2.49)$$

where  $K = K_1 K_2$  is a positive constant. This final expression for  $u(v)$  is going to play a vital role for what's to come.

So far we have only discussed the collapse of a star as it forms a Schwarzschild black hole. We have only used tools from general relativity. Now we move on to introduce aspects of quantum field theory.

### 2.2.2 Quantum Fields in a Schwarzschild Background

From the Einstein-Hilbert action,

$$S = \int d^4x \sqrt{-g} \left( \frac{1}{16\pi G_N} R + \frac{1}{2} \partial_\mu \phi \partial^\mu \phi \right), \quad (2.50)$$

we get the following equation of motion for a massless scalar field,  $\phi$ ,

$$\frac{1}{\sqrt{-g}} \partial_\mu (\sqrt{-g} g^{\mu\nu} \partial_\nu \phi) = 0. \quad (2.51)$$

Note that  $R$ , the Ricci scalar, is zero for the Schwarzschild black hole.  $g$  is the determinant of the metric, which is

$$g = \begin{vmatrix} -\left(1 - \frac{2G_N M}{r}\right) & 0 & 0 & 0 \\ 0 & \left(1 - \frac{2G_N M}{r}\right)^{-1} & 0 & 0 \\ 0 & 0 & r^2 & 0 \\ 0 & 0 & 0 & r^2 \sin^2 \theta \end{vmatrix} = r^4 \sin^2 \theta. \quad (2.52)$$

If  $f_1(x)$  and  $f_2(x)$  are solutions to equation (2.51), then the following scalar product is conserved,

$$(f_1, f_2) = i \int dV_x [f_1^*(\vec{x}, t) \partial_0 f_2(\vec{x}, t) - (\partial_0 f_1^*(\vec{x}, t)) f_2(\vec{x}, t)]. \quad (2.53)$$

Let us list two properties of this scalar product:

$$(i) \quad (f_1, f_2 + f_3) = (f_1, f_2) + (f_1, f_3), \quad (2.54)$$

$$(ii) \quad (f_1, cf_2) = c(f_1, f_2), \quad (2.55)$$

where  $c$  is some constant. The proofs of these two properties are as follows:

$$\begin{aligned} (i) \quad (f_1, f_2 + f_3) &= i \int dV [f_1^* \partial_0 (f_2 + f_3) - (\partial_0 f_1^*) (f_2 + f_3)] \\ &= i \int dV [f_1^* \partial_0 (f_2) + f_1^* \partial_0 (f_3) - (\partial_0 f_1^*) f_2 + (\partial_0 f_1^*) f_3] \\ &= i \int dV [f_1^* \partial_0 (f_2) - (\partial_0 f_1^*) f_2] + i \int [f_1^* \partial_0 (f_3) - (\partial_0 f_1^*) f_3] \\ &= (f_1, f_2) + (f_1, f_3) \\ (ii) \quad (f_1, cf_2) &= i \int dV [f_1^* \partial_0 (cf_2) - (\partial_0 f_1^*) (cf_2)] \\ &= ci \int dV [f_1^* \partial_0 (f_2) - (\partial_0 f_1^*) (f_2)] \\ &= c(f_1, f_2). \end{aligned}$$

Let us write

$$\phi = \int d\omega (a_\omega f_\omega + a_\omega^\dagger f_\omega^*), \quad (2.56)$$

where  $\{f_\omega\}$  and  $\{f_\omega^*\}$  are a complete set of solutions to (2.51) satisfying the normalisation condition  $(f_{\omega_1}, f_{\omega_2}) = \delta(\omega_1 - \omega_2)$ . The operators  $a_\omega$  and  $a_\omega^\dagger$  behave in the usual manner, i.e.

$$[a_{\omega_1}, a_{\omega_2}^\dagger] = \delta(\omega_1 - \omega_2) \quad (2.57)$$

$$[a_{\omega_1}, a_{\omega_2}] = [a_{\omega_1}^\dagger, a_{\omega_2}^\dagger] = 0. \quad (2.58)$$

On past null infinity,  $f_{\omega lm} \sim \frac{1}{\sqrt{\omega r}} e^{-i\omega v} Y_{lm}(\theta, \varphi)$ . The operators  $a_\omega$  annihilate particles on  $\mathcal{I}^-$ . This is at early times and at large distances from the collapsing star.

Let the  $p_\omega$  be solutions on  $\mathcal{I}^+$ , satisfying  $(p_{\omega_1}, p_{\omega_2}) = \delta(\omega_1 - \omega_2)$ , and  $p_{\omega lm} \sim \frac{1}{\sqrt{\omega r}} e^{-i\omega u} Y_{lm}(\theta, \varphi)$ . (From now on, we will drop the subscripts  $l$  and  $m$ ).

To generalise the solution, we need to accommodate for a part of the wave equation that will be incoming at late times. This means that we must introduce a set of solutions  $\{q_\omega\}$ . At late times, a superposition of the  $\{q_\omega\}$  is localised near the event horizon. They have no Cauchy data on  $\mathcal{I}^+$ . (When we refer to Cauchy data, we are referring to the boundary conditions that a differential equation, ordinary or partial, must satisfy to ensure that a unique solution exists). Observations on  $\mathcal{I}^+$  will not be affected by the  $\{q_\omega\}$ , since they depend only on  $\{p_\omega\}$ . The  $\{q_\omega\}$  satisfy the same normalisation conditions as the other solutions.

Since the horizon and the region outside the horizon are disjoint, we have  $(q_{\omega_1}, p_{\omega_2}) = 0$ . The most general solution for outgoing and incoming particles on  $\mathcal{I}^+$  is of the form

$$\phi = \int d\omega (b_\omega p_\omega + c_\omega q_\omega + b_\omega^\dagger p_\omega^* + c_\omega^\dagger q_\omega^*), \quad (2.59)$$

where the operators  $\{b_\omega\}$  and  $\{c_\omega\}$  satisfy the same conditions as the  $\{a_\omega\}$  operators discussed above.

For all  $\omega$ ,  $a_\omega |0\rangle = 0$  for particles incoming from  $\mathcal{I}^-$ . The  $\{f_\omega\}$  and  $\{f_\omega^*\}$  are a complete set, so we can write

$$p_\omega = \int (\alpha_{\omega\omega'} f_{\omega'} + \beta_{\omega\omega'} f_{\omega'}^*) d\omega'. \quad (2.60)$$

Using equations (2.59) and (2.60), we have

$$b_\omega = (p_\omega, \phi). \quad (2.61)$$

From equations (2.59) and (2.61), we can write

$$b_\omega = d\omega' (\alpha_{\omega\omega'}^* a_{\omega'} - \beta_{\omega\omega'}^* a_{\omega'}^\dagger). \quad (2.62)$$

Playing around with more of these expressions, we can also show that

$$\alpha_{\omega\omega'} = (f_{\omega'}, p_\omega) \quad \text{and} \quad \beta_{\omega\omega'} = (f_{\omega'}^*, p_\omega). \quad (2.63)$$

As the star collapses to form a Schwarzschild black hole, we consider a range of frequencies near a given value  $\omega$ . We can then form a wave packet from a superposition of the  $p_\omega$ . The coefficients of the superposition can be chosen such that the null geodesic that describes the outgoing wave packet approaching  $\mathcal{I}^+$  has a large constant value of  $u$  (i.e. at late times).

We can express the components  $p_\omega$  of this wave packet in terms of  $f_{\omega'}$  and  $f_{\omega'}^*$ , as in equation (2.60). Now suppose this wave were propagated backward in time. The curved spacetime would scatter part of this wave back toward infinity, where it would reach  $\mathcal{I}^-$  as a superposition of the  $f_{\omega'}$ . The frequencies  $\omega'$  would be close to the original frequency  $\omega$ . Another part of this wave packet would pass through the star (we will ignore interactions with the star's material), where it would eventually reach  $\mathcal{I}^-$  as a superposition of  $f_{\omega'}$  and  $f_{\omega'}^*$ . In this case, however, the frequencies will be highly blue-shifted, i.e.  $\omega' \gg \omega$ .

At late times (i.e.  $u \rightarrow \infty$ ), the values for  $\omega'$  become quite large. The spectrum of the outgoing particles is determined by the asymptotic form of the coefficients  $\beta_{\omega\omega'}$ .

At early times, the form on  $\mathcal{I}^-$  (with  $v < v_0$ ) is  $p_\omega \sim \frac{1}{\sqrt{\omega r}} e^{-i\omega u(v)} Y(\theta, \varphi)$ . Using Fourier's theorem, we have

$$\alpha_{\omega\omega'} = C \int_{-\infty}^{v_0} dv \sqrt{\frac{\omega'}{\omega}} e^{i\omega'v} e^{-i\omega u(v)} \quad (2.64)$$

$$\beta_{\omega\omega'} = C \int_{-\infty}^{v_0} dv \sqrt{\frac{\omega'}{\omega}} e^{-i\omega'v} e^{-i\omega u(v)}. \quad (2.65)$$

Setting  $s \equiv v_0 - v$  in equation (2.64), and  $s \equiv v - v_0$  in equation (2.65), we have

$$\alpha_{\omega\omega'} = -C \int_{+\infty}^0 ds \sqrt{\frac{\omega'}{\omega}} e^{-i\omega' s} e^{i\omega' v_0} e^{i\omega 4G_N M \ln\left(\frac{s}{K}\right)} \quad (2.66)$$

$$\beta_{\omega\omega'} = C \int_{-\infty}^0 ds \sqrt{\frac{\omega'}{\omega}} e^{-i\omega' s} e^{-i\omega' v_0} e^{i\omega 4G_N M \ln\left(-\frac{s}{K}\right)}. \quad (2.67)$$

To evaluate these integrals, we have to turn to complex analysis. For equation (2.66), we draw a contour from 0 to  $\infty$  on the real axis, and from  $-i\infty$  to 0 on the imaginary  $s$ -axis. The region enclosed contains no poles, and the integrand vanishes at infinity on the boundary. For equation (2.67), instead the contour is drawn from 0 to  $-\infty$  on the real axis. By making the substitution  $s \equiv i\sigma$ , equations (2.66) and (2.67) become

$$\alpha_{\omega\omega'} = -iC \int_{-\infty}^0 d\sigma \sqrt{\frac{\omega'}{\omega}} e^{\omega'\sigma} e^{i\omega' v_0} e^{i\omega 4G_N M \ln\left(\frac{i\sigma}{K}\right)} \quad (2.68)$$

$$\beta_{\omega\omega'} = iC \int_{-\infty}^0 d\sigma \sqrt{\frac{\omega'}{\omega}} e^{\omega'\sigma} e^{-i\omega' v_0} e^{i\omega 4G_N M \ln\left(-\frac{i\sigma}{K}\right)}. \quad (2.69)$$



(a) Sketch corresponding to equation (2.66). (b) Sketch corresponding to equation (2.67).

Figure 2: Two sketches of the contours drawn in the complex plane. Sketch (a) corresponds to equation (2.66), while sketch (b) corresponds to equation (2.67).

For  $\sigma < 0$ ,

$$\ln\left(\frac{i\sigma}{K}\right) = \ln\left(\frac{-i|\sigma|}{K}\right) = -i\frac{\pi}{2} + \ln\left(\frac{|\sigma|}{K}\right) \quad (2.70)$$

$$\ln\left(\frac{-i\sigma}{K}\right) = \ln\left(\frac{i|\sigma|}{K}\right) = i\frac{\pi}{2} + \ln\left(\frac{|\sigma|}{K}\right). \quad (2.71)$$

Thus, we have

$$\alpha_{\omega\omega'} = -iC e^{i\omega'v_0} e^{2\pi\omega G_N M} \int_{-\infty}^0 d\sigma \sqrt{\frac{\omega'}{\omega}} e^{\omega'\sigma} e^{i\omega 4G_N M \ln\left(\frac{|\sigma|}{K}\right)} \quad (2.72)$$

$$\Rightarrow |\alpha_{\omega\omega'}|^2 = |C|^2 e^{4\pi\omega G_N M} \int_{-\infty}^0 d\sigma d\sigma' \frac{\omega'}{\omega} e^{\omega'(\sigma+\sigma')} e^{i\omega 4G_N M \ln\left(\frac{|\sigma|}{|\sigma'|}\right)} \quad (2.73)$$

$$\beta_{\omega\omega'} = iC e^{-i\omega'v_0} e^{-2\pi\omega G_N M} \int_{-\infty}^0 d\sigma \sqrt{\frac{\omega'}{\omega}} e^{\omega'\sigma} e^{i\omega 4G_N M \ln\left(-\frac{|\sigma|}{K}\right)} \quad (2.74)$$

$$\Rightarrow |\beta_{\omega\omega'}|^2 = |C|^2 e^{-4\pi\omega G_N M} \int_{-\infty}^0 d\sigma d\sigma' \frac{\omega'}{\omega} e^{\omega'(\sigma+\sigma')} e^{i\omega 4G_N M \ln\left(\frac{|\sigma|}{|\sigma'|}\right)}. \quad (2.75)$$

The relationship between  $\alpha_{\omega\omega'}$  and  $\beta_{\omega\omega'}$  is

$$|\alpha_{\omega\omega'}|^2 = e^{8\pi G_N M \omega} |\beta_{\omega\omega'}|^2. \quad (2.76)$$

This corresponds to the part of the wave packet that was propagated back in time to just before the black hole formed. For this part of the wave packet,

$$(p_{\omega_1}, p_{\omega_2}) = \Gamma(\omega_1) \delta(\omega_1 - \omega_2), \quad (2.77)$$

where  $\Gamma(\omega_1)$  is a factor accounting for the fraction of an outgoing wave packet of frequency  $\omega_1$  at  $\mathcal{I}^+$  that would propagate through the star backward in time to  $\mathcal{I}^-$ . See [8] for more details. It can be shown that [8]

$$\Gamma(\omega_1) \delta(\omega_1 - \omega_2) = \int d\omega' (\alpha_{\omega_1\omega'}^* \alpha_{\omega_2\omega'} - \beta_{\omega_1\omega'}^* \beta_{\omega_2\omega'}). \quad (2.78)$$

From this, we encounter an infinity if we try to evaluate

$$\langle 0 | b_{\omega}^{\dagger} b_{\omega} | 0 \rangle = \int d\omega' |\beta_{\omega\omega'}|^2, \quad (2.79)$$

where the operators  $\{b_{\omega}\}$  contain the information about the particles created by the black hole.

Due to the steady flux of particles reaching  $\mathcal{I}^+$  at late times, we expect  $\langle 0 | b_{\omega}^{\dagger} b_{\omega} | 0 \rangle$ , the total number of particles created per unit frequency, to be infinite. To get around this problem, we replace  $\delta(\omega_1 - \omega_2)$  by  $\lim_{T \rightarrow \infty} \frac{1}{2\pi} \int_{-T/2}^{T/2} dt e^{i(\omega_1 - \omega_2)t}$ . When  $\omega_1 = \omega_2 = \omega$ , then

$$\begin{aligned} \lim_{T \rightarrow \infty} \Gamma(\omega) \left( \frac{T}{2\pi} \right) &= \int d\omega' (|\alpha_{\omega\omega'}|^2 - |\beta_{\omega\omega'}|^2) \\ &= \int d\omega' (e^{8\pi G_N M \omega} |\beta_{\omega\omega'}|^2 - |\beta_{\omega\omega'}|^2) \\ &= (e^{8\pi G_N M \omega} - 1) \int d\omega' |\beta_{\omega\omega'}|^2, \end{aligned}$$

and thus, we have

$$\int d\omega' |\beta_{\omega\omega'}|^2 = \frac{1}{e^{8\pi G_N M \omega} - 1} \lim_{T \rightarrow \infty} \Gamma(\omega) \left( \frac{T}{2\pi} \right). \quad (2.80)$$

Therefore,

$$\langle 0 | b_\omega^\dagger b_\omega | 0 \rangle = \lim_{T \rightarrow \infty} \left( \frac{T}{2\pi} \right) \frac{\Gamma(\omega)}{e^{8\pi G_N M \omega} - 1}. \quad (2.81)$$

$\Gamma(\omega)$  is the fraction of how much of the purely outgoing wave packet can be propagated backward in time from  $\mathcal{I}^+$  such that it would enter the collapsing star just before it became a black hole.

By studying the analytic extension of the Schwarzschild spacetime, we see that  $\Gamma(\omega)$  is also the fraction that a purely incoming wave packet starting from  $\mathcal{I}^-$  at late times would be absorbed by the black hole. This analysis suggests that the black hole behaves like a grey body of absorptivity  $\Gamma(\omega)$  and temperature given by

$$k_B T = \frac{1}{8\pi G_N M}. \quad (2.82)$$

In units where  $k_B = 1$ , and recalling that  $\kappa = \frac{1}{4G_N M}$ , we see that the black hole temperature is given by

$$T = \frac{\kappa}{2\pi}. \quad (2.83)$$

It is important to realise that the matter/radiation produced from the black hole comes from empty space, due to the gravitational disturbance, and not from the star as a source. The material of the star is not necessarily coupled to the quantum field. Even if two stars of equal mass ( $J, Q = 0$ ) are made from different materials, they would both produce the same Hawking radiation. This is because Hawking radiation is a property obtained from studying the quantum mechanical vacuum near the black hole horizon.

The above derivation is very similar to Hawking's original derivation [10]. However, it is important to note that there are several ways in which Hawking's argument can be presented. For instance, the authors in [11] provide a description in which Hawking radiation is viewed as a quantum tunneling process. The idea is that if a pair of particles are created just inside or outside the event horizon, the particle's energy will change sign if it crosses the horizon. There is no energy violation, since the pair of particles would have come into existence with a total energy of zero, provided one of the members tunneled to the other side. We shall discuss this idea of particle/anti-particle production in more detail in the next chapter, when we look at the black hole information paradox.

In the next section, we shall look at a Schwarzschild black hole in Anti-de Sitter (AdS) spacetime. Before we move on to the next section, let us compute the specific heat of a Schwarzschild black hole. We see that

$$\text{specific heat} = \frac{\partial T}{\partial M} = -\frac{1}{8\pi G_N M^2} < 0. \quad (2.84)$$

The black hole gets hotter as it gives off energy. This is a common feature of self-gravitating systems. In AdS space, however, we shall see something different.

## 2.3 Schwarzschild Black Hole in Anti-de Sitter Spacetime

For this section, we shall set  $c = \hbar = k_B = 1$ . In this system of units, the black hole temperature is given by

$$T = \frac{\kappa}{2\pi}, \quad (2.85)$$

and the entropy is

$$S_{BH} = \frac{A}{4G_N}, \quad (2.86)$$

where  $A$  is the surface area of the black hole, and  $\kappa$  is the surface gravity.

### 2.3.1 Anti-de Sitter Spacetime

In the previous section, we saw that the specific heat of a Schwarzschild black hole is negative. We deduce from this that an increase in mass results in a decrease in temperature. In fact, as the temperature decreases, the mass grows indefinitely.

Let us place the black hole in a box of finite volume and finite heat capacity. If  $E_{\text{rad}} < \frac{1}{4}M$ , then thermodynamic equilibrium can be reached. Equilibrium implies that  $S = S_{\text{rad}} + S_{\text{BH}}$  is at a maximum, subject to  $E = E_{\text{rad}} + M$ . The energy radiated by a black body is proportional to the fourth power of temperature, thus

$$\frac{\partial T_{\text{rad}}}{\partial E_{\text{rad}}} = \frac{1}{4} \frac{T_{\text{rad}}}{E_{\text{rad}}}. \quad (2.87)$$

We can conclude that  $E_{\text{rad}} < \frac{1}{4}M$ .

Instead of placing the black hole in an unphysical box, let us rather place it in a spacetime that is *not* asymptotically flat. As one approaches asymptotic infinity of anti-de Sitter (AdS) space, there is a type of potential wall. This makes AdS space “box-like”. The AdS space is a solution to the Einstein equations with a negative cosmological constant, i.e.

$$R_{\mu\nu} = \Lambda g_{\mu\nu}. \quad (2.88)$$

The metric for AdS spacetime is given by

$$ds^2 = - (dx^0)^2 - (dx^{d+1})^2 + \sum_{i=1}^d (dx^i)^2. \quad (2.89)$$

The set of points of the  $(d + 1)$ -dimensional AdS space,  $\text{AdS}_{d+1}$ , is defined as

$$\text{AdS}_{d+1} = \{(x^0, x^1, \dots, x^{d+1}) \mid -(x^0)^2 - (x^{d+1})^2 + \sum_{i=1}^d (x^i)^2 = -L^2\}. \quad (2.90)$$

We write the Einstein-Hilbert action for the AdS metric as

$$S = \frac{1}{16\pi G_N} \int \sqrt{-g} (R - 2\Lambda) d^{d+1}x. \quad (2.91)$$

The equations of motion from this action are the Einstein equations, i.e.

$$R_{\mu\nu} - \frac{1}{2}Rg_{\mu\nu} = -\Lambda g_{\mu\nu}. \quad (2.92)$$

To get an expression for the Ricci scalar, we take the trace of both sides of equation (2.92). We get

$$R - \frac{1}{2}R(d + 1) = -\Lambda(d + 1), \quad (2.93)$$

and thus

$$R = 2\frac{d + 1}{d - 1}\Lambda. \quad (2.94)$$

Plugging this back into equation (2.92) yields

$$R_{\mu\nu} = \frac{2}{d - 1}\Lambda g_{\mu\nu}. \quad (2.95)$$

However, a calculation of the Ricci tensor directly from the metric gives us [13]

$$R_{\mu\nu} = -\frac{d}{L^2}g_{\mu\nu}. \quad (2.96)$$

Comparing these two expressions for the Ricci tensor allows us to get an expression for both the cosmological constant and the Ricci scalar, i.e.

$$\Lambda = -\frac{d(d - 1)}{2L^2} \quad (2.97)$$

$$R = -\frac{d(d + 1)}{L^2}. \quad (2.98)$$

Since  $R \neq 0$ , we see that this metric is *not* asymptotically flat.

It is common to describe AdS spacetime using the following set of coordinates:

$$x_0 = L \cosh(\rho) \cos(\tau), \quad x_{d+1} = L \cosh(\rho) \sin(\tau), \quad x_i = R \sinh(\rho) \Omega_i,$$

where  $\tau \in [0, 2\pi)$ ,  $\rho \geq 0$ ,  $i = 1, \dots, d$ , and  $\sum_i \Omega_i^2 = 1$ . Using these coordinates, the metric becomes

$$ds^2 = L^2 \left( -\cosh^2(\rho) d\tau^2 + d\rho^2 + \sinh^2(\rho) d\Omega_{d-1}^2 \right), \quad (2.99)$$

where  $d\Omega_{d-1}^2$  is the metric on  $S^{d-1}$ . Since the entire space is covered,  $(\tau, \rho, \Omega_i)$  are called global coordinates.

Near  $\rho = 0$ ,  $ds^2 \approx L^2 (-d\tau^2 + d\rho^2 + \rho^2 d\Omega_{d-1}^2)$ . A closed timelike geodesic is contained in the spacetime, represented by the circle  $S^1$ . The spacetime has topology  $S^1 \times \mathbb{R}^d$ . To restore causality, we have to “unwrap” the circle so that  $-\infty < \tau < \infty$ . After this process of “unwrapping”, the spacetime now has topology  $\mathbb{R}^{1,d}$ .

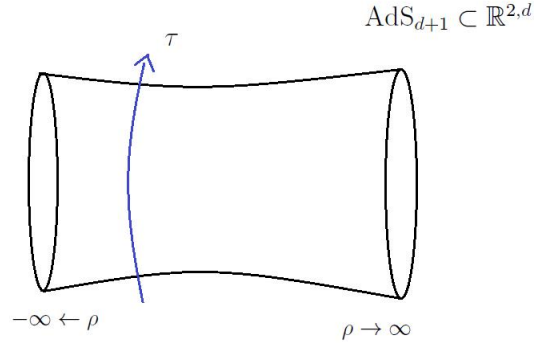


Figure 3: A sketch of  $\text{AdS}_{d+1}$  as it is embedded in  $\mathbb{R}^{2,d}$ .

We can conformally compactify AdS by setting  $\tan(\theta) = \cosh(\rho)$ . This is useful, as it allows us to see the topology of the spacetime more clearly. After making this substitution, the metric becomes

$$ds^2 = \frac{L^2}{\cos(\theta)} (-d\tau^2 + d\theta^2 + \sin^2(\theta) d\Omega_{d-1}^2). \quad (2.100)$$

For the Einstein static universe, the  $d$ -dimensional Minkowski metric is  $ds^2 = -d\tau^2 + d\theta^2 + \sin^2(\theta) d\Omega_{d-1}^2$ . This means that (2.100) is conformal to the conformally compactified Minkowski space. For the Minkowski case,  $\theta$  runs from 0 to  $\pi$ , while it runs from 0 to  $\pi/2$  in the AdS case. This means that the AdS spacetime is conformal to one half of the Einstein static universe. The conformal boundary of  $\text{AdS}_{d+1}$  is at  $\theta = \pi/2$ , where  $d\tilde{s}^2 = -d\tau^2 + d\Omega_{d-1}^2$ , which has topology  $\mathbb{R} \times S^{d-1}$ . The conformal boundary of  $\text{AdS}_{d+1}$  is identical to the conformally compactified  $d$ -dimensional Minkowski spacetime, i.e.  $\mathbb{R} \times S^{d-1}$ . The  $d$ -dimensional Minkowski spacetime, which has topology  $\mathbb{R}^{1,d-1}$ , is conformally compactified to  $\mathbb{R} \times S^{d-1}$ .

Let us now discuss the Poincaré coordinates  $(t, \tilde{x}_i, u)$ , defined by [14]

$$\begin{aligned}
x^0 &= \frac{1}{2u} \left( 1 + u^2 \left( L^2 + \sum_i (\tilde{x}^i)^2 - t^2 \right) \right), \\
x^i &= Lu\tilde{x}^i, \\
x^d &= \frac{1}{2u} \left( 1 - u^2 \left( L^2 - \sum_i (\tilde{x}^i)^2 + t^2 \right) \right), \\
x^{d+1} &= Lut,
\end{aligned} \tag{2.101}$$

where  $i = 1, \dots, d-1$ . The metric now becomes

$$ds^2 = L^2 \left( \frac{du^2}{u^2} + u^2 \left( -dt^2 + \sum_i (d\tilde{x}^i)^2 \right) \right). \tag{2.102}$$

It is often convenient to make the coordinate substitution,  $z \equiv \frac{1}{u}$ . With this  $z$  coordinate, the Poincaré coordinates become defined by

$$\begin{aligned}
x^0 &= \frac{1}{2z} \left( z^2 + L^2 + \sum_i (\tilde{x}^i)^2 - t^2 \right), \\
x^i &= \frac{L\tilde{x}^i}{z}, \\
x^d &= \frac{1}{2z} \left( z^2 - L^2 + \sum_i (\tilde{x}^i)^2 - t^2 \right), \\
x^{d+1} &= \frac{Lt}{z},
\end{aligned} \tag{2.103}$$

and the metric becomes

$$ds^2 = \frac{L^2}{z^2} \left( -dt^2 + dz^2 + \sum_i (d\tilde{x}^i)^2 \right). \tag{2.104}$$

The  $z$  coordinate behaves like a radial coordinate. It cuts the AdS space into two regions. Because of this, the Poincaré coordinates do not cover the entire space of AdS, as can be seen in figure 4. The region of AdS space that is covered by the Poincaré coordinates is known as the *Poincaré patch*.

In the Poincaré coordinates, the boundary of AdS is the plane  $z = 0$ . This boundary is flat space, with topology  $\mathbb{R}^{1,d-1}$ . This differs from the boundary of AdS in global coordinates, which has topology  $\mathbb{R} \times S^{d-1}$  (this is not flat, but rather cylindrical). From this, we see that the boundary of the Poincaré patch is *not* the same as the boundary of global AdS.

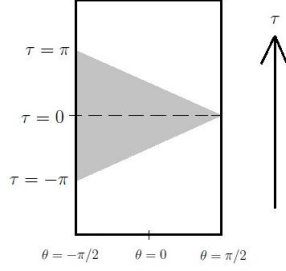


Figure 4: Poincaré coordinates covering only half of AdS space. The shaded region is known as the Poincaré patch.

Let us examine how a particle moving in AdS space would behave. Consider a particle with four-momentum  $P^\mu = (-E, p^1, p^2, p^3)$ . At infinity, a static observer has four-velocity  $U^\mu = \frac{k^\mu}{\sqrt{-k^2}}$ , where  $k = \frac{\partial}{\partial t}$ . The local observer measures an energy  $E = g_{\mu\nu} U^\mu P^\nu = \frac{E_\infty}{\sqrt{-k^2}} = \frac{E_\infty}{\sqrt{-g_{00}}} = \frac{E_\infty}{\sqrt{1+r^2/L^2}}$ . We see that the energy,  $E$ , is red-shifted by a factor of  $\sqrt{1+r^2/L^2}$ . It gets red-shifted to zero as  $r \rightarrow \infty$ . Since energy and temperature scale the same way, the temperature gets red-shifted by the same factor.

### 2.3.2 Temperature of the Schwarzschild-AdS Black Hole

The Schwarzschild-AdS metric is given by

$$ds^2 = - \left( 1 - \frac{2G_N M}{r} + \frac{r^2}{L^2} \right) dt^2 + \left( 1 - \frac{2G_N M}{r} + \frac{r^2}{L^2} \right)^{-1} dr^2 + r^2 d\Omega^2. \quad (2.105)$$

We see that for small  $r$ , the metric looks like the Schwarzschild black hole; and for large  $r$ , AdS space. The black hole has an event horizon at  $r = r_+$ , the largest root of the potential,  $V(r) = 1 - \frac{2G_N M}{r} + \frac{r^2}{L^2}$ . To determine the temperature of the black hole, we can perform a Wick rotation,  $\tau = it$ , and then look at the metric near the horizon. By performing a Wick rotation, we are compactifying Euclidean time. This allows us to identify the period with the inverse of the black hole temperature, i.e.  $\frac{1}{T} = \beta$ , where  $\beta$  is the period.

Let  $r = r_+ + \rho^2$ , where  $\rho \ll 1$ . Then

$$\begin{aligned} V(r) &= 1 - \frac{2G_N M}{r} + \frac{r^2}{L^2} = \frac{L^2 r - 2G_N M L^2 + r^3}{r L^2} \\ &= \frac{L^2 (r_+ + \rho^2) - 2G_N M L^2 + (r_+ + \rho^2)^3}{(r_+ + \rho^2) L^2}. \end{aligned} \quad (2.106)$$

To leading order in  $\rho$ ,

$$\begin{aligned}
V(r) &= \frac{L^2 \rho^2 + 3r_+^2 \rho^2 + 3r_+ \rho^4 + \rho^6}{(r_+ + \rho^2) L^2} \\
&= \frac{b^2 + 3r_+^2 + 3r_+ \rho^2 + \rho^4}{(r_+ + \rho^2) L^2} \rho^2 \\
&\approx \frac{L^2 + 3r_+^2}{L^2 r_+} \rho^2.
\end{aligned} \tag{2.107}$$

Since  $r = r_+ + \rho^2$  and  $t = -i\tau$ , we have that  $dr^2 = 4\rho^2 d\rho^2$  and  $dt^2 = -d\tau^2$ . This allows us to write the metric (2.94) as

$$\begin{aligned}
ds^2 &= -V(r)dt^2 + V(r)^{-1}dr^2 + r^2 d\Omega^2 \\
&= V(\rho)d\tau^2 + 4V(\rho)^{-1}\rho^2 d\rho^2 + r_+^2 d\Omega^2 + \underbrace{\rho^4 d\Omega^2 + 2r_+ \rho^2 d\Omega^2}_{\text{very small}} \\
&\approx V(\rho)d\tau^2 + 4V(\rho)^{-1}\rho^2 d\rho^2 + r_+^2 d\Omega^2 \\
&= \frac{L^2 + 3r_+^2}{L^2 r_+} \rho^2 d\tau^2 + 4 \frac{L^2 r_+}{b^2 + 3r_+^2} d\rho^2 + r_+^2 d\Omega^2 \\
&= \frac{4L^2 r_+}{L^2 + 3r_+^2} \left[ \left( \frac{L^2 + 3r_+^2}{2L^2 r_+} \right)^2 \rho^2 d\tau^2 + d\rho^2 \right] + r_+^2 d\Omega^2.
\end{aligned} \tag{2.108}$$

In this form, we can determine the temperature,

$$T = \frac{1}{\beta} = \frac{L^2 + 3r_+^2}{4\pi L^2 r_+}. \tag{2.109}$$

The temperature is a function of  $r$ , i.e.  $T(r) = \frac{L^2 + 3r^2}{4\pi L^2 r}$ . The minimum temperature is found when  $r = r_0$ . Let us calculate  $r_0$ ,

$$\begin{aligned}
\left. \frac{dT_{BH}}{dr} \right|_{r=r_0} = 0 &\Leftrightarrow \frac{6r(4\pi L^2 r_0) - (L^2 + 3r_0^2)4\pi L^2}{(4\pi L^2 r_0)^2} = 0 \\
&\Leftrightarrow r_0 = \pm \frac{L}{\sqrt{3}}.
\end{aligned} \tag{2.110}$$

Now that we know what  $r_0$  is, we can calculate  $T_0 = T(r_0)$ ,

$$T_0 = T(r_0) = \frac{L^2 + 3r_0^2}{4\pi L^2 r_0} = \frac{\sqrt{3}}{2\pi L}. \tag{2.111}$$

$T_0$  is the minimum temperature. By calculating the second derivative of  $T$  with respect to  $r$ , we see that it is positive, i.e.

$$\frac{d^2 T}{dr^2} = \frac{d}{dr} \left( \frac{3}{4\pi L^2} - \frac{1}{4\pi r^2} \right) = \frac{1}{2\pi r^3} > 0. \tag{2.112}$$

The Schwarzschild-AdS black hole reaches a minimum temperature, but then the temperature increases indefinitely. This behaviour is very different from that of the Schwarzschild black hole in Minkowski space, where the temperature keeps decreasing as the black hole gets bigger.



(a) Black hole in Minkowski space.

(b) Black hole in AdS space.

Figure 5: Both figures show the relationship between the temperature and the mass of a Schwarzschild black hole. Figure (a) is for a black hole in Minkowski space, while figure (b) corresponds to a black hole in AdS space.

For  $T < T_0$ , there are no black holes. The space is filled with pure radiation. Smaller black holes,  $r < r_0$ , have negative specific heat and are thermodynamically unstable. The larger black holes, i.e.  $r > r_0$ , have positive specific heat and are thermodynamically stable. This is what makes studying Schwarzschild-AdS black holes convenient: they are thermodynamically stable.

The black hole reaches thermal equilibrium in AdS space because of the boundaries of the spacetime. We can think of the Hawking radiation as “bouncing” off from the walls of the AdS space, which is shaped like a cylinder. This “bounced” off radiation makes its way back to the black hole. See figure 6.

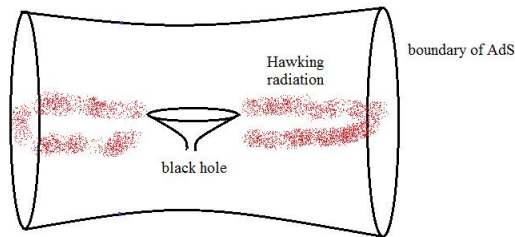


Figure 6: A sketch of how the Hawking radiation “bounces” off from the boundaries of the AdS cylinder, and makes its way back to the black hole.

Radiation follows null geodesics. In AdS, particles which follow null geodesics take a finite coordinate time to go from  $r = 0$  to  $r = \infty$ . Let us begin with the AdS metric,

$$ds^2 = - \left( 1 + \frac{r^2}{L^2} \right) dt^2 + \left( 1 + \frac{r^2}{L^2} \right)^{-1} dr^2 + r^2 d\Omega^2. \quad (2.113)$$

For null geodesics,  $ds^2 = 0$ . Due to rotational symmetry, we can ignore the  $r^2 d\Omega^2$  term. We can derive an expression for time as a function of radial distance, i.e.

$$\left(1 + \frac{r^2}{L^2}\right) dt^2 = \left(1 + \frac{r^2}{L^2}\right)^{-1} dr^2 \quad (2.114)$$

$$\Rightarrow dt = \pm \frac{L^2 dr}{L^2 + r^2}, \quad (2.115)$$

and thus

$$t(r) = \pm L \arctan\left(\frac{r}{L}\right). \quad (2.116)$$

From equation (2.116), we see that as  $r \rightarrow \infty$ ,  $t \rightarrow \frac{\pi L}{2}$ . This means that in the AdS spacetime, it takes a ray of light a finite time to travel an infinite distance.

We shall conclude this chapter by discussing what it means for a black hole to be in equilibrium in AdS space.

### 2.3.3 The Eternal Black Hole

In order for us to discuss the eternal black hole, we have to review the Anti-de Sitter/Conformal Field Theory (AdS/CFT) correspondence. Let us begin by briefly discussing conformal field theory. [15]

A conformal field theory is a quantum field theory that enjoys conformal symmetry. A conformal transformation is one that preserves the angles between lines. By angles, we mean the angle between the tangent vectors. In a conformal transformation, the spacetime metric transforms as

$$ds^2 \rightarrow \Omega^2(x) ds^2. \quad (2.117)$$

CFT's have a large amount of symmetry, which makes them simpler to study. The following is a list of finite conformal transformations:

- (i) Translations:  $x^\mu \rightarrow x^\mu + b^\mu$ ,
- (ii) Lorentz transformations:  $x^\mu \rightarrow \Lambda^\mu_\nu x^\nu$ ,
- (iii) Scaling:  $x^\mu \rightarrow e^\lambda x^\mu$  (when  $\lambda$  is infinitesimal,  $e^\lambda \approx 1 + \lambda$ ),
- (iv) Special conformal transformation:  $x^\mu \rightarrow \frac{x^\mu - b^\mu x^2}{1 - 2b^\mu x^\mu + b^2 x^2}$ .

Together, these transformations form the conformal group. There are many things about conformal field theories which we can discuss at great length, however, that is not our intention. We merely wish to state an important result pertaining to a certain class of CFT's, the state-operator map.

Consider a CFT where the cylinder is mapped to the complex plane, i.e.  $R \times S^{D-1} \rightarrow R^D$ . The states live in the cylinder, while the operators live on the complex plane. The state-operator map says that the states are in a one-to-one correspondence with the local operators. This is a powerful result that is unique to CFT's. For an ordinary quantum theory, the map only goes one way: by acting on the vacuum with an operator, we obtain a state. In CFT's, every state uniquely corresponds to a local operator. [16]

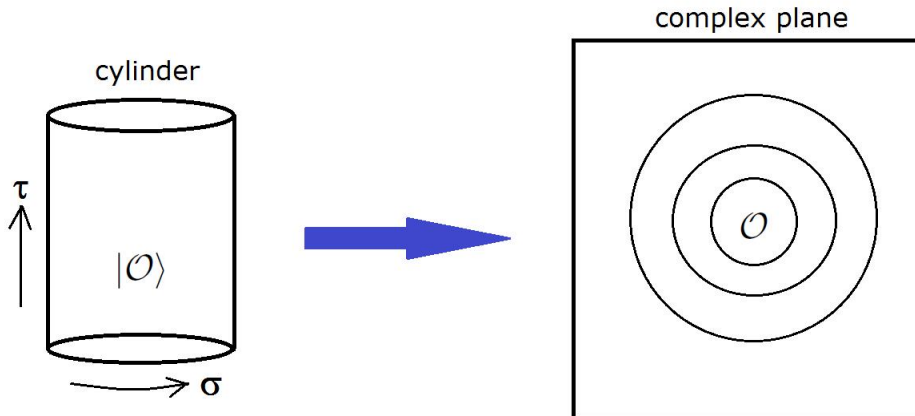


Figure 7: A sketch showing the state-operator map. States live in the cylinder, and can be mapped to operators in the complex plane.

Now we can discuss the AdS/CFT correspondence, which is also known as the gauge/gravity duality. This duality claims that a strongly coupled 4-dimensional gauge theory is equivalent to a gravitational theory in 5-dimensional AdS spacetime [17]. The gauge theory describes the electromagnetic force, the weak nuclear force, and the strong nuclear force. At strong coupling, it is not easy to study a gauge theory. For instance, there are still many unanswered questions in quantum chromodynamics (QCD), the gauge theory which describes the strong nuclear force.

The AdS space is a vacuum solution to the Einstein equations. The boundary of AdS space is Minkowski space. This boundary is used as the background for a conformal field theory. The bulk (i.e. inside the cylinder) of the AdS space is where the gravitational physics takes place. The AdS/CFT correspondence creates a “dictionary” [19] between the boundary and the bulk. The two theories, the CFT without gravity, and the quantum gravity on AdS space (formulated in terms of string theory), are exactly equivalent. We can do calculations in either and get the same answer.

In Maldacena’s original paper [20], it was argued that the 10-dimensional Type IIB superstring theory on  $AdS_5 \times S^5$  is equivalent to  $\mathcal{N} = 4$  supersymmetric Yang-Mills (SYM) theory with gauge group  $SU(N)$ . The  $\mathcal{N} = 4$  SYM theory lives on the 4-dimensional boundary of  $AdS_5$ , which is flat. A field of mass  $m$  in  $AdS_5$  is associated with an operator in SYM of

conformal dimension  $\Delta$ , with the relationship being

$$m^2 = \Delta(\Delta - 4). \quad (2.118)$$

Now that we have a basic idea about the AdS/CFT correspondence, we can move on to discuss eternal black holes and equilibrium. An eternal black hole has a full, two-sided Penrose diagram [21]. In AdS space, the extended Schwarzschild-AdS black hole is eternal. It has two boundaries, and thus it is dual to two copies of a CFT. Two copies of a CFT suggests that there is a “doubling” of the degrees of freedom of the theory. This is known as the thermofield double (TFD) formalism. The thermofield double formalism allows us to treat a thermal, mixed state, which we shall call a TFD state, as a pure state in a larger system (the “doubled” system). Using the AdS/CFT dictionary, it was shown in [22] that the eternal black hole is dual to the TFD state.

Let us call the two CFT’s on the two respective boundaries  $\text{CFT}_1$  and  $\text{CFT}_2$ . Let  $\mathcal{O}_1$  be an operator in  $\text{CFT}_1$  and  $\mathcal{O}_2$  an operator in  $\text{CFT}_2$ . Let us perturb the TFD state, i.e.

$$|\text{TFD}\rangle \rightarrow |\tilde{\text{TFD}}\rangle = (1 + \epsilon\mathcal{O}_2) |\text{TFD}\rangle. \quad (2.119)$$

The expectation value of  $\mathcal{O}_1$  in the perturbed state in  $\text{CFT}_1$  is

$$\begin{aligned} \langle \mathcal{O}_1 \rangle &\equiv \langle \tilde{\text{TFD}} | \mathcal{O}_1 | \tilde{\text{TFD}} \rangle \\ &= \langle \text{TFD} | (1 + \epsilon\mathcal{O}_2)^\dagger \mathcal{O}_1 (1 + \epsilon\mathcal{O}_2) | \text{TFD} \rangle \\ &= \langle \text{TFD} | (1 + \epsilon\mathcal{O}_2)^\dagger (\mathcal{O}_1 + \epsilon\mathcal{O}_1\mathcal{O}_2) | \text{TFD} \rangle \\ &= \langle \text{TFD} | \mathcal{O}_1 | \text{TFD} \rangle + \epsilon \left( \langle \text{TFD} | \mathcal{O}_2^\dagger \mathcal{O}_1 | \text{TFD} \rangle + \langle \text{TFD} | \mathcal{O}_1 \mathcal{O}_2 | \text{TFD} \rangle \right) + O(\epsilon^2). \end{aligned}$$

To first order,

$$\langle \mathcal{O}_1 \rangle \sim \langle \text{TFD} | \mathcal{O}_1 \mathcal{O}_2 | \text{TFD} \rangle. \quad (2.120)$$

In the bulk, which is the gravity side, if we keep  $\mathcal{O}_2$  at a specific time while allowing  $\mathcal{O}_1$  to go to very late times, the geodesic distance between these two points increases forever, i.e.

$$\langle \mathcal{O}_1 \rangle_{\text{gravity}} \sim e^{-t/\beta} \rightarrow 0, \quad (2.121)$$

for  $t \gg \beta$ .

This creates a contradiction in the CFT, since

$$\langle \mathcal{O}_1 \rangle_{\text{CFT}} \sim e^{-S}, \quad (2.122)$$

for  $t \gg \beta$ .  $S$ , the entropy, is finite. This means that  $\langle \mathcal{O}_1 \rangle_{\text{CFT}}$  doesn’t decay to zero, as in the gravity case. But the AdS/CFT correspondence asserts that the two values should be equal. It turns out that by considering non-perturbative effects in gravity, of the order  $e^{-1/G_N} \sim e^{-S}$ , the contradiction is avoided. The non-perturbative effects ensure that the expectation value of the observable doesn’t decay to zero.

The CFT describes a system in thermal equilibrium. Since the gravitational theory is dual to the CFT, we can conclude that the black hole in AdS, which is an eternal black hole, reaches thermal equilibrium.

## 3 Quantum Information and Black Holes

### 3.1 Measurements in Quantum Physics

In order to make sense of anything in the physical universe, we need to have some notion of what it means to perform a *measurement*.

#### 3.1.1 POVM Formalism

The measurement postulate of quantum mechanics states that a quantum measurement is described by a collection of measurement operators, denoted  $\{M_m\}$ . These operators act on the state space of the system being measured. If the state before the measurement is  $|\psi\rangle$ , then the probability of the result  $m$  occurring is given by

$$p(m) = \langle \psi | M_m^\dagger M_m | \psi \rangle, \quad (3.1)$$

and the system's state after the measurement is  $\frac{M_m|\psi\rangle}{\sqrt{\langle \psi | M_m^\dagger M_m | \psi \rangle}}$ . The completeness relation is satisfied by these measurement operators, i.e.

$$\sum_m M_m^\dagger M_m = \mathbb{I}. \quad (3.2)$$

These observables are Hermitian. The completeness relation ensures that the probabilities sum to one, i.e.

$$\sum_m p(m) = \langle \psi | \sum_m M_m^\dagger M_m | \psi \rangle = \langle \psi | \mathbb{I} | \psi \rangle = 1. \quad (3.3)$$

In many cases, we are not interested in the state of the system after the measurement. Our main interest generally lies in the probabilities of the respective measurement outcomes. An example of such a case is in an experiment where the system is only measured once, upon the experiment's conclusion. This is where the Positive Operator-Valued Measure (POVM) is particularly useful [22]. It is a mathematical tool well adapted to measurement analysis.

At this point, it is useful to define what it means for an operator to be positive [23]. An operator  $P$  is said to be positive if  $\langle \psi | P | \psi \rangle \geq 0$  for all  $|\psi\rangle$ . Here we list three properties pertaining to positive operators:

- (i)  $|k\rangle\langle k|$  is positive for any  $|k\rangle$ ,
- (ii) if  $P$  is a positive operator and  $\pi$  a projection operator, then  $\pi P \pi$  is also positive;
- (iii) if  $P$  is a positive operator and  $|\psi\rangle$  is normalised, then  $\langle \psi | P | \psi \rangle \leq \text{Tr}(P)$ .

Proof:

(i) Let  $|k\rangle$  be some vector. Then  $\langle k|\psi\rangle$  is a complex number.

So  $\langle\psi|(|k\rangle\langle k|)|\psi\rangle = |\langle\psi|k\rangle|^2 \geq 0 \Rightarrow |k\rangle\langle k|$  is positive.

(ii)  $\pi$  is a projection operator, so  $\pi|\psi\rangle = |\psi\rangle$ . (Note that this is only true if  $|\psi\rangle$  is an eigenstate of  $\pi$ ).

We see that  $\pi P \pi |\psi\rangle = \pi P (\pi |\psi\rangle) = \pi P |\psi\rangle = \pi (P |\psi\rangle) = P |\psi\rangle$ , thus  $\pi P \pi$  is positive.

(iii) Let  $\{|n\rangle\}$  be the basis for  $|\psi\rangle$ , then  $\langle\psi|\psi\rangle = \langle n|n\rangle = 1$ , since  $|\psi\rangle$  is normalised. For the positive operator  $P$ , we write  $\text{Tr}(P) = \sum_n \langle n|P|n\rangle$ . By stating that  $n \leq \sum_n n$  for  $n \in \mathbb{Z}$ , we conclude that  $\langle\psi|P|\psi\rangle \leq \sum_n \langle n|P|n\rangle = \text{Tr}(P)$ .

Suppose a quantum system is in a state  $|\psi\rangle$ . Using measurement operators  $M_m$  to perform a measurement on the system, the probability for outcome  $m$  is given by  $p(m) = \langle\psi|M_m^\dagger M_m|\psi\rangle$ . For convenience, let us define

$$E_m \equiv M_m^\dagger M_m. \quad (3.4)$$

From the properties of  $M_m$ , it follows that  $E_m$  is a positive operator such that  $\sum_m E_m = \mathbb{I}$  and  $p(m) = \langle\psi|E_m|\psi\rangle$ . The complete set of operators,  $\{E_m\}$ , is known as a POVM. The elements of this set are known as POVM elements. They are sufficient to determine the probabilities of the various measurement outcomes. In summary, we can define a POVM to be any set of operators  $\{E_m\}$  such that

- (i) every operator  $E_m$  is positive; and
- (ii) the completeness relation,  $\sum_m E_m = \mathbb{I}$ , holds.

### 3.1.2 Density Operators

Suppose we make statistical predictions on a collection of physical systems that have been identically prepared. This collection is called an *ensemble*. If every member of this collection is described by the same ket, say  $|\psi\rangle$ , then the ensemble is pure. On the other hand, if  $p_1$  members of the ensemble are described by the ket  $|\psi_1\rangle$ , and  $p_2$  members are described by the ket  $|\psi_2\rangle$ , then the ensemble is mixed.

We can view a mixed ensemble as a mixture of pure ensembles. The following normalisation condition must be satisfied,

$$\sum_i p_i = 1. \quad (3.5)$$

Furthermore, it is not necessary for  $|\psi_1\rangle$  and  $|\psi_2\rangle$  to be orthogonal. The number of terms in the sum need not equal the dimension of the Hilbert space inside which the ket lives, it can be greater than the dimension. To see this [24], consider a spin  $\frac{1}{2}$  system which has  $d = 2$ , where  $d$  is the dimension of the Hilbert space. We may have a situation in which 40% of the

elements in the ensemble have spin in the positive  $z$ -direction, 25% have spin in the positive  $x$ -direction, and the remaining 35% have spin in the negative  $y$ -direction. In this case, the summation index  $i$  runs from 1 to 3, even though the dimension of the Hilbert space is only 2.

Consider an ensemble of systems, where every individual system is prepared in one of the various possible states, with a fraction  $p_i$  of them prepared in  $|\psi_i\rangle$ . For an observable  $A$ , the average measured value will be  $\langle A \rangle_i = \langle \psi_i | A | \psi_i \rangle$ . Over the entire ensemble,  $\langle A \rangle = \sum_i p_i \langle A \rangle_i = \sum_i p_i \text{Tr}(|\psi_i\rangle \langle \psi_i| A)$ .

We define the density operator  $\rho$  to be  $\rho = \sum_i p_i |\psi_i\rangle \langle \psi_i|$ . The density operator is used to describe mixed states. If the  $\psi_i$  form an orthonormal basis, then the maximally mixed state is the state for which the  $p_i$  are the uniform probability distribution, i.e.  $p_i = \frac{1}{d}$ , where  $d$  is the dimension of the Hilbert space in which the  $\psi_i$  live. Due to the linearity of the trace, the density operator  $\rho$  allows us to calculate the expectation value for any observable  $A$ , i.e.  $\langle A \rangle = \text{Tr}(\rho A)$ .

Before we continue, let us briefly discuss the *trace* of an operator. The trace of an operator is a linear functional. If the operator is represented as a matrix, then the trace is the sum of its diagonal elements. Mathematically, we have

$$\text{Tr}(|n\rangle \langle m|) = \sum_i \langle \phi_i | n \rangle \langle m | \phi_i \rangle, \quad (3.6)$$

where  $|\phi_i\rangle$  is some basis.

In matrix form, the trace is the sum of all the diagonal elements of the square matrix. It is independent of the choice of basis. For instance, let  $\{|n\rangle\}$  and  $\{|m\rangle\}$  be two orthonormal bases. Then

$$\begin{aligned} \sum_n \langle n | A | n \rangle &= \sum_n \langle n | A \left( \underbrace{\sum_m |m\rangle \langle m|}_{=I} \right) | n \rangle \\ &= \sum_m \langle m | \left( \sum_n |n\rangle \langle n| \right) A | m \rangle \\ &= \sum_m \langle m | A | m \rangle. \end{aligned}$$

Thus,

$$\sum_n \langle n | A | n \rangle = \sum_m \langle m | A | m \rangle. \quad (3.7)$$

For operators  $A$  and  $B$ ,  $\text{Tr}(AB) = \text{Tr}(BA)$ . The trace also satisfies the cyclic property, i.e.  $\text{Tr}(A...BC) = \text{Tr}(CA...B)$ .

The trace of a density matrix is always equal to 1. For pure states, we have the following property,

$$\rho^2 = \rho, \quad (3.8)$$

from which it follows that  $\text{Tr}(\rho^2) = 1$ . This property exhibited in equation (3.8) is known as idempotency. For a mixed state,  $\rho^2 \neq \rho$ , and consequently  $\text{Tr}(\rho^2) < 1$ . The  $\text{Tr}(\rho^2)$  is called the purity of a state.

The Schrödinger equation,  $H |\psi(t)\rangle = i\hbar \frac{d}{dt} |\psi(t)\rangle$ , describes how the state vector  $|\psi(t)\rangle$  of an informationally isolated system evolves in time. (By informationally isolated, we mean that the system's time evolution is governed by a unitary operator [23]). Over the time interval 0 to  $t$ , the unitary operator  $U(t)$  describes the evolution  $|\psi(t)\rangle = U(t) |\psi(0)\rangle$ . For this pure state, the density operator is described by  $\rho(t) = |\psi(t)\rangle \langle \psi(t)| = U(t) |\psi(0)\rangle \langle \psi(0)| U^\dagger(t) = U(t)\rho(0)U^\dagger(t)$ .

For an infinitesimal time interval  $dt$ ,  $U(dt) = e^{-iH/\hbar dt} \approx \mathbb{I} - \frac{i}{\hbar} dt H$ , where we ignore  $\mathcal{O}(dt^2)$  terms. Thus, the time evolution from  $t$  to  $t + dt$  is

$$\begin{aligned} \rho(t + dt) &= \left( \mathbb{I} - \frac{i}{\hbar} dt H \right) \rho(t) \left( \mathbb{I} + \frac{i}{\hbar} dt H \right) \\ &= \rho(t) - \frac{i}{\hbar} (H\rho(t) - \rho(t)H) dt \\ \Rightarrow \rho(t + dt) - \rho(t) &= -\frac{i}{\hbar} [H, \rho(t)] dt \\ \Rightarrow \frac{\rho(t + dt) - \rho(t)}{dt} &= \frac{1}{i\hbar} [H, \rho(t)]. \end{aligned}$$

At time  $t$ ,

$$\lim_{dt \rightarrow 0} \frac{\rho(t + dt) - \rho(t)}{dt} = \lim_{dt \rightarrow 0} \frac{1}{i\hbar} [H, \rho(t)],$$

and thus,

$$\frac{d\rho}{dt} = \frac{1}{i\hbar} [H, \rho]. \quad (3.9)$$

The relations  $\rho(t) = U(t)\rho(0)U^\dagger(t)$  and the Schrödinger equation applies to mixed states as well, i.e.  $\rho(0) = \sum_i p_i |\psi_i(0)\rangle \langle \psi_i(0)|$ . The matrix representation of a density operator is called a density matrix. In terms of the basis  $\{|n\rangle\}$ , we write  $\rho = \sum_{m,n} \rho_{mn} |m\rangle \langle n|$ . The probability that a basic measurement will yield a result  $n$  is given by  $\rho_{nn} = \langle n | \rho | n \rangle$ . The off-diagonal elements of the density matrix are called coherences. This is because there is a definite phase relation between the terms of a superposition of basis states. We say that the superposition is coherent.

Before we move onto the next subsection, it would be wise to discuss the reduced density matrix. Suppose we have a composite system  $AB$ , made up of subsystems  $A$  and  $B$  respectively. The reduced density matrix for subsystem  $A$  is given by

$$\rho_A = \text{Tr}_B(\rho_{AB}), \quad (3.10)$$

where  $\rho_{AB}$  is the density matrix of the composite system, and  $\text{Tr}_B$  is the partial trace. The partial trace “traces” over the degrees of freedom of subsystem  $B$ , and we are only left with information pertaining to subsystem  $A$ . By performing the partial trace, we end up “losing” information about the composite system. This loss of information, or uncertainty, is related to entropy.

### 3.1.3 Classical and Quantum Entropy

In quantum information theory, entropy measures how much uncertainty there is in a state of a system. In classical information theory, we speak about Shannon entropy. Suppose  $X$  is a random variable whose value we learn after performing a measurement. The Shannon entropy of  $X$  is a quantity that tells us how much information we have gained, on average, by learning the value of  $X$ . Another way of thinking about the Shannon entropy is that it measures the amount of uncertainty that we had about  $X$  before we learned its value.

The *Shannon entropy* associated with a probability distribution is defined as

$$H(X) \equiv H(p_1, p_2, \dots, p_n) \equiv - \sum_x p_x \log_2 p_x, \quad (3.11)$$

where we use the logarithm to the base 2, so that the entropy is measured in bits. This is the convention used in the quantum computation and quantum information literature [22]. However, for convenience, we shall drop the subscript 2.

Note that  $\lim_{x \rightarrow 0} x \log x = 0$ . An event that cannot occur would have no effect on the entropy.

If we wish to measure the closeness of two probability distributions  $p(x)$  and  $q(x)$  over the same index set  $x$ , then we define the *relative entropy* of  $p(x)$  to  $q(x)$  as

$$H(p(x)||q(x)) \equiv \sum_x p(x) \log \left( \frac{p(x)}{q(x)} \right) \equiv -H(X) - \sum_x p(x) \log q(x). \quad (3.12)$$

The *joint entropy* of  $X$  and  $Y$  is defined as

$$H(X, Y) \equiv - \sum_{x,y} p(x, y) \log p(x, y). \quad (3.13)$$

It gives us a measure of the total uncertainty about the pair  $(X, Y)$ . If we know what the value of  $Y$  is, then that means we have acquired  $H(Y)$  bits of information about the pair,  $(X, Y)$ . Since we don't know what the value of  $X$  is, there still exists some uncertainty about the pair,  $(X, Y)$ . The entropy of  $X$  conditional on knowing  $Y$  is defined by

$$H(X|Y) \equiv H(X, Y) - H(Y). \quad (3.14)$$

This is known as *conditional entropy*. It gives us a way of measuring how uncertain we are about the value of  $X$ , given that we know the value of  $Y$ . The *mutual information*, also referred to as the *mutual entropy*, of  $X$  and  $Y$  is defined as

$$H(X : Y) \equiv H(X) + H(Y) - H(X, Y). \quad (3.15)$$

This measures how much information is shared in common between  $X$  and  $Y$ . The joint entropy term is subtracted so that we do not count the information which is common to both  $X$  and  $Y$  twice.

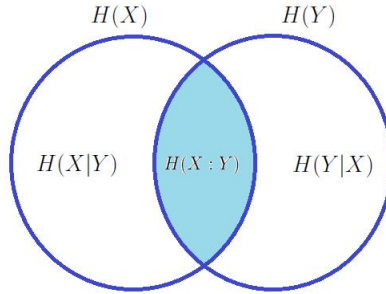


Figure 8: This is an entropy Venn diagram. It provides a graphical representation of the different entropy measures discussed above.

Shannon entropy measures the uncertainty associated with classical probability distributions. In quantum theory, we replace probability distributions with density operators. We generalise the definition of Shannon entropy to quantum states. The *Von Neumann entropy* of a quantum state  $\rho$  is given by the formula [22],

$$S(\rho) \equiv -\text{Tr}(\rho \log \rho). \quad (3.16)$$

We can re-express this definition as

$$S(\rho) = -\sum_k \lambda_k \log \lambda_k, \quad (3.17)$$

where the  $\lambda_k$  are the eigenvalues of  $\rho$  and  $0 \log 0 \equiv 0$ . In a  $d$ -dimensional space, the completely mixed density operator,  $\frac{1}{d}\mathbb{I}$ , has entropy  $\log d$ .

If  $\rho$  and  $\sigma$  are density operators, then the *relative entropy* of  $\rho$  to  $\sigma$  is

$$S(\rho||\sigma) \equiv \text{Tr}(\rho \log \rho) - \text{Tr}(\rho \log \sigma). \quad (3.18)$$

Let  $AB$  be a composite system made up of systems  $A$  and  $B$ . Then the *joint entropy* is defined as

$$S(A, B) \equiv -\text{Tr}(\rho_{AB} \log(\rho_{AB})), \quad (3.19)$$

where  $\rho_{AB}$  is the density matrix of the system  $AB$ . The *conditional entropy* and the *mutual information* are defined similarly as in the classical case, i.e.

$$S(A|B) \equiv S(A, B) - S(B), \quad (3.20)$$

and

$$S(A : B) \equiv S(A) + S(B) + S(A, B). \quad (3.21)$$

The *mutual entropy*,  $S(A : B)$ , accounts for both entanglement and classical correlations between the systems  $A$  and  $B$ . (By classical correlations, we mean the manner in which the two systems affect or influence each other). In the case where the entangled state of  $A$  and  $B$  is a pure state, we have that  $S(A) = S(B)$ , no classical correlations exist, and the joint entropy is zero, i.e.  $S(A, B) = 0$ . In such a case, the mutual information is

$$S(A : B) = 2S(A), \quad (3.22)$$

and becomes a measure of entanglement. This measure goes by the name of entanglement entropy.

We wish to study the relationship between measurement and entropy. Suppose we perform a projective measurement on a quantum system, but we never find out the result of the measurement. If the projectors,  $P_i$ , describe the projective measurement and the initial state is  $\rho$ , then the state after the measurement is  $\rho' = \sum_i P_i \rho P_i$ . There exists a theorem [22] which states that the entropy never decreases due to this process, i.e.  $S(\rho') \geq S(\rho)$ , with equality if and only if  $\rho = \rho'$ .

Klein's inequality declares that the quantum relative entropy between two states  $\rho$  and  $\sigma$  is non-negative,  $S(\rho||\sigma) \geq 0$ , with equality if and only if  $\rho = \sigma$ .

There are many identities for both Shannon entropy and Von Neumann entropy [22]. However, it is not our goal to list all of them, only those of which we might need to apply at some point. One these important identities goes by the name of the *strong subadditivity inequality*, i.e. for three quantum systems  $A$ ,  $B$ , and  $C$ , the following is true:

$$S(A, B, C) + S(B) \leq S(A, B) + S(B, C). \quad (3.23)$$

A proof for this inequality can be found in [25].

## 3.2 Information and Distinguishability

In order for us to reliably depend on the information we obtain from a measurement, we must have a way of distinguishing between the sources of the information. In this section, we shall look at ways in which to distinguish between quantum states. We shall also look at entanglement and cloning in the quantum sense.

### 3.2.1 Distance Measures

It is often useful for us to have a way of determining how “close” two quantum states are to each other. In order to do this, we need to introduce a distance measure. In this subsection, we shall only discuss the trace distance (also known as the  $L_1$  distance or the Kolmogorov distance).

Let us consider two probability distributions,  $\{p_k\}$  and  $\{q_k\}$ , over the same index set  $k$ . The *trace distance* is defined as

$$D(p_k, q_k) \equiv \frac{1}{2} \sum_k |p_k - q_k|. \quad (3.24)$$

The trace distance is a metric, i.e.

- (i)  $D(p_k, q_k) = D(q_k, p_k)$
- (ii)  $D(p_k, p_k) = 0$
- (iii)  $D(p_k, r_k) \leq D(p_k, q_k) + D(q_k, r_k)$ .

In quantum mechanics, the trace distance between two quantum states  $\rho$  and  $\sigma$  is

$$D(\rho, \sigma) \equiv \frac{1}{2} \text{Tr} |\rho - \sigma|, \quad (3.25)$$

where  $|A| = \sqrt{A^\dagger A}$  for some operator  $A$ . If  $\rho$  and  $\sigma$  commute, then they can be expressed as diagonal matrices in the same basis, i.e.

$$\rho = \sum_i r_i |i\rangle \langle i|, \quad \sigma = \sum_i s_i |i\rangle \langle i|,$$

where  $\{|i\rangle\}$  is some orthonormal basis. Upon calculating, we see that

$$\begin{aligned} D(\rho, \sigma) &= \frac{1}{2} \text{Tr} |\rho - \sigma| \\ &= \frac{1}{2} \text{Tr} \left| \sum_i (r_i - s_i) |i\rangle \langle i| \right| \\ &= \frac{1}{2} |r_i - s_i| \\ &= D(r_i, s_i). \end{aligned}$$

Let us now discuss quantum entanglement.

### 3.2.2 Quantum Entanglement

We begin by considering a composite system  $AB$ , made up of distinct systems  $A$  and  $B$ . Let  $|\psi^{(A)}\rangle$  and  $|\phi^{(B)}\rangle$  be the quantum state vectors of system  $A$  and system  $B$  respectively. By

enumerating the states of the subsystems, we can describe the joint state of the composite system  $AB$ ,  $|\psi^{(A)}\rangle \otimes |\phi^{(B)}\rangle$ . Mathematically, the joint state is represented as the tensor product of states from each Hilbert space. The tensor product of the subsystem Hilbert spaces satisfies the following properties:

- (i) For any  $|a\rangle$  in  $\mathcal{H}^{(A)}$  and  $|b\rangle$  in  $\mathcal{H}^{(B)}$ , the space  $\mathcal{H}^{(AB)}$  contains the product vector  $|a\rangle \otimes |b\rangle$ .
- (ii)  $|a\rangle \otimes (\lambda_1 |b_1\rangle + \lambda_2 |b_2\rangle) = \lambda_1(|a\rangle \otimes |b_1\rangle) + \lambda_2(|a\rangle \otimes |b_2\rangle)$ , where  $\lambda_i$  are constants.
- (iii)  $(\langle a_1| \otimes \langle b_1|)(|a_2\rangle \otimes |b_2\rangle) = \langle a_1|a_2\rangle \langle b_1|b_2\rangle$ .
- (iv) Any  $|\Psi^{(AB)}\rangle$  in  $\mathcal{H}^{(AB)}$  is either a product vector or a linear combination of product vectors.

If we make measurements on  $A$  and  $B$  respectively, where  $|a^{(A)}\rangle$  and  $|b^{(B)}\rangle$  are the basis vectors associated with the outcomes  $a$  and  $b$ , then the probabilities are

$$P^{(A)}(a) = |\langle a^{(A)}|\psi^{(A)}\rangle|^2, \quad \text{and} \quad (3.26)$$

$$P^{(B)}(b) = |\langle b^{(B)}|\phi^{(B)}\rangle|^2. \quad (3.27)$$

If the subsystems have been prepared completely independently, then

$$P^{(AB)}(a, b) = P^{(A)}(a)P^{(B)}(b). \quad (3.28)$$

In quantum mechanics,

$$P^{(AB)}(a, b) = |(\langle a^{(A)}| \otimes \langle b^{(B)}|)(|\psi^{(A)}\rangle \otimes |\phi^{(B)}\rangle)|^2. \quad (3.29)$$

We need to reconcile equations (3.28) and (3.29), i.e.

$$\begin{aligned} (\langle a^{(A)}| \otimes \langle b^{(B)}|)(|\psi^{(A)}\rangle \otimes |\phi^{(B)}\rangle) &= \langle a^{(A)}|\psi^{(A)}\rangle \langle b^{(B)}|\phi^{(B)}\rangle \\ |(\langle a^{(A)}| \otimes \langle b^{(B)}|)(|\psi^{(A)}\rangle \otimes |\phi^{(B)}\rangle)|^2 &= |\langle a^{(A)}|\psi^{(A)}\rangle|^2 |\langle b^{(B)}|\phi^{(B)}\rangle|^2 \\ \Rightarrow P^{(AB)}(a, b) &= P^{(A)}(a)P^{(B)}(b). \end{aligned}$$

From the superposition principle, there exists composite system states of the form

$$|\Psi^{(AB)}\rangle = \alpha_1 |\psi_1^{(A)}\rangle \otimes |\phi_1^{(B)}\rangle + \alpha_2 |\psi_2^{(A)}\rangle \otimes |\phi_2^{(B)}\rangle + \dots$$

The subsystems  $A$  and  $B$  are described by Hilbert spaces  $\mathcal{H}^{(A)}$  and  $\mathcal{H}^{(B)}$  respectively. The composite system is described by the Hilbert space  $\mathcal{H}^{(AB)} = \mathcal{H}^{(A)} \otimes \mathcal{H}^{(B)}$ . We call such a system a bipartite system, since it's made up of two parts.

If  $|a_1\rangle$  is orthogonal to  $|a_2\rangle$  in  $\mathcal{H}^{(A)}$ , then  $|a_1, b_1\rangle$  is orthogonal to  $|a_2, b_2\rangle$  in  $\mathcal{H}^{(AB)}$ . The argument goes as follows:

$$\begin{aligned} |a_1\rangle \text{ is orthogonal to } |a_2\rangle &\Rightarrow \langle a_1|a_2\rangle = \langle a_2|a_1\rangle = 0 \\ (\langle a_1| \otimes \langle b_1|)(|a_2\rangle \otimes |b_2\rangle) &= \langle a_1|a_2\rangle \langle b_1|b_2\rangle = 0. \end{aligned}$$

Let  $\{|n\rangle\}$  be a basis for  $\mathcal{H}^{(A)}$  and  $\{|k\rangle\}$  be a basis for  $\mathcal{H}^{(B)}$ . Then the set  $\{|n, k\rangle\}$ , which includes all products  $|n\rangle \otimes |k\rangle$  of basis vectors, is a basis for  $\mathcal{H}^{(AB)}$ . If  $\dim \mathcal{H}^{(A)} = d_A$  and  $\dim \mathcal{H}^{(B)} = d_B$ , then we can write

$$|\psi^{(A)}\rangle = \alpha_1 |n_1\rangle + \alpha_2 |n_2\rangle + \cdots + \alpha_{d_A} |n_{d_A}\rangle \quad (3.30)$$

$$|\phi^{(B)}\rangle = \beta_1 |k_1\rangle + \beta_2 |k_2\rangle + \cdots + \beta_{d_B} |k_{d_B}\rangle, \quad (3.31)$$

and thus

$$|\psi^{(A)}\rangle \otimes |\phi^{(B)}\rangle = \sum_{i=1}^{d_A} \sum_{j=1}^{d_B} \alpha_i \beta_j |n_i\rangle \otimes |k_j\rangle. \quad (3.32)$$

Some states of  $AB$  are not product states. For instance, consider

$$|\Psi^{(AB)}\rangle = \sum_{n,k} \alpha_{nk} |n\rangle \otimes |k\rangle = \sum_n |n\rangle \otimes \left( \sum_k \alpha_{nk} |k\rangle \right) = \sum_n |n\rangle \otimes |\phi_n\rangle, \quad (3.33)$$

where  $|\phi_n\rangle$  are not necessarily normalised in  $\mathcal{H}^{(B)}$ .

Let  $|\Psi^{(AB)}\rangle = |\psi\rangle \otimes |\phi\rangle$ . By expanding the  $A$ -state using the  $\{|n\rangle\}$  basis, we have  $|\Psi^{(AB)}\rangle = \sum_n |n\rangle \otimes (\alpha_n |\phi\rangle)$ . If  $|\phi_n\rangle = \alpha_n |\phi\rangle$  for all  $n$  in (3.33), then  $|\Psi^{(AB)}\rangle$  must be a product state, i.e.  $|\Psi^{(AB)}\rangle = \sum_{n,k} \alpha_{nk} |n\rangle \otimes |k\rangle$ .

We have a product state if and only if the various  $|\phi_n\rangle$  vectors are all multiples of a single vector. A non-product state is called an entangled state. If  $AB$  is in an entangled state, it is not possible to assign state vectors to the individual subsystems. Entanglement arises when a dynamical interaction takes place.

Systems  $A$  and  $B$  are non-interacting if the Hamiltonian of  $AB$  is  $H^{(AB)} = H^{(A)} + H^{(B)}$ . Non-interacting systems are dynamically isolated or uncoupled from each other. If  $A$  and  $B$  are non-interacting, they will not become entangled by their own autonomous time evolution.

The mutual entropy,  $S(A : B)$ , accounts for both entanglement and classical correlations between the systems  $A$  and  $B$ . (By classical correlations, we mean the manner in which the two systems affect or influence each other). In the case where the entangled state of  $A$  and  $B$  is a pure state, we have that  $S(A) = S(B)$ , no classical correlations exist, and the joint entropy is zero, i.e.  $S(A, B) = 0$ . In such a case, the mutual information is

$$S(A : B) = 2S(A), \quad (3.34)$$

and becomes a measure of entanglement. It is known as the entanglement entropy. Let us discuss what it means for a state to be maximally entangled.

A pure state from  $\mathcal{H}^{(AB)}$  is maximally entangled if the reduced density matrix of any one of the subsystems is maximally mixed. Another way of determining if a state is maximally entangled is by calculating the von Neumann entropy. If the von Neumann entropy is a maximum for each bipartition, then the state is said to be maximally entangled. [26]

Let us look at an example in which we can see some of the physical implications of entanglement. We shall look at the EPR state. For this example, let us define the observable,

$$\vec{v} \cdot \vec{\sigma} \equiv v_1 \sigma_1 + v_2 \sigma_2 + v_3 \sigma_3, \quad (3.35)$$

which has the eigenvalues  $\pm 1$ . The measurement of this observable is known as measurement of spin along the  $\vec{v}$  axis [22]. Let us prepare an entangled state of the two qubit system,  $|\psi\rangle = \frac{|0\rangle \otimes |1\rangle - |1\rangle \otimes |0\rangle}{\sqrt{2}}$ . Let us introduce two players, named Alice and Bob. Each member of the entangled pair belongs to Alice and Bob respectively, who are very far apart from each other. If Alice measures  $\vec{v} \cdot \vec{\sigma}$  along the  $\vec{v}$  axis and obtains a result of  $+1$ , then she can predict, with absolute certainty, that Bob's result will yield  $-1$ . It appears as if Bob's qubit has knowledge of the result of a measurement performed on Alice's qubit.

To see this, let  $|a\rangle$  and  $|b\rangle$  be eigenstates of  $\vec{v} \cdot \vec{\sigma}$ . Then we can write

$$|0\rangle = \alpha_1 |a\rangle + \alpha_2 |b\rangle, \quad (3.36)$$

$$|1\rangle = \beta_1 |a\rangle + \beta_2 |b\rangle, \quad (3.37)$$

where  $\alpha_i, \beta_i \in \mathbb{C}$ . Now we can write the EPR state as

$$\begin{aligned} \frac{|0\rangle \otimes |1\rangle - |1\rangle \otimes |0\rangle}{\sqrt{2}} &= \frac{1}{\sqrt{2}} (\alpha_1 \beta_2 |a\rangle \otimes |b\rangle + \alpha_2 \beta_1 |b\rangle \otimes |a\rangle - \beta_1 \alpha_2 |a\rangle \otimes |b\rangle - \alpha_1 \beta_2 |b\rangle \otimes |a\rangle) \\ &= (\alpha_1 \beta_2 - \beta_1 \alpha_2) \frac{|a\rangle \otimes |b\rangle - |b\rangle \otimes |a\rangle}{\sqrt{2}}. \end{aligned}$$

The factor  $(\alpha_1 \beta_2 - \beta_1 \alpha_2)$  is the determinant of the unitary matrix,

$$\begin{pmatrix} \alpha_1 & \alpha_2 \\ \beta_1 & \beta_2 \end{pmatrix}.$$

This implies that  $\alpha_1 \beta_2 - \beta_1 \alpha_2 = e^{i\theta}$ , for some real  $\theta$ . We conclude that  $\frac{|0\rangle \otimes |1\rangle - |1\rangle \otimes |0\rangle}{\sqrt{2}} = \frac{|a\rangle \otimes |b\rangle - |b\rangle \otimes |a\rangle}{\sqrt{2}}$  up to a global phase factor which is not observed. These calculations demonstrate to us that if the first qubit yields a measurement result of  $+1$ , then the second qubit is guaranteed to yield a result of  $-1$ .

The bothersome aspect of this situation arises when Alice and Bob perform their respective measurements at the *same time*. If Bob's qubit can have knowledge of Alice's qubit's result, how can the information from Alice's qubit be transmitted to Bob's one instantaneously? Nothing can travel faster than light, not even information. This problem is what gave rise to Einstein's famous phrase of "spooky action at a distance". It turns out that this apparent paradox is resolved by Bell's theorem [23]. The main point is that our "common sense" view of nature is not to be trusted. In the next section, we shall look at the idea of quantum cloning.

### 3.2.3 Quantum Xerox Machine

Suppose we have three systems  $A$ ,  $B$ , and  $M$ , with Hilbert spaces  $\mathcal{H}_A$ ,  $\mathcal{H}_B$ , and  $\mathcal{H}_M$  respectively. Let system  $A$  be the input system,  $B$  the output system, and  $M$  the “machine”. The job of this machine is to take any state from  $\mathcal{H}_A$  and produce the original state and a copy of it, undergoing unitary time evolution. We can call this machine a “unitary cloning machine.” It turns out that such a machine cannot be invented. The no-cloning theorem states that no unitary cloning machine exists that works on arbitrary initial states of the input  $A$ . Two different proofs of this theorem can be found in [23].

We shall not go over the proof of this theorem, instead we shall look at an example from [27]. In this example, let us call this machine a *Quantum Xerox Machine*, i.e. a machine that can take any system as its input, and then produce the original system and a duplicate.

Suppose we have a spin-up state and a spin-down state as our initial states, both with respect to the  $z$ -axis. We would expect the Xerox machine to do the following:

$$\begin{aligned} |\uparrow\rangle &\rightarrow |\uparrow\rangle |\uparrow\rangle, \\ |\downarrow\rangle &\rightarrow |\downarrow\rangle |\downarrow\rangle. \end{aligned}$$

Now let us consider a spin which had its polarisation along the  $x$ -axis, i.e.

$$\frac{1}{\sqrt{2}} (|\uparrow\rangle + |\downarrow\rangle) = \frac{1}{\sqrt{2}} |\uparrow\rangle + \frac{1}{\sqrt{2}} |\downarrow\rangle. \quad (3.38)$$

According to quantum mechanics, this state must evolve linearly, i.e.

$$\frac{1}{\sqrt{2}} (|\uparrow\rangle + |\downarrow\rangle) \rightarrow \frac{1}{\sqrt{2}} (|\uparrow\rangle |\uparrow\rangle + |\downarrow\rangle |\downarrow\rangle). \quad (3.39)$$

However, the Xerox machine would have

$$\frac{1}{\sqrt{2}} (|\uparrow\rangle + |\downarrow\rangle) \rightarrow \frac{1}{\sqrt{2}} (|\uparrow\rangle + |\downarrow\rangle) \frac{1}{\sqrt{2}} (|\uparrow\rangle + |\downarrow\rangle) \quad (3.40)$$

$$= \frac{1}{2} (|\uparrow\rangle |\uparrow\rangle + |\downarrow\rangle |\downarrow\rangle + |\uparrow\rangle |\downarrow\rangle + |\downarrow\rangle |\uparrow\rangle). \quad (3.41)$$

This is in violation of the principle of linear evolution. The linearity principle from quantum mechanics disallows the cloning of states.

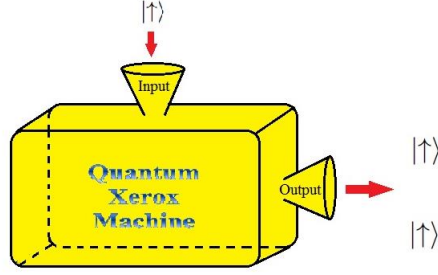


Figure 9: A simple drawing of the hypothetical Quantum Xerox Machine.

### 3.3 Black Holes and Information

In the previous chapter, we discussed the thermodynamics of black holes. We saw that black holes have a finite entropy, but due to our inability to probe what goes on beyond the black hole horizon, we know very little about the microstates of black holes. From our previous discussions in the current chapter, we looked at the relationship between entropy and information. In this section, we wish to discuss the black hole information paradox.

#### 3.3.1 Black Hole Information Paradox

In order to understand the black hole information paradox, we need to discuss Hawking radiation in the context of particle pair production on the horizon. Suppose the gravitational field around the black hole horizon produces particle pairs. These pairs consist of a real particle (with positive energy) and a virtual particle (with negative energy). The particle with the negative energy falls into the black hole to reduce its mass. The particle with the positive energy escapes to infinity, where it can be observed by a physicist.

These particles are entangled with each other, i.e.

$$|\psi\rangle_{\text{pair}} \sim |0\rangle_r |0\rangle_v + |1\rangle_r |1\rangle_v + |2\rangle_r |2\rangle_v + \dots,$$

where the subscripts  $r$  and  $v$  stand for real and virtual, respectively. As more particle pairs are created, the entanglement of the radiation of the black hole keeps increasing. But the black hole decreases in size. The smaller the black hole becomes, the greater the entanglement of the radiation. We need to answer the question of how a small residual black hole, which is called a remnant, can carry all this entanglement. Furthermore, once the black hole completely evaporates away, we are left wondering what happened to all the information.

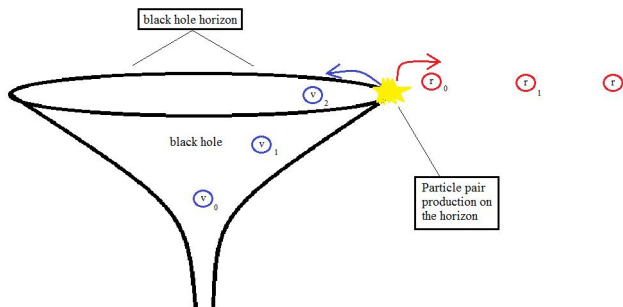


Figure 10: A simple sketch depicting the creation of particle/anti-particle pairs on the horizon of a black hole.

In [28], the author introduces “niceness conditions”. These conditions ensure that for a quantum state specified on an initial spacelike slice, the state will evolve under the action of a Hamiltonian operator to later spacelike slices. Furthermore, locality always holds. We would like to list these conditions. However, it would probably be a good idea to first discuss what is meant by intrinsic and extrinsic curvature. [29]

Extrinsic curvature arises when a surface curves into a higher dimension in an embedding space. For instance, a flat sheet of paper being rolled up into a cylinder. Intrinsic curvature arises when the geometry within the surface is no longer flat, Euclidean geometry. We use geodesic deviation to determine if intrinsic curvature is present. It is possible for a surface to exhibit extrinsic curvature without exhibiting intrinsic curvature. This can be demonstrated by drawing a triangle on a flat sheet of paper. The sum of the interior angles of the triangle is  $180^\circ$ . If we fold the sheet of paper to form a cylinder, then the surface would have acquired extrinsic curvature. However, the surface is still intrinsically flat. If someone measured the angles of the triangle (this would be a rather awkward task), they would find it to all add up to  $180^\circ$ .

Now we are ready to list the “niceness” conditions:

- (N1) We define our quantum state on a spacelike slice. This spacelike slice should have an intrinsic curvature,  ${}^{(3)}R$ , that is much smaller than the Planck scale everywhere, i.e.  ${}^{(3)}R \ll \frac{1}{l_p^2}$ .
- (N2) The spacelike slice lives in a 4-dimensional spacetime. We require that the extrinsic curvature of the slice  $K$  be small everywhere:  $K \ll \frac{1}{l_p}$ .
- (N3) In the neighbourhood of the slice, the 4-curvature of the full spacetime should be small everywhere, i.e.  ${}^{(4)}R \ll \frac{1}{l_p^2}$ .
- (N4) All matter on the slice is required to be “good”. By this, we mean that the wavelength of any quanta should be much longer than the Planck length ( $\lambda \gg l_p$ ), and both the

energy and the momentum density should be small everywhere compared to the Planck density. Furthermore, we expect all matter to satisfy the usual energy conditions.

- (N5) The quantum state on the initial slice should evolve to a later slice. The vectors needed to specify the evolution should change smoothly with position.

The niceness conditions allow us to discuss Hawking radiation within the context of, as the author in [28] calls it, “solar system physics”. We shall now go through the mechanism of particle pair production on the horizon, using figure as our guide.

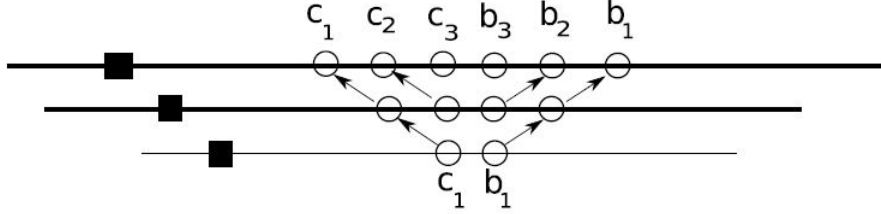


Figure 11: A diagram depicting the creation of particle pairs, labelled  $b_i$  and  $c_i$  respectively, due to the “stretching” of spacelike slices. This figure is taken directly from [28].

### Hawking Radiation Mechanism

- (i) Let  $|\psi\rangle_M$  denote the matter state of the star that collapses to form the black hole on some initial spacelike slice.
- (ii) Evolving to the next spacelike slice results in the “middle part” of the spacelike slice stretching, while no changes occur to the left and right parts. Due to this stretching, correlated pairs labelled  $b_1$  and  $c_1$  are created. On the entire slice, the state is given by

$$|\Psi\rangle \approx |\psi\rangle_M \otimes \left( \frac{1}{\sqrt{2}} |0\rangle_{c_1} |0\rangle_{b_1} + \frac{1}{\sqrt{2}} |1\rangle_{c_1} |1\rangle_{b_1} \right). \quad (3.42)$$

The entanglement entropy of  $b_1$  with  $\{M, c_1\}$  is

$$S_{\text{entanglement}} = \log 2. \quad (3.43)$$

- (iii)  $|\psi\rangle_M$  remains approximately constant, since no evolution occurs in this part of the slice. However, more stretching of the spacelike slice occurs, resulting in the creation of a new set of pairs  $b_2, c_2$ . Additionally, the pairs  $b_1, c_1$  move further away from each other and from the region of stretching. At the end of this step, we can write the state of the whole slice as

$$|\Psi\rangle \approx |\psi\rangle_M \otimes \left( \frac{1}{\sqrt{2}} |0\rangle_{c_1} |0\rangle_{b_1} + \frac{1}{\sqrt{2}} |1\rangle_{c_1} |1\rangle_{b_1} \right) \otimes \cdots \otimes \left( \frac{1}{\sqrt{2}} |0\rangle_{c_2} |0\rangle_{b_2} + \frac{1}{\sqrt{2}} |1\rangle_{c_2} |1\rangle_{b_2} \right) \quad (3.44)$$

The entanglement entropy of the set  $\{b_1, b_2\}$  with  $\{M, c_1, c_2\}$  is

$$S_{\text{entanglement}} = 2 \log 2. \quad (3.45)$$

(iv) After this process occurs  $n$  times, we have the state

$$\begin{aligned} |\Psi\rangle \approx & |\psi\rangle_M \otimes \left( \frac{1}{\sqrt{2}} |0\rangle_{c_1} |0\rangle_{b_1} + \frac{1}{\sqrt{2}} |1\rangle_{c_1} |1\rangle_{b_1} \right) \otimes \cdots \\ & \cdots \otimes \left( \frac{1}{\sqrt{2}} |0\rangle_{c_2} |0\rangle_{b_2} + \frac{1}{\sqrt{2}} |1\rangle_{c_2} |1\rangle_{b_2} \right) \otimes \cdots \\ & \cdots \otimes \left( \frac{1}{\sqrt{2}} |0\rangle_{c_n} |0\rangle_{b_n} + \frac{1}{\sqrt{2}} |1\rangle_{c_n} |1\rangle_{b_n} \right) \end{aligned} \quad (3.46)$$

The entanglement entropy of the sets  $\{b_i\}$  and  $\{M, c_i\}$  is

$$S_{\text{entanglement}} = n \log 2. \quad (3.47)$$

(v) The mass of the black hole decreases as more quanta  $\{b_i\}$  are emitted. Once  $M_{BH} \sim m_{pl}$ , the niceness conditions fail to be satisfied, i.e. quantum gravity enters the picture. This is because  ${}^{(4)}R \ll \frac{1}{l_{pl}^2}$  is no longer true. Consequently, the evolution of the spacelike slice comes to an end.

At one stage, it was believed that sub-leading terms in the expression for the black hole entropy could remove the entanglement. This turned out not to be the case. By recasting Hawking's argument as a theorem [28], it became clear that no such resolution was possible. This is the Hawking argument cast as a theorem:

*Consider the following two conditions:*

- (i) *The low energy modes at the horizon undergo an evolution that is within a fraction,  $\epsilon$ , of what is expected semi-classically.*
- (ii) *Quanta at  $r \gg M$ , i.e. particles that are very far away from the horizon, are essentially independent of the black hole.*

*If these two conditions hold, then the entanglement entropy at the  $n^{\text{th}}$  emission step,  $S_n$ , must keep increasing as*

$$S_{n+1} > S_n + \log 2 - 2\epsilon. \quad (3.48)$$

The Hawking theorem states that, assuming niceness conditions, the formation and evaporation of a traditional black hole will ultimately give rise to either mixed states or remnants. The formation of mixed states violates the unitarity principle of quantum mechanics, since it describes a process in which a pure state evolves into a mixed state. The formation of remnants does not necessarily violate a law of physics, however it is quite hard to digest the idea of a small, bounded region having unbounded degeneracy.

There is no hope of wishing that sub-leading terms can remove the entanglement, since the entanglement entropy increases every time quanta are emitted.

The main idea behind the proof of this “theorem” lies in the fact that as the black hole evaporates, more and more entangled pairs of particles are produced. By the time the size of the black hole is near the Planck length,  $l_{pl}$ , the entropy of entanglement will be large. If the black hole evaporates away completely, then we are left with radiation which is “entangled with nothing.” This violates the unitarity of quantum mechanics. Alternatively, if the Planck-size black hole remains (this is the remnant), then our theory would have to admit for remnants with an arbitrarily large degeneracy.

Over the years, there have been several proposed resolutions to the black hole information paradox. However, the quantum strong sub-additivity theorem has reduced the number of possible resolutions to three main categories. We will briefly discuss these three main categories. [30]

(i) If the effects of quantum gravity are only applicable at distances  $d \leq l_p$ , then the information would be trapped inside a remnant. This remnant could evaporate away (this would entail the loss of information), take the form of a baby universe, or slowly allow information to be leaked away over times  $t \gg M^3$ . This cubic dependence on  $M$  comes from the distance between the matter which makes up the black hole and the region in which the particles are created. The creation of these particles comes about as a consequence of the spacelike slices stretching.

(ii) The no-hair theorem can be violated by non-trivial effects at the horizon  $r \sim M$ . In string theory, the assumptions inherent in the no-hair theorem are bypassed as a consequence of the behaviour of extra dimensions. Fuzzballs are a realisation of this idea. They provide unitary evaporation. However, the traditional horizon does not exist in string theory. For more information on fuzzballs, the reader is encouraged to consult [31].

(iii) Non-local effects could occur. For instance, wormholes connect locations of the entangled quanta [32]. We know that the regions inside a black hole are causally disconnected from the regions outside a black hole. A wormhole could form a bridge between these regions.

For a more thorough discussion of the black hole information paradox, the reader is encouraged to read [28]. Let us see if it is possible, at least in theory, to retrieve information from a black hole.

### 3.3.2 Information Recovery from a Black Hole

The authors in [1] argue that it should be possible to identify a particular underlying quantum state that gives rise to the entropy of a black hole. To identify this state, the observer needs to make measurements that require Planck scale precision. Without such precision, the observer will experience information loss. We shall present a summary of the main points of

their idea.

Suppose we have a gravitating system of total energy  $E$  and entropy  $S(E)$ . We let it interact with a measuring device that has an energy resolution of  $\Delta E$ . The number of states between  $E$  and  $E + \Delta E$  is of the order  $e^S$ . Since we have a non-degenerate spectrum, the spacing of the energy levels must be  $\delta E \sim \Delta E e^{-S}$ .

Let us place a black hole “in a box” [1]. We do this because uncharged black holes do not come to equilibrium in an asymptotically flat spacetime. They eventually evaporate away completely. Furthermore, we assume that a black hole has a finite number of microstates. By arguing that all the information concerning the black hole microstates is available in the asymptotic region of spacetime, the density of states in the regime dominated by the black hole is

$$\frac{dN}{dE} \approx \frac{d}{dE} e^S = e^S \frac{dS}{dE}. \quad (3.49)$$

The measuring device, of energy resolution  $\Delta E$ , will interact with  $N(E)\Delta E \approx e^S \times \Delta E \frac{dS}{dE}$  many states. The entropy,

$$\ln(N(E)\Delta E) = S + \ln(\Delta E) + \ln\left(\frac{dS}{dE}\right), \quad (3.50)$$

is the same as the black hole entropy up to logarithmic corrections. We need the precision of the measuring device to be  $\delta E \sim e^{-S}$ . From the Heisenberg uncertainty principle,  $\delta t \sim \frac{1}{\delta E} \sim e^S$ . In the classical limit, where  $\hbar \rightarrow 0$  or  $l_p \rightarrow 0$ , there is an exponential divergence of this time scale since  $S = \frac{A}{4l_p^2} + \text{corrections}$ .

For a black hole with a finite number of states, the energy spectrum should be discrete and non-degenerate. It would then be possible to determine the quantum state by knowing the precise energy. In a generic gravitating theory, the energy of the black hole is given by boundary terms, so complete knowledge of the state of a black hole is contained in the asymptotic region.

Suppose we identically prepare a large number of black holes in the state  $|\psi\rangle$ , where

$$|\psi\rangle = \sum_n a_n |E_n\rangle. \quad (3.51)$$

In order for us to show that the information is available at infinity, we would need to be able to measure the  $a_n$  to arbitrary accuracy. When measuring the black hole’s energy, the number of times we get the value  $E_n$  is determined by the  $|a_n|^2$ . However, we would also need to obtain phase information. For phase information, we would need to consider measurements performed on time-dependent operators. Let us call  $\mathcal{B}$  such an operator, where  $[\mathcal{B}, H] \neq 0$ , and the eigenvalues of  $\mathcal{B}$  are  $B_n$ .

For ease of calculation, let us only consider the state  $|\psi\rangle$  to be a superposition of two energy eigenstates, i.e.  $|\psi\rangle = a_1 |E_1\rangle + a_2 |E_2\rangle$ . We also consider two eigenstates of the operator  $\mathcal{B}$ ,

i.e.

$$|B_1\rangle = \sum_n b_{1,n} |E_n\rangle,$$

$$|B_2\rangle = \sum_n b_{2,n} |E_n\rangle.$$

We take the coefficients  $b_{i,j}$  to be known quantities, based on the underlying theory. By underlying theory, we mean that the necessary properties of the operator  $\mathcal{B}$  are known. By calculating the overlaps,

$$|\langle B_1|\psi\rangle|^2 = |a_1 b_{1,1} + a_2 b_{1,2}|^2 \tag{3.52}$$

$$|\langle B_2|\psi\rangle|^2 = |a_1 b_{2,1} + a_2 b_{2,2}|^2, \tag{3.53}$$

we can obtain the relative frequencies of measurements  $B_1$  and  $B_2$ . Since we know what the  $b_{i,j}$  are, and we learned what the  $|a_n|$  are from our measurements of the energy, it is possible for us to determine the relative phase of  $a_1$  and  $a_2$  by taking the ratio between the overlaps, i.e. equations (3.52) and (3.53). Now we would be able to completely reconstruct  $|\psi\rangle$ . This means that we have obtained full information about the black hole's microstate, and from outside the black hole.

The authors used conventional physics in their argument, and thereupon successfully showed that information can be retrieved from a black hole. This would have been excellent news if it were not for the fact that we do not have the resources to perform this task. We would need very large energies or very long times.

## 3.4 Quantum Typicality

In this section, we shall discuss quantum typicality. Before jumping straight into the definition, we shall first try to gain some intuition. We shall then move on to a more mathematical discussion of these ideas. Levy's lemma is very important for what is to come in later chapters.

### 3.4.1 Typicality in an Intuitive Sense

Classical mechanics provides us with a model of the universe in which the laws of physics are deterministic. This means that if we are given adequate information about the initial state of a system, i.e. initial conditions, then we can accurately predict how the state will evolve in time.

Suppose we perform an experiment in which we prepare the initial state of a system in a specific way, and then record the outcome of the experiment. If we perform an identical

experiment with all the same initial conditions, we expect to get the same outcome every time. This is known as repeatability. (We should note that there exist systems which are very sensitive to their initial conditions. The study of such systems falls under the topic of chaos, or dynamical instability).

Quantum mechanics is not deterministic like classical mechanics. The time-dependent Schrödinger equation describes how the wave function, which is a probability distribution when we compute the square of its modulus, evolves in time. The wave function does not tell us where a particle is at a given time, but rather what the probability is of the particle being at a particular position at a given time. This probabilistic aspect of the theory means that even if the initial conditions of the Schrödinger equation are set with very high precision, we shall always have some degree of indeterminacy.

Quantum typicality is the phenomenon in which the outcome of a measurement does not depend on how the state was initially prepared [33]. To see this, suppose we perform an experiment. We need to be able to confidently assert that the wave function for our system belongs to a suitable ensemble, i.e. it should lie in a given subspace of the total Hilbert space of the system. By the very nature of the wave function, it is not meaningful to speak about two particles having identical wave functions. It is for this reason that we rather work with a statistical ensemble. This means that the quantum state is described by a density matrix. Every time we repeat the experiment, we merely need to select the wave function from the statistical ensemble. This saves us from having to have a particular wave function identically re-prepared every time we perform the experiment.

Unlike in the classical case, a particular observable may or may not yield the same outcome every time we perform a measurement on the system. If we calculate the expectation value for some observable at a later time, and we see that it is almost the same as the expectation value at the initial time, and this is true for the majority of pure states within the ensemble, then we say that the observable is typical. Some observables are typical, some are atypical.

Let us now move on to a more mathematical discussion of these ideas. We shall discuss the phenomenon of measure concentration, as well as Levy's lemma. We shall try not to make our discussion too technical, as we do not want to lose sight of the physics amidst all the technical mathematics. A rigorous discussion of Levy's lemma would involve a decent knowledge of measure theory. The interested reader is invited to consult [34] for such a discussion.

### 3.4.2 Levy's Lemma

Suppose we have an  $n$ -dimensional Hilbert space  $\mathcal{H}$ . We prepare a state by randomly selecting a given pure state  $|\psi\rangle$  from a subspace  $\mathcal{H}_E \subset \mathcal{H}$ , whose dimension is  $\dim(\mathcal{H}_E) = d_E$ . Given

a basis  $\{|k\rangle\}$  of  $\mathcal{H}_E$ , we can write

$$|\psi\rangle = \sum_k z_k |k\rangle. \quad (3.54)$$

The  $\{z_k\}$  are complex coefficients assumed to be sampled uniformly over the surface of the unit sphere, i.e.  $\sum_k |z_k|^2 = 1$ . This is important, since our discussion of Levy's lemma involves higher dimensional unit spheres.

Before we continue, we need to define a metric measure space. A measure on a set provides a generalisation for the concepts of length, area, and volume. The manner in which distance is defined in a given space depends on the metric. If we say that the measure of two sets  $X$  and  $Y$  are the same, i.e.  $\mu(X) = \mu(Y)$ , then we are saying that the two sets share the same notion of length, area, and volume. For the precise mathematical definition of these concepts, the reader should consult [34]. We shall now list a few definitions and an important result.

Definition (Median  $M_f$ )

Let  $X$  be a metric measure space, and  $f : X \rightarrow \mathbb{R}$  a continuous function. Then a median  $M_f$  is defined by

$$\mu\{x \in X | f(x) \leq M_f\} = \frac{1}{2}. \quad (3.55)$$

It is important to note that the median  $M_f$  is not necessarily unique, and that  $\mathbb{E} \neq M_f$  (here  $\mathbb{E}$  is the expectation value).

Definition (Concentration function)

Let  $X$  be a metric measure space. For every  $\epsilon > 0$ , we define the concentration function as

$$\alpha_X(\epsilon) := \sup\{\mu(X \setminus N_\epsilon(S)) | S \text{ is measurable and } \mu(S) = \frac{1}{2}\}, \quad (3.56)$$

where  $N_\epsilon(S)$  is the  $\epsilon$ -neighbourhood of  $S$ . This is defined as

$$N_\epsilon(S) = \{x \in X | \exists s \in S \text{ such that } |s - x| < \epsilon\}. \quad (3.57)$$

If  $\alpha_X$  is small, then we say that the space has a strong concentration of measure.

Definition (Lipschitz continuous function)

A function  $f : X \rightarrow \mathbb{R}$  is said to be Lipschitz continuous, with Lipschitz constant  $\eta$ , if

$$|f(x) - f(y)| \leq \eta \|x - y\|, \quad (3.58)$$

for all  $x, y \in X$ .

Lemma (Isoperimetric inequality for the sphere)

Let  $A \subset S^{(2n-1)}$  be a closed subset of the sphere, and let  $B := B(a, r) \subset S^{(2n-1)}$  be a spherical cap around any point  $a \in S^{(2n-1)}$ , where the radius  $r$  is chosen such that  $\mu(B) = \mu(A)$ . Then

$$\mu(N_\epsilon(A)) \geq \mu(N_\epsilon(B)).$$

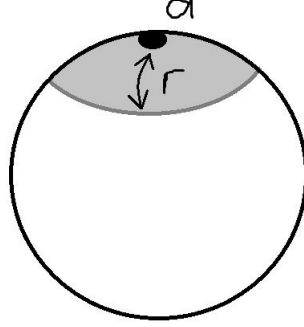


Figure 12: A sketch of a sphere with a spherical cap of radius  $r$ .

For this case, the metric measure space is  $X = S^{(2n-1)}$ , the  $(2n - 1)$  - dimensional sphere. The metric is  $d(x, y) = \arccos\langle x, y \rangle$ , where  $x, y \in S^{(2n-1)}$ , which is the angle between  $x$  and  $y$ . The concentration function for this sphere is

$$\begin{aligned} \alpha_X(\epsilon) &= \alpha_{S^{(2n-1)}}(\epsilon) = 1 - \inf\{\mu(N_\epsilon(S))\} \\ &= 1 - \mu(N_\epsilon(B(a, \frac{\pi}{2}))) \\ &= 1 - \mu(B(a, \frac{\pi}{2} + \epsilon)). \end{aligned}$$

We define  $A(r) := \mu(B(a, r))$ , the surface of the spherical cap, as

$$A(\phi) = \frac{1}{S_{2n-1}} \int_0^\phi \sin^{((2n-1)-1)}(\phi') d\phi', \quad (3.59)$$

where  $S_{2n-1} = \int_0^\pi \sin^{(2n-1)-1}(\phi') d\phi'$ . We could derive an explicit expression for  $\alpha_{S^{(2n-1)}}(\epsilon)$ , but the calculation is long and tedious. The full derivation can be found in [34]. We shall merely state the result:

$$\alpha_{S^{(2n-1)}}(\epsilon) \leq e^{-(2n-1)\frac{\epsilon^2}{2}}. \quad (3.60)$$

The important thing to notice here is that the concentration function is exponentially suppressed by the dimension of the sphere. If the dimension is large, then  $\alpha_{S^{(2n-1)}}(\epsilon)$  is small. We stated earlier that a small concentration function implies a strong concentration of measure.

Levy's Lemma

Let  $f : S^{(2n-1)} \rightarrow \mathbb{R}$  be a Lipschitz-continuous function with Lipschitz constant  $\eta$ , then by

choosing a random point  $x \in S^{(2n-1)}$  with respect to the uniform measure on the sphere, we have

$$\text{Prob}\{|f(x) - M_f| \geq \varepsilon\} \leq 2e^{-n\frac{\varepsilon^2}{\eta^2}}, \quad (3.61)$$

for all  $\varepsilon \geq 0$ .

Suppose we replace  $f(x)$  with the expectation value of an observable in some randomly chosen state in  $\mathcal{H}_E$ , and we replace  $M_f$  with the expectation value of the observable over the entire ensemble. Then we learn from Levy's lemma that for a high dimensional Hilbert space, it is highly unlikely to distinguish between the two values.

To see Levy's lemma in action, we must choose an ensemble that is approximated by typical states. This means that almost all states in the ensemble are typical. For a particular observable  $\mathcal{O}$ , two randomly chosen typical states in the ensemble, say  $|\psi\rangle$  and  $|\phi\rangle$ , will have

$$\langle\psi|\mathcal{O}|\psi\rangle \approx \langle\phi|\mathcal{O}|\phi\rangle. \quad (3.62)$$

If there exists a state in the ensemble, say  $|\chi\rangle$ , for which

$$\langle\chi|\mathcal{O}|\chi\rangle \neq \langle\psi|\mathcal{O}|\psi\rangle, \quad (3.63)$$

then the state  $|\chi\rangle$  is said to be atypical. However, Levy's lemma tells us that it is very rare to encounter atypical states.

One way of quantifying the rarity of atypical states is by calculating the relative entropy for different states in the ensemble. For instance, we can choose  $|\psi\rangle$  as a reference state. Then by creating a plot which shows the values of the relative entropy for all the states in the ensemble with respect to the reference state, we can count the number of atypical states. The relative entropy for typical states would be effectively zero, so we merely need to count the number of states which yield non-zero values for the relative entropy. We can then determine the probability of finding an atypical state within the ensemble.

In the next chapter, we shall look at ways in which we can apply Levy's lemma to a simple quantum system.

## 4 Quantum Typicality in Simple Quantum Systems

In this chapter, we shall use a simple quantum mechanical model to study quantum typicality. Mathematically, we shall make use of tools from mathematical statistics, namely Chebyshev's inequality and Levy's lemma. By studying the microstates of a simple quantum model, we hope to deduce some universal properties of microstates, with the intention of applying these ideas to the study of black hole microstates.

We shall begin by discussing some important results from mathematical statistics and measure theory. [35]

*Chebyshev's Inequality.* Let  $X$  be a random variable with mean  $\mu$  and variance  $\sigma^2$ . Then, for any  $\varepsilon > 0$ ,

$$P(|X - \mu| > \varepsilon) \leq \frac{\sigma^2}{\varepsilon^2}. \quad (4.1)$$

Chebyshev's inequality tells us that the probability of the value of a random variable of a population to significantly deviate from the mean value of the population is highly unlikely.

*Law of Large Numbers.* Let  $X_1, X_2, \dots, X_i, \dots$  be a sequence of independent random variables with  $\langle X_i \rangle = \mu$  and  $\text{Var}(X_i) = \sigma^2$ . Let  $\bar{X}_n = \frac{1}{n} \sum_{i=1}^n X_i$ . Then, for any  $\varepsilon > 0$ ,

$$P(|\bar{X}_n - \mu| > \varepsilon) \rightarrow 0 \quad \text{as } n \rightarrow \infty. \quad (4.2)$$

The law of large numbers is also commonly referred to as the law of averages. It tells us that given large enough trials, the events will occur with equal probability.

Let  $\mathcal{H}_E \subset \mathcal{H}$  be the Hilbert space consisting of all pure states  $\psi = |\psi\rangle\langle\psi|$  that live in the microcanonical ensemble of energy  $[E - \delta E, E + \delta E]$ . We consider large energies, such that  $\delta E \ll E$ . We shall work with a Hamiltonian which has a non-degenerate spectrum. Since the spectrum is non-degenerate, the dimension of this Hilbert space, denoted  $d_E$ , is the number of states that live in the energy range.

For our purposes, we shall treat  $\langle\psi_i| A |\psi_i\rangle$  as a random variable  $X_i$ , where  $A$  is an observable. Our goal is to identify the conditions that the set of observables  $\mathcal{A}$  must satisfy such that a random pure state  $\psi \in \mathcal{H}_E$  can be distinguished from the maximally mixed state in  $\mathcal{H}_E$ . We know that in the microcanonical formalism, all microscopic configurations of a thermodynamic system have equal likelihood of occurring. Since the number of states in  $\mathcal{H}_E$  is  $d_E$ , the maximally mixed state is

$$\Omega_E = \frac{1}{d_E} \mathbb{I} = \frac{1}{d_E} \sum_i |\psi_i\rangle\langle\psi_i|, \quad (4.3)$$

where  $\mathbb{I}$  is the identity matrix in  $\mathcal{H}_E$ , and  $|\psi_i\rangle \in \mathcal{H}_E$ . In the context of studying pure states in the microcanonical ensemble, a maximally mixed state is also maximally entangled. It is important to note that this is not true in general: maximally mixed does *not* imply maximally entangled!

We can construct a density matrix out of the pure states  $|\psi\rangle \in \mathcal{H}_E$ , i.e.  $\hat{\rho} = |\psi\rangle\langle\psi|$ . We can define an operator  $\hat{A}$  as

$$\hat{A} = A\hat{\rho} = \begin{pmatrix} A|\psi_1\rangle\langle\psi_1| & A|\psi_2\rangle\langle\psi_1| & \cdots & A|\psi_n\rangle\langle\psi_1| \\ A|\psi_1\rangle\langle\psi_2| & A|\psi_2\rangle\langle\psi_2| & \cdots & A|\psi_n\rangle\langle\psi_2| \\ \vdots & \vdots & \ddots & \vdots \\ A|\psi_1\rangle\langle\psi_n| & A|\psi_2\rangle\langle\psi_n| & \cdots & A|\psi_n\rangle\langle\psi_n| \end{pmatrix}. \quad (4.4)$$

Let  $\psi \in \mathcal{H}_E$  be a random pure state. Then, since  $X_\psi = \langle\psi|A|\psi\rangle$  is the random variable distributed over  $\mathcal{H}_E$ , its average value  $\langle A \rangle_E$  is

$$\langle A \rangle_E = \frac{1}{d_E} \text{Tr} A = \text{Tr}(A\Omega_E), \quad (4.5)$$

where  $\Omega_E = \frac{1}{d_E}\mathbb{I}$  is the maximally mixed state. The quantity  $\langle A \rangle_E$  is the average over the expectation values of the observable  $A$  for every state in the ensemble. We shall refer to it as the ensemble average.

For the random variable, the variance is

$$\sigma_A^2 \equiv \langle (\langle\psi|A|\psi\rangle - \langle A \rangle_E)^2 \rangle_\psi = \frac{1}{d_E + 1} \left( \frac{1}{d_E} \text{Tr}(A^2) - \left( \frac{\text{Tr}(A)}{d_E} \right)^2 \right). \quad (4.6)$$

This is the variance over the entire ensemble. We see that it is inversely proportional to the dimension of the ensemble.

Now we can apply Chebyshev's inequality,

$$\text{Prob}(|\langle\psi|A|\psi\rangle - \text{Tr}(A\Omega_E)| \geq \varepsilon) \leq \frac{\sigma_A^2}{\varepsilon^2}. \quad (4.7)$$

In this context, Chebyshev's inequality says that it is not likely to find a state in the ensemble whose expectation value of the observable  $A$  deviates significantly from the ensemble average. The larger the deviation, the more unlikely it is to find such a state. Let us now discuss Levy's lemma, which is a stronger result than Chebyshev's inequality.

By considering a subspace  $\mathcal{H}_E$  of a large Hilbert space, we can treat a random pure state  $\psi \in \mathcal{H}_E$  as a random point on a sphere of dimension  $d = 2d_E - 1$ . Levy's lemma allows us to apply these ideas to expectation values, i.e. functions over this sphere. We discussed Levy's lemma in the previous chapter. However, we shall state it again within this context.

#### Levy's Lemma

Let  $f(\psi)$  be a bounded function defined over the set of pure states  $\psi \in \mathcal{H}_E$ . Then for any random state  $\psi$  and  $\varepsilon > 0$ , we have

$$\text{Prob}(|f(\psi) - \langle f(\psi) \rangle_\psi| \geq \varepsilon) \leq 2e^{-4cd_E\varepsilon^2/\lambda^2}, \quad (4.8)$$

where  $c = \frac{1}{18\pi^3}$ ,  $d_E$  is the dimension of  $\mathcal{H}_E$ , and  $\lambda = \sup|\nabla f|$  is the Lipschitz constant of the function  $f(\psi)$ .

Let's apply these ideas to the ensemble average. For the ensemble average, the uniform probability distribution is indeed the normalised measure over the sphere which describes the microstates in our microcanonical ensemble  $\mathcal{H}_E$ . This means that the expectation values can be described as functions over the sphere, i.e.  $f(\psi) = \langle \psi | A | \psi \rangle$ , with  $\langle f(\psi) \rangle_\psi = \text{Tr}(A\Omega_E)$  being the ensemble average. It was proved in [37] that

$$\lambda = \sup |\nabla \langle \psi | A | \psi \rangle| \leq 2\|A\|. \quad (4.9)$$

We learn from this that unless the largest eigenvalue of  $A$  scales like  $\sqrt{d_E}$ , the probability of a random pure state deviating from the mean of the ensemble is suppressed exponentially in  $d_E$ .

These results generalise to time averages as well [2]. The time dependent wave function is

$$\psi_n(x, t) = \psi_n(x)e^{-iE_n t}, \quad (4.10)$$

where  $\hbar = 1$ . By taking the square of the modulus, the time dependence disappears. When dealing with time averages, our goal is to determine the probability of a given state differing from its equilibrium configuration at a given instant in time. Consider a general pure state  $|\psi\rangle \in \mathcal{H}_E$ . At an initial time  $t = 0$ , we can expand our pure state in its energy eigenbasis, i.e.

$$|\psi(0)\rangle = \sum_E c_E |E\rangle, \quad (4.11)$$

where  $\sum_E |c_E|^2 = 1$ . At a time  $t$ , using the time independent Schrödinger equation for a time independent Hamiltonian, the state will evolve to

$$|\psi(t)\rangle = \sum_E c_E e^{-iEt} |E\rangle. \quad (4.12)$$

The time average is defined as

$$\omega_\psi \equiv \langle \psi(t) \rangle_t = \lim_{T \rightarrow \infty} \frac{1}{T} \int_0^T |\psi(t)\rangle \langle \psi(t)| dt = \sum_E |c_E|^2 |E\rangle \langle E|. \quad (4.13)$$

For an observable  $A$ , the time averaged expectation value is given by

$$\langle A \rangle_t = \lim_{T \rightarrow \infty} \frac{1}{T} \int_0^T \langle \psi(t) | A | \psi(t) \rangle dt = \sum_E |c_E|^2 \langle E | A | E \rangle = \text{Tr}(A\omega_\psi). \quad (4.14)$$

When averaging over time, dephasing occurs. This dephasing allows us to set to zero all the off-diagonal elements in the density matrix,  $\hat{\rho}(t) = |\psi(t)\rangle \langle \psi(t)|$ , in the energy eigenbasis. Since the Hamiltonian we shall be considering in the next section has no explicit time dependence, we need not devote too much study to time averages. The important thing to note is that the typicality arguments apply to both ensemble averages as well as time averages [2]. Let us now move on to applying these ideas to actual quantum systems.

## 4.1 Quantum Models

We wish to find a simple quantum model that has certain properties. These properties are:

- (i) It must have non-degenerate energy gaps.
- (ii) The energy level spacing must not be constant as the state number increases.
- (iii) The expectation values of a particular observable for two distinct states, corresponding to energy eigenvalues in a narrow window of energy, must be indistinguishable to a classical observer. (By classical observer, we mean an observer without access to a measuring device which has Planck-scale precision).

The first system that comes to mind is the simple harmonic oscillator, which has the following Hamiltonian,

$$\hat{H} = \frac{\hat{p}^2}{2m} + \frac{m\omega^2}{2}\hat{x}^2. \quad (4.15)$$

However, it fails to meet all of the above criteria. Its energy spectrum is given by

$$E_n = \left(n + \frac{1}{2}\right) \hbar\omega. \quad (4.16)$$

The spacing between consecutive energy levels is constant, it doesn't decrease with increasing state number. We see this by

$$\begin{aligned} E_{n+1} - E_n &= \left(n + 1 + \frac{1}{2}\right) \hbar\omega - \left(n + \frac{1}{2}\right) \hbar\omega \\ &= \hbar\omega, \end{aligned}$$

which has no  $n$  dependence, i.e. the energy level spacing is constant.

We could try perturbing the system with a quartic potential of the form  $V = \gamma x^4$ , where  $\gamma$  is some constant. Using the ladder operator method, we can determine the perturbative contribution to the energy spectrum.

The creation and annihilation operators for the simple harmonic oscillator are defined as

$$\hat{a}^\dagger \equiv \sqrt{\frac{m\omega}{2\hbar}}\hat{x} - \frac{i}{\sqrt{2m\omega\hbar}}\hat{p}; \quad \hat{a} \equiv \sqrt{\frac{m\omega}{2\hbar}}\hat{x} + \frac{i}{\sqrt{2m\omega\hbar}}\hat{p}, \quad (4.17)$$

and they satisfy the following identities:

$$\hat{a}|n\rangle = \sqrt{n}|n-1\rangle; \quad \hat{a}^\dagger|n\rangle = \sqrt{n+1}|n+1\rangle. \quad (4.18)$$

From the definitions above, we can express  $\hat{x}$  as

$$\hat{x} = \sqrt{\frac{\hbar}{2m\omega}}(\hat{a} + \hat{a}^\dagger). \quad (4.19)$$

Now we can derive an expression for the energy spectrum due to the perturbation,

$$\begin{aligned}\Delta E_n &= \gamma \langle n | \Delta \hat{x}^4 | n \rangle \\ &= \gamma \left( \frac{\hbar}{2m\omega} \right)^2 \langle n | (\hat{a} + \hat{a}^\dagger)^4 | n \rangle \\ &= 3\gamma \left( \frac{\hbar}{2m\omega} \right)^2 (2n^2 + 2n + 1).\end{aligned}$$

Thus, the eigenvalues for this perturbed system are

$$E_n = \left( n + \frac{1}{2} \right) \hbar\omega + 3\gamma \left( \frac{\hbar}{2m\omega} \right)^2 (2n^2 + 2n + 1). \quad (4.20)$$

This spectrum is ideal for our purposes, since we can observe the spacing between successive energy levels,

$$\begin{aligned}E_{n+1} - E_n &= \left( n + 1 + \frac{1}{2} \right) \hbar\omega + 3\gamma \left( \frac{\hbar}{2m\omega} \right)^2 (2(n+1)^2 + 2(n+1) + 1) - \dots \\ &\dots - \left( n + \frac{1}{2} \right) \hbar\omega - 3\gamma \left( \frac{\hbar}{2m\omega} \right)^2 (2n^2 + 2n + 1) \\ &= \hbar\omega + 3\gamma \left( \frac{\hbar}{2m\omega} \right)^2 (4n + 4) \\ &= \hbar\omega + 12\gamma \left( \frac{\hbar}{2m\omega} \right)^2 (n + 1),\end{aligned}$$

which has an  $n$  dependence. The Schrödinger equation for this system is

$$-\frac{\hbar^2}{2m} \frac{\partial^2 \psi(x)}{\partial x^2} + \frac{1}{2} \omega^2 m x^2 \psi(x) + \gamma x^4 \psi(x) = E \psi(x), \quad (4.21)$$

which cannot be solved analytically. This is not in our best interest, since we would profit from a setup in which we have an analytic expression for the wave function,  $\psi(x)$ .

Before we move on to explicitly show the results for the models we considered. It might be useful to mention that not all quantum systems with a non-degenerate, unequally spaced energy spectrum works. As will be explicitly shown with the Morse potential, some models fail to exhibit typicality. We hypothesise that this failure to exhibit typicality is associated with wave functions which consist of orthogonal polynomials.

#### 4.1.1 Infinite Potential Well

Since the simple harmonic oscillator fails to meet the desired criteria, and adding a perturbation provides us with an unsolvable differential equation, it appears as though we have to

settle for arguably the simplest quantum system known to physics: the particle in an infinite potential well. This system is governed by the potential described by

$$V(x) = \begin{cases} +\infty & \text{if } x < -\frac{L}{2}, \\ 0 & \text{if } -\frac{L}{2} \leq x \leq \frac{L}{2}, \\ +\infty & \text{if } x > \frac{L}{2}. \end{cases}$$

where the length of the well is  $L$ .

The energy spectrum is

$$E_n = \frac{\hbar^2 \pi^2}{2mL^2} n^2, \quad (4.22)$$

and the state number as a function of the energy is

$$n(E) = \sqrt{\frac{2mL^2 E}{\hbar^2 \pi^2}}. \quad (4.23)$$

For convenience, let us set  $\frac{\hbar^2 \pi^2}{2m} = 1$ , so that equations (4.22) and (4.23) become

$$E_n = \frac{n^2}{L^2} \quad (4.24)$$

and

$$n(E) = L\sqrt{E} \quad (4.25)$$

respectively.

The wave function for this system is

$$\psi_n(x) = \sqrt{\frac{2}{L}} \sin \left[ \frac{\pi n}{L} \left( x + \frac{L}{2} \right) \right] = \begin{cases} \sqrt{\frac{2}{L}} \cos \left( \frac{\pi n}{L} x \right) & \text{for } n = 1, 3, 5, \dots \\ \sqrt{\frac{2}{L}} \sin \left( \frac{\pi n}{L} x \right) & \text{for } n = 2, 4, 6, \dots \end{cases} \quad (4.26)$$

The number of states in  $\mathcal{H}_E$  can be calculated using (4.25). We have

$$\begin{aligned} d_E &= n(E + \delta E) - n(E - \delta E) \\ &= L \left( \sqrt{E + \delta E} - \sqrt{E - \delta E} \right) \\ &= L \left( \sqrt{E \left( 1 + \frac{\delta E}{E} \right)} - \sqrt{E \left( 1 - \frac{\delta E}{E} \right)} \right) \\ &\approx L\sqrt{E} \left[ \left( 1 + \frac{\delta E}{2E} \right) - \left( 1 - \frac{\delta E}{2E} \right) \right] \\ &= L\sqrt{E} \frac{\delta E}{E}. \end{aligned}$$

The number of states within the narrow energy range is

$$d_E \approx \frac{L}{\sqrt{E}} \delta E. \quad (4.27)$$

Since  $\delta E \ll E$ , if we want the number of states to be large, we need to make the size of the well,  $L$ , large.

Let  $\mathcal{A} = \{A^i\}$  be a set of observables, where  $i = 1, 2, \dots, N(A)$ .  $N(A)$  is the number of possible outcomes after performing a measurement on the observable  $A$ . The observables we will be studying are the moments of the probability distribution. The  $k^{\text{th}}$  moment is denoted  $\langle \psi | x^k | \psi \rangle$ , where  $k = 1, 2, \dots, K$ . This means that the size, or cardinality, of the set  $\mathcal{A}$  is  $K$ , i.e.  $N(\mathcal{A}) = K$ .

Since the spectrum is non-degenerate, there is only one outcome for every measurement of the observable  $A$  for every individual state in  $\mathcal{H}_E$ . There are  $d_E$  states in  $\mathcal{H}_E$ , thus  $N(\mathcal{A}) = K d_E$ .

Using integration by parts repeatedly, we found it possible to derive an analytic expression for the  $k^{\text{th}}$  moment of the  $n^{\text{th}}$  state. We have

$$\begin{aligned} \langle \psi_n | x^k | \psi_n \rangle &= \frac{L^k}{2^{k+1}(k+1)} (1 - (-1)^{k+1}) \pm \\ &\frac{L^k}{\pi^{k+1}} \sum_{m=0}^k (-1)^m \frac{(k)_{2m+1}}{(2n)^{2m+2}} \left(\frac{\pi}{2}\right)^{k-2m-1} (-1)^n (1 - (-1)^{k-2m-1}), \end{aligned} \quad (4.28)$$

where  $(k)_m = k(k-1)(k-2) \dots (k-m+1)$  is the Pochhammer symbol. It is also denoted  $k^{\underline{m}}$ . The  $\pm$  in equation (4.28) corresponds to the odd/even states. For odd states, we add; for even states, we subtract.

We can be more concise, and write

$$\langle \psi_n | x^k | \psi_n \rangle = \begin{cases} 0 & \text{for odd } k, \\ \frac{L^k}{2^{k+1}(k+1)} \pm \frac{L^k}{\pi^{k+1}} \sum_{m=0}^k (-1)^m \frac{(k)_{2m+1}}{(2n)^{2m+2}} \left(\frac{\pi}{2}\right)^{k-2m-1} (-1)^n & \text{for even } k. \end{cases} \quad (4.29)$$

By considering a large energy,  $E$ , we know that the state numbers,  $n$ , are also large. In the case where  $k \ll n$  (we need not consider large values for  $k$ ), we see that

$$\lim_{n \rightarrow \infty} \langle \psi_n | x^k | \psi_n \rangle = \begin{cases} 0 & \text{for odd } k, \\ \frac{L^k}{2^{k+1}(k+1)} & \text{for even } k. \end{cases} \quad (4.30)$$

This means that for large  $n$ , the expectation value for a given observable,  $A$ , converges to a constant value. In such a scenario, it will be very difficult for an observer to know which state he/she is in, based on the outcome of a measurement made on the observable  $A$ .

Furthermore, in the limit of large  $n$ , we notice that the difference between the values for the  $k^{\text{th}}$  moment of two adjacent states tends to zero, i.e.

$$\lim_{n \rightarrow \infty} (\langle \psi_n | x^k | \psi_n \rangle - \langle \psi_{n-1} | x^k | \psi_{n-1} \rangle) = 0. \quad (4.31)$$

For practical purposes, working with the moments turns out to be rather inconvenient. In integral form, the  $k^{\text{th}}$  moment of the  $n^{\text{th}}$  state is given by

$$\int_{-L/2}^{L/2} dx x^k |\psi_n(x)|^2. \quad (4.32)$$

The wave function is normalised, i.e.  $\int_{-L/2}^{L/2} dx |\psi_n(x)|^2 = 1$ . This means that the values for the moments scale like  $\lambda^k$ , for some number  $\lambda$ . This poses many problems, since we have to deal with very large numbers. For this reason, we shall not study the raw moments of the wave function, but rather the standardised moments. Before we can define the standardised moments, we need to first define the mean, standard deviation, and centralised moments. [35]

The mean of the probability distribution is defined by

$$\mu = \int_{-L/2}^{L/2} dx x |\psi_n(x)|^2. \quad (4.33)$$

It is merely the first moment of the probability distribution. For the particle in an infinite potential well, the mean is given by

$$\mu = \frac{2}{L} \int_{-L/2}^{L/2} dx x \sin^2 \left( \frac{\pi n}{L} x \right) = 0. \quad (4.34)$$

The standard deviation of the probability distribution is defined as

$$\sigma = \sqrt{\int_{-L/2}^{L/2} dx (x - \mu)^2 |\psi_n(x)|^2}, \quad (4.35)$$

which is the square root of the variance. For our system the variance is

$$\sigma^2 = \frac{2}{L} \int_{-L/2}^{L/2} dx x^2 \sin^2 \left( \frac{\pi n}{L} x \right) - \mu^2 = \left( \frac{1}{24} \pm \frac{(-1)^n}{(2\pi n)^2} \right) L^2, \quad (4.36)$$

and thus the standard deviation is

$$\sigma = \sqrt{\frac{1}{24} \pm \frac{(-1)^n}{(2\pi n)^2}} L. \quad (4.37)$$

(Note that for large  $n$ ,  $\sigma \rightarrow \frac{L}{2\sqrt{6}}$ ).

The  $k^{\text{th}}$  centralised moment of the  $n^{\text{th}}$  state is given by

$$\int_{-L/2}^{L/2} dx (x - \mu)^k |\psi_n(x)|^2. \quad (4.38)$$

The centralised moment is merely the moment about the mean. Finally, we can define the standardised moments. The  $k^{\text{th}}$  standardised moment is the ratio between the  $k^{\text{th}}$  centralised moment and the standard deviation raised to the  $k^{\text{th}}$  power, i.e.

$$\frac{1}{\sigma^k} \int_{-L/2}^{L/2} dx (x - \mu)^k |\psi_n(x)|^2. \quad (4.39)$$

Let us plot the raw moments and standardised moments on the same graph to see how they differ graphically. Let us use the fourth moment and the third state, with  $L = 10$ :

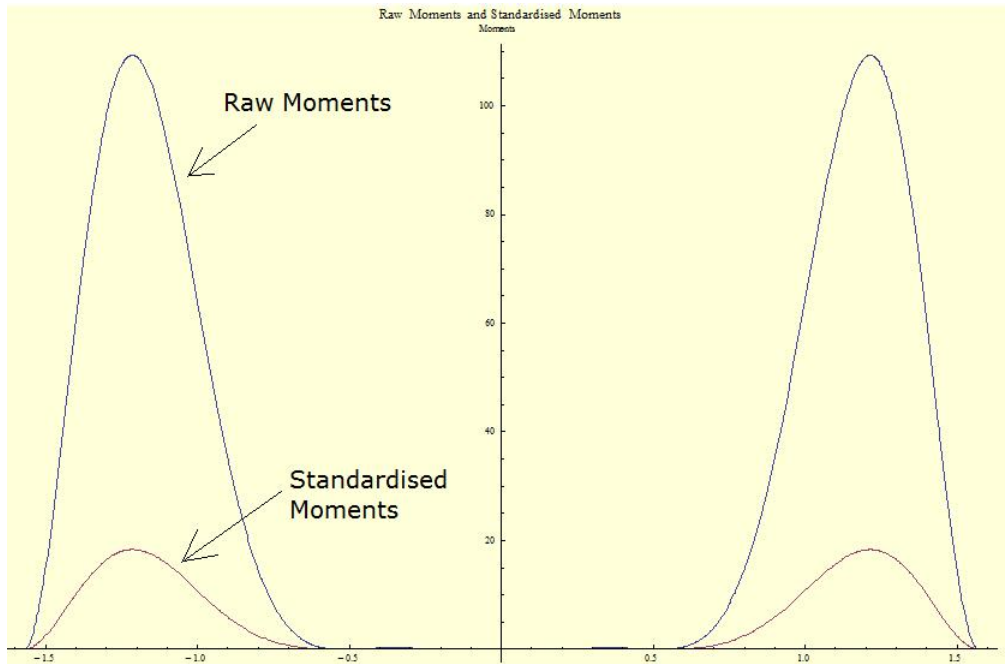


Figure 13: A plot showing the difference between raw moments and standardised moments for the third state and fourth moment, with  $L = 10$ .

We see from figure 13 that the standardised moments are scaled down by a certain factor.

For the particle in an infinite potential well, we need to evaluate the integral

$$\frac{2}{\sigma^k L} \int_{-L/2}^{L/2} dx (x - \mu)^k \sin^2 \left( \frac{n\pi x}{L} \right). \quad (4.40)$$

We can use the binomial theorem to derive an expression for equation (4.40). We have

$$\frac{2}{\sigma^k L} \int_{-L/2}^{L/2} dx (x-\mu)^k \sin^2\left(\frac{n\pi x}{L}\right) = \begin{cases} 0 & \text{for odd } k-j, \\ \frac{2}{\sigma^k L} \sum_{j=0}^k \binom{k}{j} (-\mu)^j \left[ \frac{L^{k-j}}{2^{k-j+1}(k-j+1)} \pm \dots \right] & \text{for even } k-j \\ \left[ \dots \frac{L^{k-j}}{\pi^{k-j+1}} \sum_{m=0}^{k-j} (-1)^m \frac{(k-j)_{2m+1}}{(2n)^{2m+2}} \left(\frac{\pi}{2}\right)^{k-j-2m-1} (-1)^n \right]. & \end{cases} \quad (4.41)$$

In the limit of large  $n$ , we have

$$\frac{1}{\sigma^k} \lim_{n \rightarrow \infty} \langle \psi_n | (x-\mu)^k | \psi_n \rangle = \frac{2}{\sigma^k L} \sum_{j=0}^k \binom{k}{j} (-\mu)^j \frac{L^{k-j}}{2^{k-j+1}(k-j+1)}. \quad (4.42)$$

We see that for a given value of  $L$  and  $k$ , the standardised moments of the wave function converges to a constant value which is independent of the state. This constant value happens to be smaller than the one we got from considering the raw moments. However, due to the presence of the  $(-\mu)^j$  term, we pick up negative values for every alternate term. This is not a problem. When we perform the numerical calculations, we shall merely take the absolute values. This way, we can avoid having negative values.

Now let us calculate the ensemble average for the moments. In the previous section, we spoke about the ensemble average in the context of matrices. It is not necessary to use matrices for now, since we are dealing with pure states. In the microcanonical ensemble, we know that every microstate has an equal probability of being realised. This probability is simply the inverse of the dimension of the space in question, i.e.  $\frac{1}{d_E}$ . To calculate the ensemble average for the observable  $A$ , we shall sum over the expectation values for  $A$  in every single state in the ensemble, and then divide by the number of states in the ensemble. So we have

$$\langle A \rangle_{\text{ens}} = \frac{1}{d_E} \sum_{k=n_1}^{n_{d_E}} \langle \psi_k | A | \psi_k \rangle. \quad (4.43)$$

Furthermore, we can also calculate the variance of the ensemble for the observable  $A$ , i.e.

$$\sigma^2(A)_{\text{ens}} = \frac{1}{d_E} \sum_{k=n_1}^{n_{d_E}} \langle \psi_k | A^2 | \psi_k \rangle - \langle A \rangle_{\text{ens}}^2. \quad (4.44)$$

If  $A = x^k$  for  $k \in \mathbb{Z}^+$ , we can derive explicit formulae for the ensemble average and the ensemble variance in the limit of large energies. By using equation (4.30), and noting that the values are independent of the state, we have

$$\langle x^k \rangle_{\text{ens}} = \frac{1}{d_E} \sum_{m=n_1}^{n_{d_E}} \langle \psi_m | x^k | \psi_m \rangle = \frac{L^k}{2^{k+2}(k+1)}, \quad (4.45)$$

and

$$\begin{aligned}
\sigma^2(x^k)_{\text{ens}} &= \frac{1}{d_E} \sum_{m=n_1}^{n_{d_E}} \langle \psi_m | x^{2k} | \psi_m \rangle - \langle x^k \rangle_{\text{ens}}^2 \\
&= \frac{1}{d_E} \sum_{m=n_1}^{n_{d_E}} \left( \frac{L^{2k}}{2^{2k+2}(2k+1)} \right) - \left( \frac{L^k}{2^{k+2}(k+1)} \right)^2 \\
&= \left( \frac{L}{2} \right)^2 \left[ \frac{1}{2^{k+1}(2k+1)} - \frac{1}{2^{k+1}(k+1)^2} \right].
\end{aligned} \tag{4.46}$$

According to [38], a good way to quantify the differences between states in the ensemble of microstates in response to the observable is by calculating to ratio between the standard deviation and the mean. This is known as the coefficient of variation [35]. It describes how “varied” the distribution is. This is useful for us, since quantum typicality implies that the “overwhelming majority” of states in an ensemble behave a certain way. For the infinite well, the coefficient of variation is

$$C_V = \frac{\sigma(x^k)_{\text{ens}}}{\langle x^k \rangle_{\text{ens}}} = \sqrt{\frac{2^{k+1}(k+1)^2}{2k+1}} - 2. \tag{4.47}$$

For sufficiently large energies, the values for the  $k^{\text{th}}$  moment all converge to a number which is independent of the state itself. This allows us to construct a set of the form [37]

$$M_E := \{ |\psi\rangle \in \mathcal{H}_E \mid \langle \psi_n | A | \psi_n \rangle = a \}. \tag{4.48}$$

The set  $M_E \subseteq \mathcal{H}_E \subset \mathcal{H}$  contains all the wave functions of the different states which yield the same expectation value for the observable  $A$ . In our case, the expectation value for the observable  $A$  is merely the  $k^{\text{th}}$  moment. We can perform a coarse-graining over the microstates of this set. Additionally, by choosing different observables, we can construct different sets of this form. If we average over all of the expectation values in  $M_E$ , we shall find that the ensemble average is merely equal to  $a$ , which is the expectation value of the observable  $A$  for every individual state in  $M_E$ . This means that the ensemble average, which is effectively a macrostate of the system, is exactly equal to the individual microstates of the system.

For such a case, Chebyshev’s inequality and Levy’s lemma are trivially satisfied. Let us define a quantity  $\text{Dev}(n)$ , which we shall call the deviation of the  $n^{\text{th}}$  state. We define this quantity as the absolute difference between the expectation value of an observable in the  $n^{\text{th}}$  state and the ensemble average, i.e.

$$\text{Dev}(n) = | \langle \psi_n | A | \psi_n \rangle - \langle A \rangle_{\text{ens}} |. \tag{4.49}$$

Using equations (4.28) and (4.30), and remembering that the observable  $A$  is  $x^k$ , we have

$$\lim_{n \rightarrow \infty} \text{Dev}(n) = \left| \frac{\pi L^{k-1}}{k+1} - \frac{\pi L^{k-1}}{k+1} \right| = 0. \tag{4.50}$$

For large energies, there is no deviation from the ensemble average for any of the states in the ensemble. This means that the probability of finding a state which deviates from the ensemble average is zero. Thus, both Chebyshev's inequality and Levy's lemma are satisfied. We therefore conclude that all the states within the ensemble behave typically.

In concluding this subsection, let us look at a numerical example of what we discussed above.

For this numerical example, we shall choose  $L = 10^4$ ,  $E = 10^4$ , and  $\delta E = 10$ . From equation (4.27), this means that our ensemble consists of  $d_E = 1000$  pure states. The lowest state in this ensemble is  $n_{\min} = 999500$ , and the largest state in this ensemble is  $n_{\max} = 1000500$ . We shall pick three representatives from this ensemble. We shall choose  $n_1 = 999750$ ,  $n_2 = 1000001$ , and  $n_3 = 1000250$ . Using Mathematica, we shall calculate the first ten standardised moments.

$k$	$n_1$	$n_2$	$n_3$
1	0	0	0
2	3183	3183	3183
3	0	0	0
4	$1.824 \times 10^7$	$1.824 \times 10^7$	$1.824 \times 10^7$
5	0	0	0
6	$1.244 \times 10^{11}$	$1.244 \times 10^{11}$	$1.244 \times 10^{11}$
7	0	0	0
8	$9.239 \times 10^{14}$	$9.239 \times 10^{14}$	$9.239 \times 10^{14}$
9	0	0	0
10	$7.219 \times 10^{18}$	$7.219 \times 10^{18}$	$7.219 \times 10^{18}$

Table 2: Numerical values for the first 10 moments of 3 states chosen arbitrarily from an ensemble.

By analysing table 2 above, we see that the moments are the same for the three states, even though the states are quite distinct. Furthermore, the values for the respective moments are exactly equal to  $\left| \frac{2}{\sigma^k L} \sum_{j=0}^k \binom{k}{j} (-\mu)^j \frac{L^{k-j}}{2^{k-j+1} (k-j+1)} \right|$ , which validates equation (4.43).

The particle in an infinite well is a very convenient model to study, since it trivially satisfies Levy's lemma. Let us now take a look at the quantum system involving a particle confined to a finite well of length  $2L$ .

### 4.1.2 Finite Potential Well

Let us consider the case in which a particle is confined to a finite well, where the potential is given by

$$V(x) = \begin{cases} 0 & \text{if } x < -L, \\ -V_0 & \text{if } -L \leq x \leq L, \\ 0 & \text{if } x > L, \end{cases}$$

and the length of the well is  $2L$ .

We shall consider only the bound states, i.e. where  $E < 0$ . The wave function for this system is given by

$$\psi_n(x) = \begin{cases} \sqrt{\frac{\kappa_n}{1+\kappa_n L}} (\cos(l_n L) - \sin(l_n L)) e^{\kappa_n(x+L)} & \text{for } x < -L, \\ \frac{1}{\sqrt{2}} \sqrt{\frac{\kappa_n}{1+\kappa_n L}} (\sin(l_n x) + \cos(l_n x)) & \text{for } -L \leq x \leq L, \\ \sqrt{\frac{\kappa_n}{1+\kappa_n L}} (\sin(l_n L) + \cos(l_n L)) e^{\kappa_n(L-x)} & \text{for } x > L, \end{cases} \quad (4.51)$$

where  $\kappa_n \equiv \frac{\sqrt{-2mE_n}}{\hbar}$ , and  $l_n \equiv \frac{\sqrt{2m(E_n+V_0)}}{\hbar}$ . To determine the eigenvalues, we need to solve the following transcendental equation,

$$\tan\left(\frac{L\sqrt{2m(E+V_0)}}{\hbar}\right) = \sqrt{\frac{V_0}{E+V_0}} - 1. \quad (4.52)$$

This equation cannot be solved analytically, only graphically and numerically. We can use Mathematica to find the eigenvalues. Since the system is non-degenerate, every individual energy eigenvalue will correspond to an individual state. Once we have a list of the energy eigenvalues, we can determine  $\kappa_n$  and  $l_n$ , thus allowing us to explicitly calculate the moments of the wave function.

The  $k^{\text{th}}$  moment of the  $n^{\text{th}}$  state is given by

$$\begin{aligned} \int_{-\infty}^{\infty} x^k |\psi_n(x)|^2 dx &= \int_{-\infty}^{-L} x^k |\psi_n(x)|^2 dx + \int_{-L}^L x^k |\psi_n(x)|^2 dx + \int_L^{\infty} x^k |\psi_n(x)|^2 dx \\ &= \frac{\kappa_n}{1+\kappa_n L} (\cos(l_n L) - \sin(l_n L))^2 e^{2\kappa_n L} \int_{-\infty}^{-L} x^k e^{2\kappa_n x} dx + \dots \\ &\dots + \frac{1}{2} \frac{\kappa_n}{1+\kappa_n L} \int_{-L}^L x^k (\sin(l_n x) + \cos(l_n x))^2 dx + \dots \\ &\dots + \frac{\kappa_n}{1+\kappa_n L} (\cos(l_n L) + \sin(l_n L))^2 e^{2\kappa_n L} \int_L^{\infty} x^k e^{-2\kappa_n x} dx. \end{aligned} \quad (4.53)$$

We can use the well known trigonometric identities to help us simplify the above expression,

i.e.

$$\begin{aligned}
\int_{-\infty}^{\infty} x^k |\psi_n(x)|^2 dx &= \frac{\kappa_n}{1 + \kappa_n L} (1 - \sin(2l_n L)) e^{2\kappa_n L} \int_{-\infty}^{-L} x^k e^{2\kappa_n x} dx + \dots \\
&\dots + \frac{1}{2} \frac{\kappa_n}{1 + \kappa_n L} \int_{-L}^L x^k (1 + \sin(2l_n x)) dx + \dots \\
&\dots + \frac{\kappa_n}{1 + \kappa_n L} (1 + \sin(2l_n L)) e^{2\kappa_n L} \int_L^{\infty} x^k e^{-2\kappa_n x} dx.
\end{aligned} \tag{4.54}$$

In the above expression, we observe that there are some integrals which are not trivial to evaluate. Let us list these integrals,

$$I_1 = \int_{-\infty}^{-L} x^k e^{2\kappa_n x} dx, \tag{4.55}$$

$$I_2 = \int_L^{\infty} x^k e^{-2\kappa_n x} dx, \text{ and} \tag{4.56}$$

$$I_3 = \int_{-L}^L x^k \sin(2l_n x) dx. \tag{4.57}$$

Finding an analytic expression for these integrals can be achieved after integrating by parts repeatedly, and then finding a pattern. We will save the reader from having to read through the brutality of the process, and merely state the results. These are the results:

$$I_1 = \sum_{m=0}^k (-1)^k \frac{(k)_m L^{k-m}}{(2\kappa_n)^{m+1}} e^{-2\kappa_n L}, \tag{4.58}$$

$$I_2 = \sum_{m=0}^k \frac{(k)_m L^{k-m}}{(2\kappa_n)^{m+1}} e^{-2\kappa_n L}, \text{ and} \tag{4.59}$$

$$\begin{aligned}
I_3 &= \sum_{m=0}^k (-1)^{m+1} \frac{(k)_{2m}}{(2l_n)^{2m+1}} (L^{k-2m} \cos(2l_n L) - (-L)^{k-2m} \cos(-2l_n L)) + \dots \\
&\dots + \sum_{m=0}^k (-1)^{m+2} \frac{(k)_{2m+1}}{(2l_n)^{2m+2}} (L^{k-2j-1} \sin(2l_n L) - (-L)^{k-2m-1} \sin(-2l_n L)).
\end{aligned} \tag{4.60}$$

Now we can use these results in our expression for the moments of the wave function. We

get

$$\begin{aligned}
& \int_{-\infty}^{\infty} x^k |\psi_n(x)|^2 dx \\
&= \frac{\kappa_n}{1 + \kappa_n L} (1 - \sin(2l_n L)) \sum_{m=0}^k (-1)^m \frac{\binom{k}{m} L^{k-m}}{(2\kappa_n)^{m+1}} + \frac{1}{2} \frac{\kappa_n}{1 + \kappa_n L} (1 - (-1)^{k+1}) \frac{L^{k+1}}{k+1} + \dots \\
&\dots + \frac{1}{2} \frac{\kappa_n}{1 + \kappa_n L} \sum_{m=0}^k (-1)^{m+1} \frac{\binom{k}{2m}}{(2l_n)^{2m+1}} (L^{k-2m} \cos(2l_n L) - (-L)^{k-2m} \cos(-2l_n L)) + \dots \\
&\dots + \frac{1}{2} \frac{\kappa_n}{1 + \kappa_n L} \sum_{m=0}^k (-1)^{m+2} \frac{\binom{k}{2m+1}}{(2l_n)^{2m+2}} (L^{k-2m-1} \sin(2l_n L) - (-L)^{k-2m-1} \sin(-2l_n L)) + \dots \\
&\dots + \frac{\kappa_n}{1 + \kappa_n L} (1 + \sin(2l_n L)) \sum_{m=0}^k \frac{\binom{k}{m} L^{k-m}}{(2\kappa_n)^{m+1}}.
\end{aligned} \tag{4.61}$$

Our goal is to study the high energy limit. For large energies,  $\kappa_n$  gets larger, while  $l_n$  gets smaller. In this limit, our expression becomes

$$\begin{aligned}
& \int_{-\infty}^{\infty} x^k |\psi_n(x)|^2 dx \\
&\approx \frac{1}{2} \frac{L^k}{k+1} (1 - (-1)^{k+1}) + \dots \\
&\dots + \lim_{l_n \rightarrow 0} \frac{1}{2L} \sum_{m=0}^k (-1)^{m+1} \frac{\binom{k}{2m}}{(2l_n)^{2m+1}} (L^{k-2m} \cos(2l_n L) - (-L)^{k-2m} \cos(-2l_n L)) + \dots \\
&\dots + \lim_{l_n \rightarrow 0} \frac{1}{2L} \sum_{m=0}^k (-1)^{m+2} \frac{\binom{k}{2m+1}}{(2l_n)^{2m+2}} (L^{k-2m-1} \sin(2l_n L) - (-L)^{k-2m-1} \sin(-2l_n L))
\end{aligned} \tag{4.62}$$

The terms which contain  $l_n$  in the denominator become larger and larger until the maximum energy is reached. This differs significantly from the particle in an infinite potential well. In the infinite well case, we observed that the expectation values converged to a common value once a certain energy was reached. This allowed us to construct a set in which different states yield the same eigenvalues. In the finite well, different states always yield different eigenvalues. Our goal now is to see how “close” these different eigenvalues are for different states within the ensemble.

Let us look at a numerical example. For this numerical example, we shall choose  $L = 500$ ,  $V_0 = 500$ ,  $E = 495.0$ , and  $\delta E = 4.95$ . We do not know the exact relationship between the state number and the corresponding energy eigenvalue. To determine the eigenvalues, we have to numerically solve equation (4.53). Using Mathematica, we find that there is a total of

3559 pure states, and that our ensemble consists of  $d_E = 465$  pure states. The lowest state in this ensemble is  $n_{\min} = 3058$ , and the largest state in this ensemble is  $n_{\max} = 3523$ . We shall pick three states at random from this ensemble. We shall choose  $n_1 = 3184$  (corresponding to energy  $E_1 = 494.435$ ),  $n_2 = 3285$  (corresponding to energy  $E_2 = 497.004$ ), and  $n_3 = 3392$  (corresponding to energy  $E_3 = 498.893$ ). Using Mathematica, we shall calculate the first ten standardised moments for these states, just as we did with the infinite well.

$k$	$n_1$	$n_2$	$n_3$
1	$1.885 \times 10^{-16}$	$1.519 \times 10^{-17}$	$4.778 \times 10^{-17}$
2	1	1	1
3	$2.023 \times 10^{-16}$	$7.260 \times 10^{-17}$	$7.433 \times 10^{-17}$
4	1.8	1.8	1.799
5	$2.434 \times 10^{-15}$	$4.321 \times 10^{-16}$	$1.569 \times 10^{-17}$
6	3.857	3.858	3.857
7	$8.794 \times 10^{-16}$	$2.064 \times 10^{-15}$	$5.160 \times 10^{-16}$
8	8.999	9.003	8.999
9	$2.515 \times 10^{-14}$	$6.970 \times 10^{-16}$	$3.979 \times 10^{-15}$
10	22.091	22.099	22.089

Table 3: Numerical values for the first 10 moments of 3 states chosen arbitrarily from an ensemble. (Finite well.)

By analysing table 3 above, we see that the values for the moments of the three states are quite close. We would like to find a way to quantify this “closeness”. A measure of the “closeness” would allow us to quantify the level of uncertainty in the measurement. The level of uncertainty is related to the entropy.

In the previous chapter, we discussed distance measures between quantum states. These measures allow us to quantify the closeness between probability distributions (for pure states) and density operators (for mixed states). Those measures are not applicable in this case, since the moments are *not* probability distributions, i.e. they are not normalised to 1. Even if we plot all of the values for the moments on a single graph, we will not have a probability distribution. (We will have a distribution, but it would be divergent).

$k$	$\langle x^k \rangle_{\text{ens}}$	$\sigma^2(x^k)_{\text{ens}}$	$C_V = \frac{\sigma(x^k)_{\text{ens}}}{\langle x^k \rangle_{\text{ens}}}$
1	$2.205 \times 10^{-7}$	$4.860 \times 10^{-14}$	0.86415755
2	1.	$7.059 \times 10^{-30}$	$2.657 \times 10^{-15}$
3	$5.303 \times 10^{-18}$	$1.258 \times 10^{-30}$	211.478
4	1.8	$1.182 \times 10^{-8}$	$6.039 \times 10^{-5}$
5	$1.139 \times 10^{-5}$	$6.033 \times 10^{-8}$	21.563

Table 4: Numerical values for the ensemble average, the variance of the ensemble, and the coefficient of variation for the ensemble.

Let us plot the fourth and fifth standardised moments for the entire ensemble respectively.

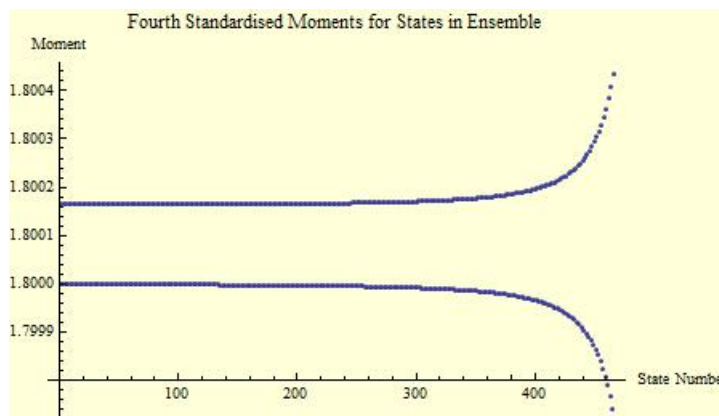


Figure 14: A plot demonstrating the values of the fourth standardised moments for all the states in the ensemble.

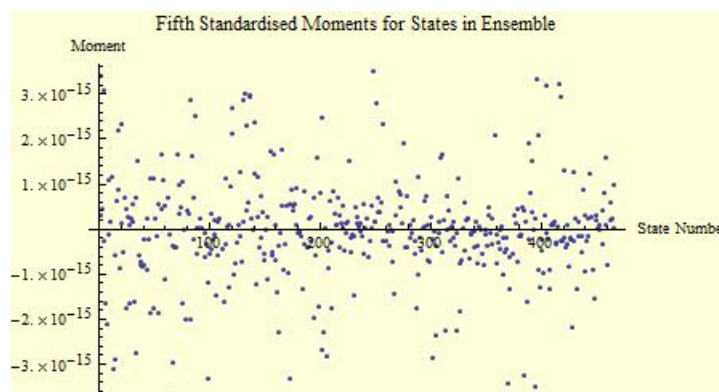


Figure 15: A plot demonstrating the values of the fifth standardised moments for all the states in the ensemble.

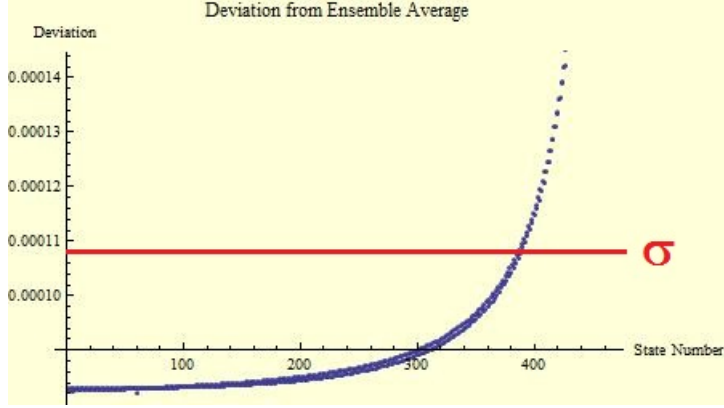


Figure 16: A plot demonstrating the deviation of the expectation value of a given state from the ensemble average. The observable is  $A = x^4$  in this case.

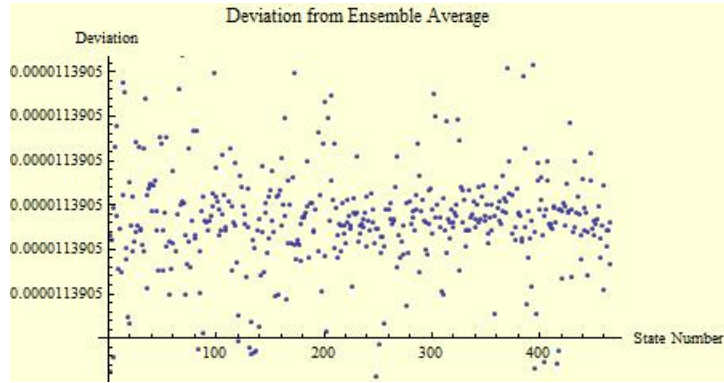


Figure 17: A plot demonstrating the deviation of the expectation value of a given state from the ensemble average. The observable is  $A = x^5$  in this case.

By referring back to Chebyshev's inequality, equation (4.1), we see that  $\varepsilon \geq \sigma$ , since probabilities can never be greater than 1. By referring to table 3 above, we notice that the standard deviation is less than the ensemble average for the fourth and fifth moments respectively. (We are only discussing the fourth and fifth moments because the two graphs above are based on these moments. It is not necessary for us to plot graphs considering all the moments. The main conclusions can be drawn by considering one odd moment and one even moment). This means that even if we choose  $\varepsilon$  to be twice the standard deviation (corresponding to an upper bound of  $\frac{1}{4}$ ), Chebyshev's inequality is still obeyed. If we choose  $\varepsilon = n\sigma$ , then the upper bound would be  $\frac{1}{n^2}$ .

Let us discuss one more example very briefly.

### 4.1.3 The Morse Potential

Let us consider a potential of the form

$$V(r) = D_e (1 - e^{-ar})^2, \quad (4.63)$$

where  $D_e$  is the dissociation energy,  $a$  is the Morse parameter, and  $r$  is the internuclear separation. The Morse potential is a useful model for describing the potential energy of a diatomic molecule.

We shall take a brief look at the moments for this model. The full derivation of the wave function can be found in the appendix.

The wave function for this model is given by [38]

$$\psi(x) = N(\alpha, n) x^{\alpha/2} e^{-x/2} L_n^{(\alpha)}(x), \quad (4.64)$$

where  $x = 2\lambda e^{-ar}$ ,  $\lambda = \frac{\sqrt{2mD_e}}{ah}$ ,  $L_n^{(\alpha)}(x)$  is the associated Laguerre polynomial, and the normalisation constant  $N(\alpha, n)$  is given by

$$N(\alpha, n) = \left[ \frac{\alpha \Gamma(n+1)}{\Gamma(n+\alpha+1)} \right]^{1/2}, \quad (4.65)$$

with  $\alpha = \lambda - n - \frac{1}{2}$ .

The energy spectrum as a function of state number is given by

$$E_n = \left[ -\frac{1}{2\lambda} \left( n + \frac{1}{2} \right)^2 + \left( n + \frac{1}{2} \right) \right] \hbar\omega, \quad (4.66)$$

where

$$\omega = a \sqrt{\frac{2D_e}{m}} \quad (4.67)$$

is the Morse frequency. The state number as a function of energy is given by

$$n(E) = \lambda \left[ 1 - \frac{1}{2\lambda} - \sqrt{1 - \frac{2E}{\lambda\hbar\omega}} \right]. \quad (4.68)$$

Let us look at a numerical example. For this example, let us set  $\lambda = 100$ ,  $E = 95$ , and  $\delta E = 5$ . Using equation (4.69), we can determine the number of states in this ensemble. There are 32 states. Thus, the dimension of the Hilbert space is 32, i.e.  $d_E = 32$ . The states are  $n \in [68, 99]$ . Let us pick three representatives from the ensemble and calculate the standardised moments as we did with the other two examples. We shall pick  $n_1 = 70$ ,  $n_2 = 80$ , and  $n_3 = 90$ . (For the numerical example, we set all the usual constants to 1, i.e.  $\frac{\hbar^2}{2m} = \hbar\omega = a = 1$ ).

$k$	$n_1$	$n_2$	$n_3$
1	$3.7873 \times 10^{-6568}$	$1.9600 \times 10^{-4743}$	$1.0575 \times 10^{-2335}$
2	1	1	1
3	$2.6806 \times 10^{6567}$	$3.9899 \times 10^{4742}$	$9.6720 \times 10^{2334}$
4	$7.2776 \times 10^{13134}$	$1.6081 \times 10^{9485}$	$9.5151 \times 10^{4669}$
5	$1.9969 \times 10^{19702}$	$6.5614 \times 10^{14227}$	$9.4824 \times 10^{7004}$

Table 5: Numerical values for the first 5 moments of 3 states chosen arbitrarily from the ensemble.

The large variations in the above values indicates to us that it is not likely to observe typicality for this model. It is not clear why this is the case. One reason could be due to the highly oscillatory nature of the associated Laguerre polynomials. Another possible reason for this non-typical behaviour could be due to the fact that the wave function for the Morse potential consists of orthogonal polynomials. In the case of the infinite well, as well as the finite well, the wave function consists of trigonometric functions, which are non-orthogonal.

To further validate our hypothesis, we have also looked at the linear potential, i.e.

$$V(x) = Fx, \quad (4.69)$$

where  $F$  is some force. The wave function for this model is

$$\psi(x) = N Ai \left[ \left( \frac{2m}{\hbar^2 F^2} \right)^{1/3} (Fx - E) \right], \quad (4.70)$$

where  $Ai(x)$  is the Airy function, and  $N$  is the normalisation constant, given by

$$N = \sqrt{\frac{F \left( \frac{2m}{\hbar^2 F^2} \right)^{1/3}}{-\lambda(0) Ai^2(\lambda(0)) + Ai'^2(\lambda(0))}}, \quad (4.71)$$

with  $\lambda(0) = - \left( \frac{2m}{\hbar^2 F^2} \right)^{1/3} E$  [39]. We shall not bore the reader with yet another numerical example of calculating moments. However, we shall mention that typicality is observed in the case of the linear potential, whose wave function consists of the Airy function, which is non-orthogonal.

Based on these few examples, it appears that typicality, by means of comparing moments, is only realised for systems in which the wave function consists of non-orthogonal functions.

## 4.2 Distinguishing Microstates

In this subsection, we shall see that even if we could find a quantum system for which there exists a set of observables such that  $N(\mathcal{A}) \sim \sqrt{d_E}$ , performing a distinguishing measurement would not be physically possible.

### 4.2.1 Distance Measures in Quantum Information

In the previous section, we used the expectation values of an observable to tell quantum states apart. However, this is not the only way to distinguish between states. In the previous chapter, we discussed distance measures in quantum information theory. Distance measures are used to determine “how close” two quantum states are to each other. Using an observable  $A$ , the *distinguishability* of two quantum states,  $\rho$  and  $\sigma$ , is defined as

$$D_A(\rho, \sigma) = \frac{1}{2} \sum_a |\text{Tr}(|a\rangle\langle a| \rho) - \text{Tr}(|a\rangle\langle a| \sigma)|, \quad (4.72)$$

where the  $\{|a\rangle\}$  are the eigenvectors of  $A$ . We can generalise this measure to any set of observables  $\mathcal{A}$ , i.e.

$$D_{\mathcal{A}}(\rho, \sigma) = \max_{A \in \mathcal{A}} D_A(\rho, \sigma), \quad (4.73)$$

even if the observables do not commute. Furthermore, if the entire set of observables in the Hilbert space is contained in  $\mathcal{A}$ , then we have

$$D(\rho, \sigma) = \frac{1}{2} \text{Tr}|\rho - \sigma|. \quad (4.74)$$

This is also commonly referred to as the *trace distance*. [22]

#### Theorem

Using the set of observables  $\mathcal{A}$ , the distinguishability of a random pure state  $\psi \in \mathcal{H}_E$  from the maximally mixed state  $\Omega_E$  satisfies

$$\text{Prob} \left( D_{\mathcal{A}}(\psi, \Omega_E) > \epsilon + \frac{N(\mathcal{A})}{2\sqrt{d_E}} \right) \leq e^{-c\epsilon^2 d_E}, \quad (4.75)$$

$$\text{Prob} \left( \langle D_{\mathcal{A}}(\psi(t), \Omega_E) \rangle_t > \epsilon + \frac{N(\mathcal{A})}{2\sqrt{d_E}} \right) \leq e^{-c\epsilon^2 d_E}, \quad (4.76)$$

for an arbitrary  $\epsilon > 0$ , and  $N(\mathcal{A})$  is the number of outcomes for measurements made on the set of observables  $\mathcal{A}$ .

From this important theorem, we learn that the probability of  $D_{\mathcal{A}}(\psi, \Omega_E)$  being larger than zero is exponentially suppressed in  $d_E$ , unless  $N(\mathcal{A}) \sim \sqrt{d_E}$ . But for the quantum models we considered in the previous section, we have that  $N(\mathcal{A}) = K d_E$ , which means that it is of the order  $d_E$ . According to the above theorem, we have

$$\text{Prob} \left( D_{\mathcal{A}}(\psi, \Omega_E) > \epsilon + \frac{K d_E}{2\sqrt{d_E}} \right) \leq e^{-c\epsilon^2 d_E}. \quad (4.77)$$

For an individual measurement using the observable  $A$ , there is only one outcome. In that case,  $N(A) \ll \sqrt{d_E}$ . The second part of the theorem tells us that for typical states, they

will remain indistinguishable from equilibrium for almost all times if  $N(A) \ll \sqrt{d_E}$  (this refers to time averages, which we have not discussed in depth).

This is similar to the result by Page [40], which states that in a composite Hilbert space, the difference between a pure state and a mixed state is exponentially small unless the number of states being measured is comparable to the square root of the dimensionality of the entire Hilbert space. Let us consider a system in contact with a heat bath. The composite Hilbert space is given by  $\mathcal{H} = \mathcal{H}_S \otimes \mathcal{H}_B$ , where the  $S$  and  $B$  symbolises system and bath respectively. Now we consider the subspace,  $\mathcal{H}_E \subseteq \mathcal{H}_S \otimes \mathcal{H}_B$ , which is associated with the microcanonical ensemble which we discussed earlier. As was also defined previously, the maximally mixed state in  $\mathcal{H}_E$  is

$$\Omega_E = \frac{\mathbb{I}}{d_E}, \quad (4.78)$$

where  $\mathbb{I}$  is the identity matrix on  $\mathcal{H}_E$ . If we wish to restrict the maximally mixed state to  $\mathcal{H}_S$ , then we would have to trace out over  $\mathcal{H}_B$ , i.e.

$$\Omega_S = \text{Tr}_B(\Omega_E), \quad (4.79)$$

where  $\text{Tr}_B$  denotes the partial trace over  $\mathcal{H}_B$ . Now using the theorem above, we obtain

$$\text{Prob} \left( D_{\mathcal{A}}(\psi, \Omega_E) > \epsilon + \frac{d_S}{2\sqrt{d_E}} \right) \leq e^{-c\epsilon^2 d_E}, \quad (4.80)$$

since  $d_S$  is the dimension of  $\mathcal{H}_S$ , and it follows that the number of outcomes is bounded by  $d_S$ . So we see that it is not possible to distinguish between a random pure state and the maximally mixed state, unless the number of outcomes scales like the square root of the dimensionality of the Hilbert space. Our result is very similar to that of Page. [40]

Now suppose we could find operators whose spectra satisfy  $N(A) \sim \sqrt{d_E}$ . We should ask ourselves if it would be possible to actually perform such a distinguishing measurement.

### 4.2.2 Making A Measurement

Let our initial state be in a product state  $|\psi\rangle \otimes |\alpha\rangle \in \mathcal{H}_E \otimes \mathcal{H}_A$ . To perform a measurement, we entangle our physical system with a quantum detector. After the measurement has taken place, we consider a sharp projection on the compound state. When performing a measurement, naturally an interaction takes place. The interaction Hamiltonian is  $H_{\text{int}} = \lambda A \otimes J$ , where  $J$  is a source acting on  $\mathcal{H}_A$ , and  $A$  is the observable we wish to measure.

By expanding the time evolution of the initial entangled state in the eigenbasis of  $A$ , we have

$$|\Psi(t)\rangle = \sum_a \psi_a(t) e^{-ia\lambda Jt} |a\rangle |\alpha\rangle.$$

For the measurement to distinguish between the outcomes  $a$  and  $a + \delta a$ , we need the wave functions of the apparatus to become orthogonal at time  $t$ , i.e.

$$S(t) = \langle \alpha | e^{-i\lambda(\delta a)t} | \alpha \rangle = 0. \quad (4.81)$$

Now we can find a lower bound on the smallest eigenvalue gap  $\delta a$  that can be resolved.

Theorem

*The smallest gap  $\delta a$  resolvable in a measurement of an observable  $A$  in time  $t$  using the interaction Hamiltonian  $H_{\text{int}} = \lambda A \otimes J$  is bounded below by*

$$\frac{\pi \hbar \langle A \rangle}{\langle H_{\text{int}} \rangle t} = \frac{\pi \hbar}{\lambda \langle J \rangle t} \leq \delta a.$$

For measurements to distinguish microstates, we must have  $N(A) \sim \sqrt{d_E}$ . These measurements involve long times or large energy resources. In the context of black holes, it would not be possible for us to distinguish among black hole microstates.

In [41], the authors qualitatively studied typical states of the Schwarzschild black hole in  $AdS_5$ . They found that very heavy pure states of quantum gravity can have an underlying quantum description. At the Planck scale, this quantum description is very complex. The details of its structure are invisible to almost all probes, thus making it appear as a “foam”.

In the second section, we mentioned that  $AdS_5 \times S^5$  is dual to  $\mathcal{N} = 4$  SYM theory. In the  $\mathcal{N} = 4$  SYM theory, the authors explicitly constructed singular spacetimes which give rise to the universal low-energy description of most of the half-BPS states which have a fixed mass. Their results were exact in this supersymmetric scenario. They found that the two sets of results: the exact results from the  $\mathcal{N} = 4$  SYM sector, and the qualitative results from the  $AdS_5$  sector, were very similar. This suggests that the supersymmetric results provide a generally correct qualitative understanding of the non-supersymmetric case.

The conclusion drawn is that a low-energy description of nature results in many quantum mechanical details, which are present at the Planck scale, being “lost”. This tells us that unless we have a full theory of quantum gravity, it is not possible to distinguish, or even probe, the microstates of black holes.

Now let us return to simple quantum models, this time in the canonical ensemble.

## 4.3 Typicality on Quantum Models in the Canonical Formalism

### 4.3.1 Simple Quantum Models in the Canonical Ensemble

In the canonical ensemble, the probability of the system being described by a particular microstate is given by

$$p_n = \frac{e^{-\beta E_n}}{\sum_k e^{-\beta E_k}} = \frac{1}{Z} e^{-\beta E_n}, \quad (4.82)$$

where  $Z = \sum_k e^{-\beta E_k}$  is the partition function and  $\beta = \frac{1}{k_B T}$ .

For the particle in an infinite potential well,  $E_n = \frac{n^2}{L^2}$ , so the partition function is  $Z = \sum_n e^{-\beta \frac{n^2}{L^2}}$ . This is an infinite sum. We can approximate its value by using an infinite integral. Let us briefly justify this approximation.

Consider the function,  $f(x) = e^{-ax^2}$ . For  $x \geq 0$ , this function is strictly decreasing, so

$$f(n+1) < \int_n^{n+1} f(x) dx < f(n) \quad \forall n \in \mathbb{N}_0.$$

Thus,

$$\sum_{n=1}^{\infty} f(n) < \int_0^{\infty} f(x) dx < f(0) + \sum_{n=1}^{\infty} f(n).$$

At most, the difference between the sum and the integral is  $f(0) = 1$ . This allows us to approximate the partition function,  $Z$ ,

$$\begin{aligned} Z &= \sum_{n=0}^{\infty} e^{-\frac{\beta}{L^2} n^2} \\ &\approx \int_0^{\infty} e^{-\frac{\beta}{L^2} x^2} dx \\ &= \frac{1}{2} \sqrt{\frac{\pi L^2}{\beta}} = L \sqrt{\frac{\pi}{4\beta}} = \frac{L}{\lambda_D}, \end{aligned}$$

where  $\lambda_D = \frac{4\beta}{\pi}$  is the thermal de Broglie wavelength. Thus, we have an approximate closed form for the partition function,

$$Z \approx \frac{L}{\lambda_D}. \quad (4.83)$$

The thermal density matrix is defined as

$$\hat{\rho} = \sum_i e^{-\beta E_i} |\psi_i\rangle \langle \psi_i|. \quad (4.84)$$

The expectation value for an operator  $A$  over the entire ensemble is given by

$$\langle A \rangle_{\text{ens}} = \frac{\text{Tr}(A\rho)}{\text{Tr}(\rho)} = \frac{1}{Z} \sum_i e^{-\beta E_i} \langle \psi_i | A | \psi_i \rangle. \quad (4.85)$$

The ensemble average is calculated by taking the trace of the following matrix,

$$\langle A \rangle_{\text{ens}} = \text{Tr} \left[ \frac{1}{Z} \begin{pmatrix} e^{-\beta E_0} \langle \psi_0 | A | \psi_0 \rangle & 0 & \cdots & 0 \\ 0 & e^{-\beta E_1} \langle \psi_1 | A | \psi_1 \rangle & \cdots & 0 \\ \vdots & \vdots & \ddots & \vdots \\ 0 & 0 & \cdots & e^{-\beta E_n} \langle \psi_n | A | \psi_n \rangle \end{pmatrix} \right]. \quad (4.86)$$

Let us return to the particle in an infinite potential well. In the canonical formalism, the density matrix can be expressed as

$$\hat{\rho} = \frac{\lambda_D}{L} \begin{pmatrix} e^{-\beta E_0} |\psi_0\rangle \langle \psi_0| & 0 & \cdots & 0 \\ 0 & e^{-\beta E_1} |\psi_1\rangle \langle \psi_1| & \cdots & 0 \\ \vdots & \vdots & \ddots & \vdots \\ 0 & 0 & \cdots & e^{-\beta E_{d_E}} |\psi_{d_E}\rangle \langle \psi_{d_E}| \end{pmatrix}, \quad (4.87)$$

where we assume that  $d_E$  is exceptionally large. (If  $d_E$  is not very large, then we shall not be permitted to make the approximation  $Z \approx \frac{L}{\lambda_D}$ ). However, to be more precise, we could always express the partition function as

$$Z = \sum_{k=0}^{d_E} e^{(\frac{-\beta}{L^2})n^2} \approx \int_0^{d_E} e^{(\frac{-\beta}{L^2})n^2} dn = \frac{L}{\lambda_D} \text{erf}(d_E), \quad (4.88)$$

where  $\text{erf}(d_E)$  is the error function, defined by

$$\text{erf}(d_E) = \frac{2}{\sqrt{\pi}} \int_0^{d_E} e^{-x^2} dx, \quad (4.89)$$

and its Taylor series is

$$\text{erf}(d_E) = \frac{2}{\sqrt{\pi}} \sum_{k=0}^{\infty} \frac{(-1)^k d_E^{2k+1}}{k!(2k+1)}. \quad (4.90)$$

We can verify that the trace of the density matrix is 1, i.e.

$$\begin{aligned} \text{Tr}(\hat{\rho}) &= \frac{\lambda_D}{\text{erf}(d_E)L} (e^{-\beta E_0} \langle \psi_0 | \psi_0 \rangle + e^{-\beta E_1} \langle \psi_1 | \psi_1 \rangle + \cdots + e^{-\beta E_{d_E}} \langle \psi_{d_E} | \psi_{d_E} \rangle) \\ &= \frac{\lambda_D}{\text{erf}(d_E)L} \sum_{k=0}^{d_E} e^{-\beta E_k} \langle \psi_k | \psi_k \rangle \\ &\approx \frac{\lambda_D}{\text{erf}(d_E)L} \frac{L}{\lambda_D} \text{erf}(d_E) = 1. \end{aligned}$$

The purity,  $\gamma$ , is defined as the trace of the square of the density matrix. The trace of the square of the density matrix is

$$\begin{aligned} \text{Tr}(\hat{\rho}^2) &= \frac{\lambda_D^2}{(\text{erf}(d_E)L)^2} \sum_{k=0}^{d_E} e^{-2\beta E_k} \\ &\approx \frac{\lambda_D^2}{(\text{erf}(d_E)L)^2} \frac{L}{\sqrt{2}\lambda_D}, \end{aligned}$$

and thus the purity is

$$\gamma = \frac{1}{\sqrt{2}} \frac{\lambda_D}{\text{erf}(d_E)L}. \quad (4.91)$$

The purity is a measure of how “mixed” an ensemble is. For a pure state, the purity is 1. For a maximally mixed state, the purity is  $\frac{1}{d_E}$ . The linear entropy is defined as

$$S_L = 1 - \gamma = 1 - \frac{1}{\sqrt{2}} \frac{\lambda_D}{\text{erf}(d_E)L}. \quad (4.92)$$

The linear entropy ranges from 0, for a pure state, and  $1 - \frac{1}{d_E}$ , for a completely mixed state. For completeness, let us compute the von Neumann entropy. The von Neumann entropy is given by

$$\begin{aligned} S(\hat{\rho}) &= -\text{Tr} [\hat{\rho} \ln(\hat{\rho})] \\ &= -\frac{\lambda_D}{\text{erf}(d_E)L} \left[ \ln \left( \frac{\lambda_D}{L} \right) \sum_{k=0}^{d_E} e^{-\beta E_k} - \beta \sum_{k=0}^{d_E} E_k \right] \\ &\approx -\frac{\lambda_D}{\text{erf}(d_E)L} \left[ \ln \left( \frac{\lambda_D}{\text{erf}(d_E)L} \right) \frac{L}{\lambda_D} \text{erf}(d_E) - \beta \sum_{k=0}^{d_E} E_k \right] \\ &= \ln \left( \frac{L}{\lambda_D} \text{erf}(d_E) \right) + \frac{\beta \lambda_D}{\text{erf}(d_E)L} \sum_{k=0}^{d_E} E_k. \end{aligned}$$

In the canonical formalism, for a particle in an infinite potential well, the von Neumann entropy is

$$S(\hat{\rho}) = \ln \left( \frac{L}{\lambda_D} \text{erf}(d_E) \right) + \frac{\beta \lambda_D}{\text{erf}(d_E)L} \sum_{k=0}^{n_{\max}} E_k. \quad (4.93)$$

We see that the larger  $d_E$  is, the larger the entropy will be. This is not at all surprising, since we know that the entropy of a system is related to the number of microstates.

Since the observables we’ve been considering are the moments, it is convenient to express the density matrix in the position representation. In this form, we have

$$\rho(x, x'; \beta) = \sum_{n=0}^{d_E} \frac{1}{Z} e^{-\beta E_n} \psi_n(x) \psi_n^*(x') = \frac{\lambda_D}{\text{erf}(d_E)L} \frac{2}{L} \sum_{n=0}^{d_E} e^{\left(\frac{-\beta}{L^2}\right)n^2} \sin \left( \frac{\pi n}{L} x \right) \sin \left( \frac{\pi n}{L} x' \right). \quad (4.94)$$

When taking the trace, we will only sum over the diagonal elements, i.e. when  $x = x'$ . Thus, the ensemble average for the  $k^{\text{th}}$  moment is

$$\langle x^k \rangle_{\text{ens}} = \frac{\lambda_D}{\text{erf}(d_E)L} \sum_{m=0}^{d_E} e^{-\beta E_m} \langle \psi_m | x^k | \psi_m \rangle. \quad (4.95)$$

This is very similar to the ensemble average found in the microcanonical ensemble (see equation (4.45)). The difference is that in this case, the microstates in the ensemble do not

have an equal likelihood of being realised. However, if we consider the high energy limit, where there is no state dependence on the expectation values, we get

$$\frac{\lambda_D}{\text{erf}(d_E)L} \sum_{m=0}^{d_E} e^{\left(\frac{-\beta}{L^2}\right)n^2} \langle \psi_m | x^k | \psi_m \rangle = \frac{\lambda_D}{\text{erf}(d_E)L} \frac{L}{\lambda_D} \text{erf}(d_E) \frac{L^k}{2^{k+2}(k+1)} = \frac{L^k}{2^{k+2}(k+1)}, \quad (4.96)$$

which is the exact result we get in the microcanonical ensemble (see equation (4.45)). We can thus conclude that typicality will also be realised in the canonical ensemble. This is expected by virtue of the thermodynamic limit.

We wish to see if we can relate these ideas to black holes. Before we do that, it is useful for us to discuss how the density matrix of one part of a composite system looks very much like the thermal density matrix found in the canonical ensemble.

### 4.3.2 Composite System and the Canonical Ensemble

Suppose we have a composite system  $AB$ , such that  $\mathcal{H}_{AB} = \mathcal{H}_A \otimes \mathcal{H}_B$ . We assume that the interaction between systems  $A$  and  $B$  is weak. Now consider a subspace  $\mathcal{H}_E \subseteq \mathcal{H}_A \otimes \mathcal{H}_B$ , which corresponds to an energy  $E$ . This subspace is spanned by a basis of vectors of the form  $|E_i\rangle_A^k \otimes |E_j\rangle_B^l$ , where  $E_i + E_j = E$ . Furthermore, the subspace of  $\mathcal{H}_A$  is spanned by  $|E_i\rangle_A^k$ , where  $k = 1, 2, \dots, g_A(E_i)$ ; and similarly for  $\mathcal{H}_B$ . (The quantity  $g_A(E_i)$  is the degeneracy of  $E_i$  in  $\mathcal{H}_A$ ).

A typical state  $|\psi\rangle \in \mathcal{H}_E$  can be expressed as

$$|\psi\rangle = \sum_i \sum_{k=1}^{g_A(E_i)} \sum_{l=1}^{g_B(E-E_i)} c_{kl}^i |E_i\rangle_A^k |E-E_i\rangle_B^l. \quad (4.97)$$

The density matrix for these states is

$$\begin{aligned} \rho &= |\psi\rangle \langle \psi| = \sum_i \sum_{k=1}^{g_A(E_i)} \sum_{l=1}^{g_B(E-E_i)} c_{kl}^i |E_i\rangle_A^k |E-E_i\rangle_B^l \sum_{i'} \sum_{k'=1}^{g_A(E_{i'})} \sum_{l'=1}^{g_B(E-E_{i'})} c_{k'l'}^{*i'} |E_{i'}\rangle_A^{k'} |E-E_{i'}\rangle_B^{l'} \\ &= \sum_{i,i'} \sum_{k,k'=1}^{g_A(E_i),g_A(E_{i'})} \sum_{l,l'=1}^{g_B(E-E_i),g_B(E-E_{i'})} \left( c_{kl}^i c_{k'l'}^{*i'} |E_i\rangle_A^{kk'} \langle E_{i'}| \otimes |E-E_i\rangle_B^{ll'} \langle E-E_{i'}| \right). \end{aligned} \quad (4.98)$$

If we want the density matrix for system  $A$  alone, then we take the trace of  $\rho$  over the degrees of freedom of  $B$ , i.e.

$$\rho_A = \text{Tr}_B(\rho) = \sum_i \sum_{l=1}^{g_B(E-E_i)} \sum_{k,k'=1}^{g_A(E_i)} c_{kl}^i c_{k'l'}^{*i'} |E_i\rangle_A^k \langle E_i|^{k'}. \quad (4.99)$$

The system  $A$  is in a mixture of states with different energies  $E_i$ . Every  $E_i$  in  $A$  is correlated with an energy  $E - E_i$  in  $B$ . We can write  $\rho_A = \sum_i p(E_i) \rho_{E_i}$ , where  $\rho_{E_i}$  is a density matrix for a system with energy  $E_i$ . The trace of this matrix is 1, and the  $p(E_i)$  are the probabilities of finding the value  $E_i$  upon performing a measurement of energy of system  $A$ . Using the knowledge we have about typicality, we know that over the entire ensemble,  $p(E_i)$  averages out to  $\frac{g_A(E_i)g_B(E-E_i)}{d_E}$ , i.e. the probability of finding a state with energy  $E_i$  is proportional to the degeneracy of those states.

Using a slightly modified form of equation (4.6), we learn that, on average,  $p(E_i)$  deviates from its most likely value by

$$\frac{1}{\sqrt{d_E + 1}} \sqrt{\frac{g_A(E_i)g_B(E-E_i)}{d_E} - \left(\frac{g_A(E_i)g_B(E-E_i)}{d_E}\right)^2} \approx \frac{\sqrt{g_A(E_i)g_B(E-E_i)}}{d_E}. \quad (4.100)$$

So the density matrix for system  $A$  alone can be written as

$$\begin{aligned} \rho_A &= \sum_i \frac{g_A(E_i)g_B(E-E_i)}{d_E} \rho_{E_i} \pm \sum_i \frac{\sqrt{g_A(E_i)g_B(E-E_i)}}{d_E} \rho_{E_i} \\ &= \frac{1}{d_E} \sum_i g_A(E_i)g_B(E-E_i) \left(1 \pm \frac{1}{\sqrt{g_A(E_i)g_B(E-E_i)}}\right) \rho_{E_i}. \end{aligned} \quad (4.101)$$

Now we know that the entropies of systems  $A$  and  $B$ ,  $S_A$  and  $S_B$  respectively, are related to the degeneracy of states in the respective systems, i.e.

$$\begin{aligned} g_A(E_i) &= e^{S_A(E_i)}, \\ g_B(E-E_i) &= e^{S_B(E-E_i)}. \end{aligned}$$

If system  $B$  has many more degrees of freedom than system  $A$ , then we may approximate

$$\begin{aligned} S_B(E-E_i) &\approx S_B(E) - \frac{\partial S_B}{\partial E} \Big|_{E=E_i} E_i \\ &= S_B(E) - \frac{E_i}{T}. \end{aligned} \quad (4.102)$$

This gives us

$$\rho_A = \frac{1}{N} \sum_i e^{-(E_i - TS_A(E_i))/T} \left(1 \pm \frac{1}{\sqrt{g_A(E_i)g_B(E-E_i)}}\right) \rho_{E_i}, \quad (4.103)$$

where  $\frac{1}{N} = \frac{e^{S_B(E)}}{d_E}$ . If the system  $B$  is a large heat bath with temperature  $T$ , then the density matrix  $\rho_A$  is very similar to the thermal density matrix we find in the canonical ensemble. In the thermodynamic limit, where  $\sqrt{g_A(E_i)g_B(E-E_i)} \rightarrow \infty$ , the probability for  $\rho_A$  to differ from a thermal density matrix is zero.

Let's apply these ideas to black holes [42]. Consider the inside of the black hole and the outside of the black hole as being two separate systems. The outside of the black hole "has temperature"  $T = \frac{1}{8\pi G_N M}$ . The form of the density matrix of the states outside the black hole is a mixture, i.e. a thermal mixture at temperature  $T = \frac{1}{8\pi G_N M}$ .

It was argued by Hawking that a black hole behaves like a black body. One of the ways to derive black hole radiance is by considering the periodicity of the Schwarzschild metric in imaginary time. However, it is important to note that the black hole is treated as a geometric object, and not a thermodynamic one. Consequently, the radiation that comes from the horizon is coherent. For a black body, the emitted radiation is *incoherent*.

It was argued by T. D. Lee [43] that black holes cannot be regarded as black bodies, since quantum fields over the whole of spacetime are coherent, whereas the radiation emitted from black bodies is incoherent. Using the argument from above about a system being in contact with a heat bath at temperature  $T$ , we can conclude that in the thermodynamic limit, coherent fields in the presence of a black hole will be indistinguishable from coherent fields in the presence of a black body.

This suggests that if an observer is at a laboratory with a radiation detector, he/she will not be able to know for certain if the radiation detected is coming from a black hole or from a black body.

In this section, we studied several quantum systems. Studying the microstates of these systems allowed us to make generalisations about black holes. As was discussed in the second section, black holes have entropy. Statistical mechanics tells us that the entropy of a system is related to the number of microstates of the system. Since there is no way for us to probe a black hole on a quantum level, due to general relativity being a classical field theory, we make use of quantum toy models. The quantum states of a system should exhibit universal properties, since all systems are quantum mechanical on a fundamental level, including black holes.

## 5 Decoherence and Black Holes

In this section, we continue our plan of trying to find simple quantum mechanical systems which may help us investigate properties of the entropy of black holes. We shall explore ideas pertaining to coherent states, squeezed states, and decoherence. Let us begin by looking at coherent states and squeezed states.

### 5.1 Coherent States and Squeezed States

#### 5.1.1 Definitions

We can think of a coherent state in two ways: as the eigenstate of the annihilation operator, and as a displaced harmonic oscillator state. If we have creation and annihilation operators  $a^\dagger$  and  $a$ , respectively, then if  $a|\alpha\rangle = \alpha|\alpha\rangle$ , we say that  $|\alpha\rangle$  is a coherent state. We can write

$$|\alpha\rangle = e^{-\frac{|\alpha|^2}{2}} \sum_{n=0}^{\infty} \frac{\alpha^n}{\sqrt{n!}} |n\rangle \quad (5.1)$$

$$= e^{-\frac{|\alpha|^2}{2}} \underbrace{\sum_{n=0}^{\infty} \frac{(\alpha a^\dagger)^n}{n!}}_{e^{\alpha a^\dagger}} |0\rangle, \quad (5.2)$$

and thus,

$$|\alpha\rangle = e^{-\frac{|\alpha|^2}{2}} e^{\alpha a^\dagger} |0\rangle. \quad (5.3)$$

According to the Baker-Campbell-Hausdorff formula [44], if  $A$  and  $B$  are any two operators such that

$$[[A, B], A] = [[A, B], B] = 0, \quad (5.4)$$

then

$$e^{A+B} = e^{-[A,B]/2} e^A e^B. \quad (5.5)$$

Replacing  $A$  with  $\alpha a^\dagger$  and  $B$  with  $-\alpha^* a$ , we have

$$\begin{aligned} e^{\alpha a^\dagger - \alpha^* a} &= e^{-[\alpha a^\dagger, -\alpha^* a]/2} e^{\alpha a^\dagger} e^{-\alpha^* a} \\ &= e^{|\alpha|^2 [a^\dagger, a]/2} e^{\alpha a^\dagger} e^{-\alpha^* a} \\ &= e^{-\frac{|\alpha|^2}{2}} e^{\alpha a^\dagger} e^{-\alpha^* a} \end{aligned}$$

since  $[a^\dagger, a] = -\mathbb{I}$ . Now we define an operator,

$$D(\alpha) = e^{-\frac{|\alpha|^2}{2}} e^{\alpha a^\dagger} e^{-\alpha^* a}, \quad (5.6)$$

which has the property

$$|\alpha\rangle = D(\alpha) |0\rangle. \quad (5.7)$$

To show that equation (5.7) is true, we need to expand the exponential, i.e.

$$\begin{aligned} D(\alpha) |0\rangle &= e^{-\frac{|\alpha|^2}{2}} e^{\alpha a^\dagger} e^{-\alpha^* a} |0\rangle \\ &= e^{-\frac{|\alpha|^2}{2}} e^{\alpha a^\dagger} \left( 1 - \alpha^* a + \frac{1}{2} (\alpha^*)^2 a^2 + \dots \right) |0\rangle \\ &= e^{-\frac{|\alpha|^2}{2}} e^{\alpha a^\dagger} (1) |0\rangle \quad (\text{since } a |0\rangle = 0) \\ &= |\alpha\rangle \quad (\text{from equation (5.3)}). \end{aligned}$$

We also see that  $D(\alpha)$  is a unitary operator, i.e.

$$D^\dagger(\alpha) = e^{\frac{|\alpha|^2}{2}} e^{-\alpha^* a} e^{\alpha a^\dagger} = D(-\alpha) = D^{-1}(\alpha). \quad (5.8)$$

We call  $D(\alpha)$  a displacement operator, since it displaces the amplitudes  $a$  and  $a^\dagger$ , i.e.

$$D^{-1}(\alpha) a D(\alpha) = a + \alpha \quad (5.9)$$

$$D^{-1}(\alpha) a^\dagger D(\alpha) = a^\dagger + \alpha^*. \quad (5.10)$$

By applying the displacement operator on the vacuum state, we obtain a coherent state. Let us discuss some properties of coherent states within the context of a radiation field.

- (i) In the coherent state  $\alpha$ , the mean number of photons is

$$\langle \alpha | a^\dagger a | \alpha \rangle = |\alpha|^2. \quad (5.11)$$

Writing  $\langle n \rangle = |\alpha|^2$ , the probability of finding  $n$  photons in the state  $|\alpha\rangle$  is given by

$$p(n) = \langle n | \alpha \rangle \langle \alpha | n \rangle = \frac{\langle n \rangle^n e^{-\langle n \rangle}}{n!}, \quad (5.12)$$

a Poisson distribution.

- (ii) For a coherent state, the Heisenberg uncertainty bound is saturated, i.e.  $\Delta p \Delta x = \frac{\hbar}{2}$ . It is a minimum uncertainty state.
- (iii) The set of all coherent states  $|\alpha\rangle$  is a complete set. We can show this by letting  $|\alpha\rangle = |\alpha| e^{i\theta}$ . Then

$$\begin{aligned} \int (\alpha^*)^n \alpha^m e^{-|\alpha|^2} d^2\alpha &= \int_0^\infty \int_0^{2\pi} |\alpha|^n e^{-in\theta} |\alpha|^m e^{im\theta} e^{-|\alpha|^2} |\alpha| d\theta d|\alpha| \\ &= \int_0^\infty d|\alpha| |\alpha|^{n+m+1} e^{-|\alpha|^2} \int_0^{2\pi} d\theta e^{i(m-n)\theta} \\ &= \pi n! \delta_{nm}, \end{aligned}$$

where the integration takes place over the entire complex plane.

Using  $|\alpha\rangle = e^{-\frac{|\alpha|^2}{2}} \sum_{n=0}^{\infty} \frac{\alpha^n}{\sqrt{n!}} |n\rangle$ , we have

$$\int d^2\alpha |\alpha\rangle \langle\alpha| = \pi \sum_n |n\rangle \langle n|. \quad (5.13)$$

The Fock states  $|n\rangle$  form a complete orthonormal set, so the sum over  $n$  is the identity operator, i.e.  $\sum_n |n\rangle \langle n| = \mathbb{I}$ . Thus, we have a completeness relation for the coherent states, namely

$$\frac{1}{\pi} \int d^2\alpha |\alpha\rangle \langle\alpha| = 1. \quad (5.14)$$

(iv) Two coherent states which correspond to different eigenstates,  $|\alpha\rangle$  and  $|\alpha'\rangle$ , are not orthogonal, i.e.

$$\langle\alpha|\alpha'\rangle = \exp\left(-\frac{1}{2}|\alpha|^2 + \alpha'\alpha^* - \frac{1}{2}|\alpha'|^2\right), \quad (5.15)$$

and

$$|\langle\alpha|\alpha'\rangle|^2 = \exp(-|\alpha - \alpha'|). \quad (5.16)$$

Due to the non-orthogonality of coherent states, any such state can be expanded in terms of the other states,

$$\begin{aligned} |\alpha\rangle &= \frac{1}{\pi} \int |\alpha'\rangle \langle\alpha'|\alpha\rangle d^2\alpha' \\ &= \frac{1}{\pi} \int |\alpha'\rangle \exp\left(-\frac{1}{2}|\alpha|^2 + \alpha'\alpha^* - \frac{1}{2}|\alpha'|^2\right) d^2\alpha'. \end{aligned}$$

We deduce that coherent states are *overcomplete*.

Now let us move on to discuss squeezed states. The unitary squeeze operator is given by

$$S(\xi) = \exp\left(\frac{1}{2}\xi^* a^2 - \frac{1}{2}\xi a^{\dagger 2}\right), \quad (5.17)$$

where  $\xi$  is some arbitrary complex number which we can write as  $\xi = r e^{i\theta}$ . The squeeze operator has the property,

$$S^\dagger(\xi) = S^{-1}(\xi) = S(-\xi). \quad (5.18)$$

Suppose  $A$  and  $B$  are operators, then we can use the following formula,

$$e^A B e^{-A} = B + [A, B] + \frac{1}{2!}[A, [A, B]] + \dots, \quad (5.19)$$

to derive unitary transformation properties of the squeeze operator. These properties are

$$S^\dagger(\xi) a S(\xi) = a \cosh r - a^\dagger e^{i\theta} \sinh r, \quad (5.20)$$

$$\text{and } S^\dagger(\xi) a^\dagger S(\xi) = a^\dagger \cosh r - a e^{-i\theta} \sinh r. \quad (5.21)$$

To obtain a squeezed coherent state  $|\alpha, \xi\rangle$ , we first act with the displacement operator  $D(\alpha)$  on the vacuum state, and then act with the squeeze operator  $S(\xi)$ , i.e.  $|\alpha, \xi\rangle = S(\xi)D(\alpha)|0\rangle$ .

We would like to study the coherent, and squeezed states, for a particle in an infinite potential well. However, before we can achieve this goal, we first need to find the appropriate ladder operators for the system.

### 5.1.2 Ladder Operators for a Particle in an Infinite Potential Square Well

Due to the fact that the energy levels for the particle in an infinite potential well are not equally spaced, the generalised creation and annihilation operators for this system are a bit more complicated to obtain compared to the harmonic oscillator.

Consider a Hamiltonian  $\frac{p^2}{2m} + V(x)$ , where  $p = \frac{\hbar}{i} \frac{d}{dx}$ . Furthermore, let us consider the well which has boundaries at  $x = 0$  and  $x = L$ . Using the factorisation method [44], we can rewrite  $H$  as

$$H_1 = a_1^\dagger a_1 + E_1, \quad (5.22)$$

a product of two first-order differential operators  $a_1^\dagger$  and  $a_1$ , and plus a constant  $E_1$ . These operators should consist of a linear term in momentum, since  $H$  has a term quadratic in momentum. Following the super-symmetric (SUSY) quantum mechanics treatment in [46], we can write

$$H_2 = a_1 a_1^\dagger + E_1. \quad (5.23)$$

By factoring  $H_2$ , we have

$$H_2 = a_2^\dagger a_2 + E_2, \quad (5.24)$$

with its SUSY partner being  $H_3 = a_2 a_2^\dagger + E_2$ . Continuing in this fashion, we have

$$\begin{aligned} H_{j+1} &= a_{j+1}^\dagger a_{j+1} + E_{j+1} \\ &= a_j a_j^\dagger + E_j, \end{aligned} \quad (5.25)$$

where  $j = 1, 2, 3 \dots$

We can express the operators  $a_j$  and  $a_j^\dagger$  as

$$\begin{aligned} a_j &= \frac{1}{\sqrt{2m}} (p + i f_j(x)), \\ a_j^\dagger &= \frac{1}{\sqrt{2m}} (p - i f_j(x)). \end{aligned} \quad (5.26)$$

These operators are *not* Hermitian, and therefore are not observable. Furthermore, we see that

$$a_j^\dagger a_j = \frac{p^2}{2m} + \frac{f_j^2(x)}{2m} + \frac{\hbar}{2m} \frac{df_j}{dx}(x), \quad (5.27)$$

which is Hermitian, and thus observable. (In the case of the harmonic oscillator, equation (5.27) is called the number operator).

For a particle in an infinite potential well,  $V(x) = 0$  inside the well. Thus, we can write

$$\begin{aligned} H_1 &= \frac{p^2}{2m} + \frac{f_1^2(x)}{2m} + \frac{\hbar}{2m} \frac{df_1}{dx}(x) + E_1 \\ \Rightarrow \frac{p^2}{2m} &= \frac{p^2}{2m} + \frac{f_1^2(x)}{2m} + \frac{\hbar}{2m} \frac{df_1}{dx}(x) + E_1 \\ \Rightarrow 0 &= \frac{f_1^2(x)}{2m} + \frac{\hbar}{2m} \frac{df_1}{dx}(x) + E_1, \end{aligned}$$

which gives us a Riccati differential equation,

$$\frac{df_1}{dx}(x) = -\frac{f_1^2(x)}{\hbar} - \frac{2mE_1}{\hbar}. \quad (5.28)$$

To solve this differential equation, we make the following substitution,  $f_1(x) = \sqrt{2mE_1} \cot(y)$ , where  $y = \frac{\sqrt{2mE_1}}{\hbar}(x - C)$ , where  $C$  is some integration constant. Since  $0 \leq x \leq L$ , the cotangent function must be finite in this region. The cotangent function has singularities at the points where the sine function is zero. Consequently, we choose our boundary conditions such that at

$$\begin{aligned} x = 0, \quad f_1(0) &\rightarrow \infty \Rightarrow C = 0; \\ x = L, \quad f_1(L) &\rightarrow \infty \Rightarrow \frac{\sqrt{2mE_1}}{\hbar}L \quad (\text{since } C = 0). \end{aligned}$$

Thus, we can write

$$\begin{aligned} f_1(x) &= \frac{\hbar\pi}{L} \cot\left(\frac{\pi}{L}x\right) \\ a_1 &= \frac{1}{\sqrt{2m}} \left( p + i \frac{\pi\hbar}{L} \cot\left(\frac{\pi}{L}x\right) \right). \end{aligned} \quad (5.29)$$

Now we wish to determine  $a_j$ . We shall consider  $f_j(x) = c_j \cot(b_j x)$ , and make use of the recurrence relation (equation (5.25)), with the restriction  $0 \leq b_j \leq \frac{\pi}{L}$ , to get

$$\begin{aligned} \frac{p^2}{2m} + \frac{c_{j+1}^2 \cot^2(b_{j+1}x)}{2m} + \frac{\hbar}{2m} \frac{d(c_{j+1} \cot(b_{j+1}x))}{dx} + E_{j+1} \\ = \frac{p^2}{2m} + \frac{c_j^2 \cot^2(b_j x)}{2m} + \frac{\hbar}{2m} \frac{d(c_j \cot(b_j x))}{dx} + E_j. \end{aligned} \quad (5.30)$$

Recalling that  $\frac{d \cot(x)}{dx} = -\csc^2(x) = -1 - \cot^2(x)$ , we get

$$\begin{aligned} 2mE_{j+1} - \hbar c_{j+1} b_{j+1} + c_{j+1}(c_{j+1} - \hbar b_{j+1}) \cot^2(b_{j+1}x) \\ = 2mE_j - \hbar c_j b_j + c_j(c_j - \hbar b_j) \cot^2(b_j x). \end{aligned} \quad (5.31)$$

For equation (5.31) to hold true, we need

$$b_{j+1} = b_j \Rightarrow b_j = b_1 = \frac{\pi}{L}, \quad (5.32)$$

$$c_{j+1}(c_{j+1} - \hbar b_{j+1}) = c_j(c_j - \hbar b_j) \Rightarrow c_{j+1} = \begin{cases} -c_j \\ c_j + \frac{\pi\hbar}{L}, \end{cases} \quad (5.33)$$

$$2mE_{j+1} - \hbar c_{j+1}b_{j+1} = 2mE_j - \hbar c_j b_j \Rightarrow E_j = \frac{c_j^2}{2m}. \quad (5.34)$$

We have two choices for  $c_{j+1}$ . We choose the one which yields the maximum value for  $E_{j+1}$ , from which we obtain

$$c_j = j \frac{\pi\hbar}{L}. \quad (5.35)$$

Finally, we have

$$a_j = \frac{1}{\sqrt{2m}} \left( p + i \frac{j\pi\hbar}{L} \cot\left(\frac{\pi}{L}x\right) \right). \quad (5.36)$$

It turns out that the  $a_j$  are not the required ladder operators. After some trial and error, we find the following creation and annihilation operators, respectively,

$$A_j^\dagger = \frac{d}{dy} + j \cot(y), \quad (5.37)$$

$$A_j = -\frac{d}{dy} + j \cot(y). \quad (5.38)$$

These operators are *not* Hermitian, and thus not observable. Let us test one of them on the wave function,  $\psi_j(y) = \sqrt{\frac{2}{L}} \sin(jy)$ , i.e.

$$\begin{aligned} A_j^\dagger \psi_j &= \sqrt{\frac{2}{L}} \left[ \frac{d}{dy} \sin(jy) + j \cot(y) \sin(jy) \right] \\ &= \sqrt{\frac{2}{L}} \left[ j \cos(jy) + j \frac{\cos(y)}{\sin(y)} \sin(jy) \right] \\ &= \frac{j}{\sin(y)} \sqrt{\frac{2}{L}} [\cos(jy) \sin(y) + \cos(y) \sin(jy)] \\ &= \frac{j}{\sin(y)} \sqrt{\frac{2}{L}} \sin((j+1)y) \\ &= \frac{j}{\sin(y)} \psi_{j+1}(y). \end{aligned}$$

Thus, we have

$$\sin(y) A_j^\dagger \psi_j(y) = j \psi_{j+1}(y), \quad (5.39)$$

$$\sin(y) A_j \psi_j(y) = j \psi_{j-1}(y). \quad (5.40)$$

Now we introduce the ladder operators which can raise and lower any eigenfunction of our physical system,

$$K_{\pm} = \pm \sin(y) \frac{d}{dy} + \cos(y) K_0, \quad (5.41)$$

where the Hermitian number operator  $K_0$  satisfies the eigenvalue equation,

$$K_0 |j\rangle = j |j\rangle. \quad (5.42)$$

Let us test these operators,

$$\begin{aligned} K_{\pm} \psi_j(y) &= \sqrt{\frac{2}{L}} \sin(y) \left( \pm \frac{d}{dy} \sin(jy) \right) + \sqrt{\frac{2}{L}} \cos(y) j \sin(jy) \\ &= j \sqrt{\frac{2}{L}} [\sin(jy) \cos(y) \pm \sin(y) \cos(jy)] \\ &= j \sqrt{\frac{2}{L}} \sin((j \pm 1)y) \\ &= j \psi_{j \pm 1}(y). \end{aligned}$$

Thus, we have

$$K_{\pm} |j\rangle = j |j \pm 1\rangle. \quad (5.43)$$

These operators satisfy the following properties,

$$K_{\pm}^{\dagger} = K_{\mp}, \quad (5.44)$$

$$[K_-, K_+] = 2K_0, \quad (5.45)$$

$$[K_0, K_{\pm}] = \pm K_{\pm}. \quad (5.46)$$

This set of operators are the generators of the  $\text{su}(1,1)$  Lie algebra [45]. From property (5.44), we see that the ladder operators are non-Hermitian. Furthermore, we can write the Hamiltonian as

$$H = \frac{\pi^2 \hbar^2}{4mL^2} \{K_+, K_-\}, \quad (5.47)$$

where the  $\{, \}$  is the anti-commutator.

### 5.1.3 Coherent States for the Infinite Square Well

Since we have the ladder operators for the particle in an infinite potential well, we should be able to construct generalised coherent states for the system. In our discussion about coherent states, we saw that there are two ways to construct such states. The eigenstate of the annihilation operator is a coherent state. We can also act with the displacement operator on the vacuum to obtain coherent states. For the harmonic oscillator, both methods yield the same coherent state. However, for the particle in an infinite well, this is not the case.

Let us begin by acting with the annihilation operator,  $K_-$ , on some state  $|\alpha\rangle$ . These type of coherent states are referred to as Barut-Girardello (BG) coherent states [45]. If  $|\alpha\rangle$  is a BG coherent state, then

$$K_- |\alpha\rangle = \alpha |\alpha\rangle. \quad (5.48)$$

Writing  $|\alpha\rangle = \sum_{j=1}^{\infty} c_j |j\rangle$ , we have

$$K_- |\alpha\rangle = \sum_{j=1}^{\infty} c_j K_- |j\rangle = \sum_{j=1}^{\infty} c_j j |j-1\rangle = \sum_{j=0}^{\infty} c_{j+1} (j+1) |j\rangle = \alpha \sum_{j=1}^{\infty} c_j |j\rangle.$$

Taking the inner product with respect to  $\langle j'|$ , we have

$$\begin{aligned} \sum_{j=0}^{\infty} c_{j+1} (j+1) \langle j'|j\rangle &= \alpha \sum_{j=1}^{\infty} c_j \langle j'|j\rangle \\ \Rightarrow c_{j+1} (j+1) &= \alpha c_j \\ \Rightarrow c_{j+1} &= \frac{\alpha}{j+1} c_j = \frac{\alpha}{j+1} \frac{\alpha}{j} c_{j-1} = \cdots = \frac{\alpha^j}{(j+1)!} c_1. \end{aligned}$$

Thus, we have

$$|\alpha\rangle_{BG} = N (|\alpha|^2) \sum_{j=0}^{\infty} \frac{\alpha^j}{(j+1)!} |j+1\rangle, \quad (5.49)$$

where  $N (|\alpha|^2) = \left( \sum_{j=0}^{\infty} \frac{|\alpha|^{2j}}{[(j+1)!]^2} \right)^{-1/2}$  is the normalisation factor.

The coherent states that we obtain by applying the displacement operator to the ground state are called Gilmore-Perelomov (GP) coherent states. Using the displacement operator  $D(\xi)$ , we have

$$\begin{aligned} |\alpha\rangle &= D(\xi) |1\rangle = \exp(\xi K_+ - \xi^* K_-) |1\rangle \\ &= e^{\alpha K_+} (1 - |\alpha|^2)^{K_0} e^{-\xi^* K_-} |1\rangle, \end{aligned}$$

where  $\alpha = \frac{\xi}{|\xi|} \tanh(\xi)$ . With a little more work, we finally have

$$|\alpha\rangle_{GP} = \sqrt{1 - |\alpha|^2} \sum_{j=0}^{\infty} \alpha^j |j+1\rangle. \quad (5.50)$$

We see that  $|\alpha\rangle_{BG} \neq |\alpha\rangle_{GP}$ .

Now let us move on to discuss squeezing. Firstly, let us define the Hermitian field operators,

$$X_1 = \frac{K_- + K_+}{2} \quad \text{and} \quad X_2 = \frac{K_- - K_+}{2i}. \quad (5.51)$$

Then we define the squeezing parameter as

$$S_{X_i} = \frac{(\Delta X_i)^2}{\sqrt{\frac{1}{4} |\langle [X_1, X_2] \rangle|^2}} - 1, \quad (5.52)$$

where  $(\Delta X_i)^2 = \langle X_i^2 \rangle - \langle X_i \rangle^2$ . We say that a state is squeezed in  $X_i$  if the following inequality is satisfied,

$$-1 < S_{X_i} < 0. \quad (5.53)$$

Let us define the Mandel parameter  $Q$  [45] as

$$Q = \frac{\langle K_+^2 K_-^2 \rangle - \langle K_+ K_- \rangle^2}{\langle K_+ K_- \rangle} - 1. \quad (5.54)$$

$Q = 0$  corresponds to Poissonian statistics (standard coherent states).

$Q < 0$  corresponds to sub-Poissonian statistics (non-classical states).

$Q > 0$  corresponds to super-Poissonian statistics (classical states).

It is often nice to have a graphical understanding of concepts in physics. In the quantum optics literature, the uncertainty in position/momentum is referred to as “noise”. In phase space, a coherent state has a Gaussian distribution which is circularly symmetric. A squeezed state, on the other hand, is asymmetrical. By “squeezing”, we suppress the noise in one direction, while increasing the noise in the other direction (we have to do this in accordance with the Heisenberg uncertainty principle). This has useful practical ramifications. By squeezing, the wave packet has a sharper peak, thus minimising interference effects. By minimising interference effects, we may perform more accurate measurements. Greater accuracy would mean less uncertainty in the outcome of measurements.



Figure 18: Two sketches comparing a coherent state to a squeezed state, as represented in phase space.

Let us play around with these ideas about coherent states and squeezed states within the context of the particle in an infinite potential well. Recall from equation (5.49) the definition of the BG coherent states. We can construct a wave function for these states by representing

the states in the position basis, i.e.

$$\langle x|\alpha\rangle_{\text{BG}} \equiv \varphi(x) = N (|\alpha|^2) \sum_{j=0}^{\infty} \frac{\alpha^j}{(j+1)!} \psi_{j+1}(x). \quad (5.55)$$

The original wave function consists of a sine function, which can be expressed as the imaginary part of an exponential. This allows us to write

$$\varphi(x) = \sqrt{\frac{2}{L}} N (|\alpha|^2) \sum_{j=0}^{\infty} \frac{\alpha^j}{(j+1)!} \text{Im} \left( e^{i\left(\frac{\pi x}{L}(j+1)\right)} \right). \quad (5.56)$$

Using Mathematica, it is possible to get a closed form expression for the infinite sum in equation (5.56). For constants  $b$  and  $c$ , we have

$$\sum_{k=0}^{\infty} \frac{c^k}{(k+1)!} e^{b(k+1)} = \frac{1}{c} \left( e^{ce^b} - 1 \right). \quad (5.57)$$

Using this identity, we can express the BG coherent state wave function as

$$\varphi(x) = \sqrt{\frac{2}{L}} N (|\alpha|^2) \text{Im} \left[ \frac{1}{\alpha} \left( e^{\alpha e^{i\frac{\pi x}{L}}} - 1 \right) \right]. \quad (5.58)$$

By expanding the terms in the square brackets, and extracting only the imaginary part, we have

$$\varphi(x) = \sqrt{\frac{2}{L}} N (|\alpha|^2) \frac{1}{\alpha} e^{\alpha \cos\left(\frac{\pi x}{L}\right)} \sin \left( \alpha \sin \left( \frac{\pi x}{L} \right) \right). \quad (5.59)$$

This expression is significantly more complicated than the ordinary wave function (equation(4.26)). However, there does exist some similarity between this BG coherent wave function and the wave function for the particle in a finite well (equation(4.51)). Apart from multiplicative constants, there is a product of an exponential function and a sine function in both types of wave functions. From our understanding of trigonometric functions, we know that the cosine function is zero when the sine function is a maximum, and vice versa. When the  $x$ -value yields a maximum for the sine function, we have

$$\varphi_{\text{max}}(x) = \sqrt{\frac{2}{L}} N (|\alpha|^2) \frac{1}{\alpha} \sin(\alpha). \quad (5.60)$$

We can also calculate the squeezed BG coherent states by acting on the BG coherent states with the squeeze operator. The squeeze operator was defined in equation (5.17). For the infinite potential well, we replace the operators  $a$  and  $a^\dagger$  with  $K_-$  and  $K_+$ , respectively. Expanding to first order, we have

$$\begin{aligned} S(\xi) &= e^{\frac{1}{2}\xi^* K_-^2 - \frac{1}{2}\xi K_+^2} \\ &= 1 - \frac{1}{2}\xi K_+^2 + \frac{1}{2}\xi^* K_-^2. \end{aligned} \quad (5.61)$$

Acting on the BG coherent states, we have

$$S(\xi) |\alpha\rangle_{\text{BG}} = N(|\alpha|^2) \sum_{j=0}^{\infty} \frac{\alpha^j}{(j+1)!} \left( |j+1\rangle - \frac{(j+1)(j+2)}{2} \xi |j+3\rangle + \frac{j(j+1)}{2} \xi^* |j-1\rangle \right). \quad (5.62)$$

We can express these squeezed BG coherent states in the position representation, i.e.

$$\langle x | S(\xi) |\alpha\rangle_{\text{BG}} = N(|\alpha|^2) \sum_{j=0}^{\infty} \frac{\alpha^j}{(j+1)!} \left( \psi_{j+1}(x) - \frac{(j+1)(j+2)}{2} \xi \psi_{j+3}(x) + \frac{j(j+1)}{2} \xi^* \psi_{j-1}(x) \right). \quad (5.63)$$

We can construct a density matrix from these wave functions and compute the von Neumann entropy. However, upon inspection, it is clear that the entropy for the BG coherent states is greater than the entropy for the ordinary states. Furthermore, the entropy of the squeezed coherent states is greater than the entropy of the coherent states. If we were to create an ensemble of these coherent states, and then calculate the ensemble average for some observable, we would certainly obtain different results from those obtained in section 4. However, we propose that quantum typicality would still be realised. This is because the wave function for the BG coherent states (equation (5.59)) is similar in structure to the wave function of the finite potential well (equation (4.51)). By calculating the moments, as we did in section 4.1.2, we would derive similar results. We would find that it is not possible to distinguish microstates, whether those states are squeezed and coherent or not. However, we shall not explicitly do this, since this section is not concerned with quantum typicality.

There is no point in performing the same analysis on the GP coherent states, since the sum in equation (5.50) diverges. This divergence prevents us from deriving closed form expressions for the wave functions of the GP coherent, and squeezed GP coherent, states.

In the next subsection, we shall look at an analysis in which the entropy of density perturbations is calculated by studying the two-mode squeezed states of the spacetime vacuum.

#### 5.1.4 Entropy of a Squeezed Vacuum

The vacuum state is the initial state for modes inside the black hole horizon. Decoupling occurs for the modes with different momenta. Using the two-mode squeeze operator formalism, it is possible to provide an accurate description of the growth of the cosmological perturbations [47]. This is because it describes the process of creation and annihilation of particle pairs in a way which preserves momentum. These particle pairs are produced with momenta equal in magnitude, but opposite in sign.

In a simple model, described by a Hamiltonian which is quadratic in a scalar field  $\hat{\phi}$  and its conjugate momentum  $\hat{\pi}$ , the authors in [47] represent the dynamics of linearised cosmological perturbations. Particles which interact with the classical background fields (spacetime) are described by the field  $\hat{\phi}$ . The quadratic Hamiltonian is then written as a sum of a free part

and an interacting part, i.e.

$$H = H^{(0)} + H^{\text{int}}, \quad (5.64)$$

where

$$H^{(0)} = \sum_{\{k, k_x > 0\}} H_k^{(0)} = \sum_{\{k, k_x > 0\}} \Omega_k \left[ a_k^\dagger a_k - a_{-k}^\dagger a_{-k} + 1 \right] \quad (5.65)$$

is the free part of the Hamiltonian. The time-dependent frequency associated with the  $k^{\text{th}}$  mode is represented by  $\Omega_k$ , and the sum is carried over half of the modes (this is why we write  $k_x > 0$ ). The interaction Hamiltonian is written as

$$H^{\text{int}} = \sum_{\{k, k_x > 0\}} H_k^{\text{int}} = \sum_{\{k, k_x > 0\}} i\lambda_k(t) \left[ e^{-2i\varphi_k} a_k a_{-k} - e^{2i\varphi_k} a_k^\dagger a_{-k}^\dagger \right], \quad (5.66)$$

where  $a_k^\dagger$  is the creation operator, and  $a_k$  is the annihilation operator for a particle with momentum  $k$ . The process of production ( $a_k^\dagger a_{-k}^\dagger$ ) and destruction ( $a_k a_{-k}$ ) of particle pairs is described in the interaction Hamiltonian.  $\lambda_k$  is a function which describes the coupling of the perturbations to the classical background (spacetime). The phase  $\varphi_k$  is related to the phase of the particle pairs which are generated. It varies slowly as a function of time (when modes cross the horizon, the variation is most significant).

Once we have the Hamiltonian, the evolution operator can be written as

$$\hat{U}(t) = \hat{S}(\{r_k, \phi_k\}) \exp \left[ -i \int^t dt' H^{(0)}(t') \right], \quad (5.67)$$

where  $\hat{S}$  is the two-mode squeeze operator, written as

$$\hat{S}(\{r_k, \phi_k\}) = \prod_{\{k, k_x > 0\}} \hat{S}(r_k, \phi_k) = \prod_{\{k, k_x > 0\}} \exp \left[ r_k \left( a_k a_{-k} e^{-2i\phi_k} - a_k^\dagger a_{-k}^\dagger e^{2i\phi_k} \right) \right]. \quad (5.68)$$

The squeezing parameter,  $r_k$ , is related to the coupling strength  $\lambda_k$  in the form  $r_k \approx \int_{t_x}^t \lambda_k(t') dt'$ , where  $t_x$  is the approximate time at which the mode leaves the horizon. The squeeze phase is  $\phi_k \approx \varphi_k - \int^{t_x} \Omega_k(t') dt'$ . For additional convenience, the two-mode squeeze operator can be written as

$$\begin{aligned} \hat{S}(r_k, \phi_k) &= \frac{1}{\cosh r_k} \exp \left[ -a_k^\dagger a_{-k}^\dagger e^{2i\phi_k} \tanh r_k \right] \exp \left[ - \left( a_k^\dagger a_k + a_{-k}^\dagger a_{-k} \right) \ln \cosh r_k \right] \times \\ &\quad \times \exp \left[ a_k a_{-k} e^{-2i\phi_k} \tanh r_k \right]. \end{aligned} \quad (5.69)$$

Applying this to the vacuum state  $|0\rangle$ , we get

$$\hat{S}(r_k, \phi_k) |0\rangle \equiv |ss_k\rangle = \sum_{n=0}^{\infty} \frac{1}{\cosh r_k} \left( -e^{2i\phi_k \tanh r_k} \right)^n |n, k; n, -k\rangle, \quad (5.70)$$

where  $|ss_k\rangle$  denotes the two-mode squeezed vacuum state, and

$$|n, k; n, -k\rangle = \frac{(a_k^\dagger a_{-k}^\dagger)^n}{n!} |0\rangle \quad (5.71)$$

denotes the two-mode occupation number state, which contains  $n$  particles with momentum  $k$ , and  $n$  particles with momentum  $-k$ .

The goal now is to calculate the entropy. We shall concern ourselves with the entropy generated by the reduction of the density matrix. In the Schrödinger picture, the density matrix is  $\hat{\rho} = |\psi, t\rangle \langle \psi, t|$ , where  $|\psi, t\rangle = \hat{U}(t) |\psi, 0\rangle$ . We use  $\hat{U}(t)$  as was defined in equation (5.67), and take  $|\psi, 0\rangle = |0\rangle_{\text{in}}$  as the *in* vacuum state. The entropy is then given by ( $k_B = 1$ )

$$S = -\langle \ln \hat{\rho} \rangle \equiv -\text{Tr}(\hat{\rho} \ln \hat{\rho}). \quad (5.72)$$

By looking at equations (5.70) and (5.71), we can write the density matrix in the occupation number basis as

$$\begin{aligned} \hat{\rho} = & \sum_{\{n_k, k_x > 0\}} \sum_{\{n_{k'}, k'_x > 0\}} \prod_{\{k, k_x > 0\}} \prod_{\{k', k'_x > 0\}} \frac{1}{\cosh r_k} \frac{1}{\cosh r_{k'}} (-e^{-2i\phi_k} \tanh r_k)^{n_k} \times \\ & \times (-e^{2i\phi_{k'}} \tanh r_{k'})^{n_{k'}} |n_k, k; n_{k'}, -k\rangle \langle n_{k'}, k'; n_k, -k|. \end{aligned} \quad (5.73)$$

We observe particles in the occupation number basis, so it is a natural choice in which to represent the density matrix. By setting all the off-diagonal elements in the two-mode occupation number basis (equation (5.73)) to zero, we can reduce the full density matrix. We can justify this procedure by observing that in the limit of large squeezing, every mode is the consequence of a superposition of a large number of particle pairs. Due to destructive interference in the off-diagonal terms, the phases  $\phi_k$  of every produced particle pair cancels. Consequently, the reduced density matrix becomes approximately diagonal [47], i.e.

$$\hat{\rho}_{\text{red}} \approx \sum_{\{n_k, k_x > 0\}} \prod_{\{k, k_x > 0\}} \frac{1}{\cosh^2 r_k} (\tanh r_k)^{2n_k} \ln \left[ \prod_{\{k', k'_x > 0\}} \frac{1}{\cosh^2 r_{k'}} (\tanh r_{k'})^{2n_{k'}} \right]. \quad (5.74)$$

We can rewrite this expression as

$$\begin{aligned} S = & \sum_{\{n_k, k_x > 0, k \neq k'\}} \prod_{\{k \neq k', k_x > 0\}} \frac{1}{\cosh^2 r_k} (\tanh r_k)^{2n_k} \times \\ & \times \left[ \sum_{\{k', k'_x > 0\}} \sum_{n_{k'}} \frac{1}{\cosh^2 r_{k'}} (\tanh r_{k'})^{2n_{k'}} \ln [\cosh^2 r_{k'} (\tanh r_{k'})^{-2n_{k'}}] \right]. \end{aligned} \quad (5.75)$$

The first part of this expression equals 1, and the second part, with  $k' \rightarrow k$ , is

$$S = \sum_{\{n_k, k_x > 0\}} [(1 + \sinh^2 r_k) \ln (1 + \sinh^2 r_k) - \sinh^2 r_k \ln \sinh^2 r_k]. \quad (5.76)$$

The coarse-graining determines the expression for the entropy. We choose the coarse-graining based on the relevant interaction with the environment fields. For instance, an alternative mechanism for coarse-graining can be chosen whereby we assume that the density matrix diagonalises in the coherent state basis. In this basis, the entropy per mode is  $s_k = \ln(1 + \sinh^2 r_k) + 2$ , which reduces to the same expression as (5.76) in the limit of large  $n_k$ . In the thermodynamic limit, or in the limit of large  $n_k$ , these differences are indistinguishable. However, if we could perform a measurement of extreme precision, we would notice detectable differences in the entropies derived from the different coarse-graining schemes. We can conclude that different coarse-graining schemes lead to different expressions for the entropy.

This conclusion shouldn't be too surprising, since we know that entropy is related to our ignorance or uncertainty with regards to a physical system. During the process of coarse-graining, we choose to ignore certain degrees of freedom. This occurs when a subsystem interacts with the environment. By choosing to leave out or ignore the degrees of freedom of the environment, we consequently introduce uncertainty into our description of our subsystem.

## 5.2 Decoherence in Quantum Systems

In this subsection, we shall discuss the phenomenon of quantum decoherence. Quantum decoherence is the process in which quantum coherence is decreased, and ultimately lost. In optics or the study of classical waves, coherence among waves can be interpreted as a definite or consistent relationship among the phases of the waves. In quantum mechanics, matter exhibits a wave-particle duality. Quantum coherence describes the phase relationship among the wave aspects of the matter.

When the phase relationship among the waves is destroyed, decoherence occurs. This makes the system lose its “quantumness”, and become classical. Decoherence occurs when a system interacts with the environment. In fact, decoherence is responsible for entangled pairs becoming disentangled.

Let us try to describe decoherence more mathematically. Suppose a quantum system is described by a density matrix. The diagonal elements of this matrix describes the respective probabilities of finding the system in the respective states. The off-diagonal elements represent quantum coherence. Decoherence occurs if it is possible to somehow reduce this density matrix so that it becomes diagonal, or at least “approximately diagonal”.

In this subsection, we shall look at a simple decoherence model [48]. We shall also discuss how Hawking radiation can come about as a consequence of decoherence [50].

### 5.2.1 A Simple Decoherence Quantum Model

Let us consider a wave function which describes the superposition of two states within an infinite potential well,

$$\Psi(x, t) = \frac{1}{\sqrt{2}} [\psi_1(x, t) + \psi_2(x, t)], \quad (5.77)$$

where

$$\psi_n(x, t) = \sqrt{\frac{2}{L}} \sin\left(\frac{n\pi x}{L}\right) e^{-i\omega_n t}, \quad (5.78)$$

and  $\omega_n = \frac{n^2\pi^2\hbar}{2mL^2}$ . The modulus squared of the superposition wave function is

$$|\Psi(x, t)|^2 = \frac{1}{2} (|\psi_1|^2 + |\psi_2|^2) + |\psi_1||\psi_2| \cos(\omega t), \quad (5.79)$$

where  $\omega = \omega_2 - \omega_1$ .

We notice that the term  $|\psi_1||\psi_2| \cos(\omega t)$  is time dependent. This is the interference term between  $\psi_1$  and  $\psi_2$ . Our goal is to show that, by allowing the boundaries of the infinite potential well to fluctuate, this interference term eventually becomes negligible after a certain amount of time.

We begin by allowing the width parameter,  $L$ , to undergo fluctuations about a mean value,  $\bar{L}$ . This mean value is defined such that

$$L = \bar{L}(1 + \varepsilon), \quad (5.80)$$

where

$$f(\varepsilon) = \sqrt{\frac{\theta}{\pi}} e^{-\theta\varepsilon^2}, \quad (5.81)$$

$$\sigma^2 = \langle \varepsilon^2 \rangle - \langle \varepsilon \rangle^2, \quad (5.82)$$

and

$$\theta = \frac{1}{2\sigma^2}. \quad (5.83)$$

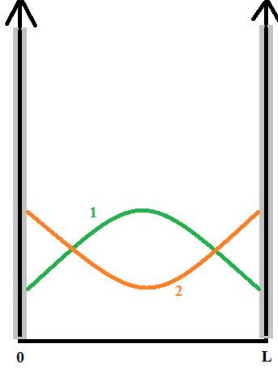


Figure 19: A simple sketch of the infinite potential well of length  $L$ . The grey regions illustrate how the length of well fluctuates.

The  $\langle \rangle$  notation is used to signify the mean value of a function, i.e.

$$\langle G \rangle = \int_{-\infty}^{+\infty} d\varepsilon G(\varepsilon) f(\varepsilon). \quad (5.84)$$

We wish to find an expression for the mean value of the superposition wave function. We have

$$\langle |\Psi|^2 \rangle = \frac{1}{2} (\langle |\psi_1|^2 \rangle + \langle |\psi_2|^2 \rangle) + \langle |\psi_1| |\psi_2| \cos(\omega t) \rangle. \quad (5.85)$$

Let us first consider the terms inside the brackets. Using equations (5.78) and (5.84), we have

$$\langle |\psi_n|^2 \rangle = \sqrt{\frac{4\theta}{\pi}} \int_{-\infty}^{+\infty} d\varepsilon \frac{e^{-\theta\varepsilon^2}}{\bar{L}(1+\varepsilon)} \sin^2 \left( \frac{n\pi x}{\bar{L}(1+\varepsilon)} \right). \quad (5.86)$$

We assume to have a narrow distribution,  $\sigma \ll 1$ , so that only small values of  $\varepsilon$  contributes to the expression in (5.86). Now we need to make use of the famous trigonometric identity,

$$\sin^2 u = 1 - \cos^2 u = \frac{1 - \cos 2u}{2} = \frac{1 - \operatorname{Re}(e^{i2u})}{2}. \quad (5.87)$$

Inside the exponential, we expand to first order in  $\varepsilon$ . This gives us

$$\operatorname{Re} \left( e^{\frac{2in\pi x}{\bar{L}(1+\varepsilon)}} \right) \approx \operatorname{Re} \left( e^{\frac{2in\pi x}{\bar{L}} - \frac{2in\pi x}{\bar{L}} \varepsilon} \right) = \cos \left( \frac{2n\pi x}{\bar{L}} \right) e^{i \left( \frac{2n\pi x}{\bar{L}} \right) \varepsilon}. \quad (5.88)$$

This allows us to write

$$\sin^2 \left( \frac{n\pi x}{\bar{L}(1+\varepsilon)} \right) \approx \frac{1}{2} - \frac{1}{2} \cos \left( \frac{2n\pi x}{\bar{L}} \right) e^{i \left( \frac{2n\pi x}{\bar{L}} \right) \varepsilon}. \quad (5.89)$$

Now we need to make use of another important identity, i.e.

$$\int_{-\infty}^{\infty} d\varepsilon e^{\pm it\varepsilon - \theta\varepsilon^2} = \sqrt{\frac{\pi}{\theta}} e^{-\frac{t^2}{4\theta}}. \quad (5.90)$$

Using equations (5.89) and (5.90), we can evaluate equation (5.86). We have

$$\begin{aligned}
\langle |\psi_n|^2 \rangle &= \sqrt{\frac{4\theta}{\pi}} \int_{-\infty}^{+\infty} d\varepsilon \frac{e^{-\theta\varepsilon^2}}{\bar{L}(1+\varepsilon)} \sin^2 \left( \frac{n\pi x}{\bar{L}(1+\varepsilon)} \right) \\
&\approx \sqrt{\frac{4\theta}{\pi}} \int_{-\infty}^{+\infty} d\varepsilon \frac{e^{-\theta\varepsilon^2}}{\bar{L}(1+\varepsilon)} \left[ \frac{1}{2} - \frac{1}{2} \cos \left( \frac{2n\pi x}{\bar{L}} \right) e^{i\left(\frac{2n\pi x}{\bar{L}}\right)\varepsilon} \right] \\
&= \sqrt{\frac{\theta}{\pi}} \int_{-\infty}^{\infty} d\varepsilon \frac{e^{-\theta\varepsilon^2}}{\bar{L}(1+\varepsilon)} - \sqrt{\frac{\theta}{\pi}} \cos \left( \frac{2n\pi x}{\bar{L}} \right) \int_{-\infty}^{\infty} \frac{1}{\bar{L}(1+\varepsilon)} e^{-i\left(\frac{2n\pi x}{\bar{L}}\right)\varepsilon - \theta\varepsilon^2} d\varepsilon \\
&\approx \frac{1}{\bar{L}} - \frac{1}{\bar{L}} \cos \left( \frac{2n\pi x}{\bar{L}} \right) e^{-\frac{n^2\pi^2\sigma^2 x^2}{\bar{L}^2}}.
\end{aligned}$$

In the limit where  $\frac{\pi\sigma x}{\bar{L}} \ll 1$ , we have  $e^{-\frac{n^2\pi^2\sigma^2 x^2}{\bar{L}^2}} \approx 1$ . Finally, we have

$$\langle |\psi_n|^2 \rangle \approx \frac{1}{\bar{L}} - \frac{1}{\bar{L}} \cos \left( \frac{2n\pi x}{\bar{L}} \right) = \frac{2}{\bar{L}} \sin^2 \left( \frac{n\pi x}{\bar{L}} \right) = |\psi_n|^2. \quad (5.91)$$

We see that the probability density is not significantly affected by the fluctuating boundaries. Our next goal is to see how the interference term is affected. We can show that [48]

$$\langle |\psi_1||\psi_2| \cos(\omega t) \rangle = \frac{1}{\bar{L}} \left[ \cos \left( \frac{\pi x}{\bar{L}} \right) - \cos \left( \frac{3\pi x}{\bar{L}} \right) \right] \cos(\bar{\omega} t) e^{-\Gamma t^2}, \quad (5.92)$$

where  $\Gamma = 2\bar{\omega}^2\sigma^2$  and  $\bar{\omega} = \omega_2(\bar{L}) - \omega_1(\bar{L}) = \frac{3h\pi^2}{2m\bar{L}^2}$ .

We see that there is a decay in (5.92), whose time scale is  $t_0 = \frac{1}{\bar{\omega}}$ . The characteristic decay time is  $t_d = \frac{1}{\sqrt{\Gamma}} = \frac{t_0}{\sqrt{2}\sigma}$ . Finally, we can write

$$\langle |\Psi|^2 \rangle = \frac{1}{2} (\langle |\psi_1|^2 \rangle + \langle |\psi_2|^2 \rangle) + \frac{1}{\bar{L}} \left[ \cos \left( \frac{\pi x}{\bar{L}} \right) - \cos \left( \frac{3\pi x}{\bar{L}} \right) \right] \cos(\bar{\omega} t) e^{-\Gamma t^2}. \quad (5.93)$$

If  $t \gg t_d$ , the term  $\frac{1}{\bar{L}} [\cos(\frac{\pi x}{\bar{L}}) - \cos(\frac{3\pi x}{\bar{L}})] \cos(\bar{\omega} t) e^{-\Gamma t^2} \rightarrow 0$ . The interference term disappears.

This model serves as a simple quantum system which illustrates decoherence. We can think of the fluctuating boundaries as analogous to spacetime. Consider gravitational waves in a flat background which has the metric, [49]

$$ds^2 = -dt^2 + h_{ij} dx^i dx^j. \quad (5.94)$$

As the metric fluctuates, the square of the proper length,

$$dl^2 = h_{ij} dx^i dx^j, \quad (5.95)$$

also fluctuates. Consequently, this causes the separation distance between geodesics in the vicinity to also fluctuate. If there is a quantum system nearby, these length fluctuations can lead to quantum phase fluctuations. This dephasing results in decoherence.

The authors in [49] replace the classical gravity wave with a bath of gravitons. This is done so that the fluctuations in the spacetime geometry can be studied. Inside this bath, quantum phase fluctuations occur, ultimately leading to dephasing and an increase in the “fuzziness” of an interference pattern. For a fixed energy density, the decoherence rate increases as the wavelengths of the gravitons increase. It also increases as the energy differences in the quantum system increase. The end result is that gravitational decoherence, i.e. the loss of quantum coherence due to the effects of gravity, is possible.

This model which consists of a graviton bath is more complicated than the simple infinite potential well model that was discussed in section 5.2.1. In the infinite potential well model, which is a quantum system, decoherence occurs as a consequence of the boundaries fluctuating. In the case of the graviton bath, the source for decoherence is studied. The fluctuations in the geometry of spacetime can affect quantum systems in such a way as to cause decoherence.

Now we shall move on to discuss Hawking radiation.

### 5.2.2 Hawking Radiation from Decoherence

The black hole information paradox violates the principle of unitarity in quantum mechanics. During the black hole evaporation process, it appears that pure quantum states evolve into mixed states. The author in [50] argues that Hawking radiation remains in a pure state. It is due to the irreversible process of decoherence that the Hawking radiation appears to be in a mixed state.

Let us consider a massless scalar field  $\phi$ , and an Unruh observer in Minkowski spacetime. We shall also consider a hypersurface of constant Rindler time (denoted  $t$ ) which connects the left and right Rindler wedges. In the Minkowski vacuum, if we trace out the modes of the left part, we get a density matrix in the right part which corresponds to a canonical ensemble with temperature  $\frac{a}{2\pi}$ , where  $a$  is the acceleration of the observer.

Alternatively, we can impose the boundary condition  $\phi = 0$  at the origin. Upon doing this, the evolution along the right part of the hypersurfaces is given by the quantum state

$$\Psi \propto \exp \left[ - \int_{-\infty}^{+\infty} k \coth \left( \frac{\pi k}{2a} + ikt \right) |\phi(k)|^2 dk \right], \quad (5.96)$$

where  $\phi(k)$  is the Fourier transform of the scalar field  $\phi$ . For a four-dimensional Schwarzschild black hole, we assume the same result holds by replacing  $a$  with the surface gravity,  $\kappa \equiv \frac{1}{4G_N M}$ . For the mode  $\vec{k}$ , the expectation value of the number operator in this state is given by

$$\langle n_{\vec{k}} \rangle = \frac{1}{e^{8\pi\omega G_N M} - 1}, \quad (5.97)$$

where  $\omega = |\vec{k}| = k$ .

In [47], as was discussed in the previous subsection, it was shown that for every mode, the vacuum quantum state in a black hole spacetime is given by a two-mode squeezed vacuum. (An inflationary phase of the early universe also yields such a state) [47]. The squeezing parameter is given by

$$\tanh r_k = e^{-4\pi\omega G_{NM}}. \quad (5.98)$$

As  $r_k \rightarrow 0$ ,  $\omega$  increases, which means the wavelength is small, since  $\lambda \sim \frac{1}{\omega}$ . As  $r_k \rightarrow \infty$ ,  $\omega$  decreases, which means the wavelength is large. We deduce that for small wavelengths, there is no squeezing. For large wavelengths, there is high squeezing.

Using equation (5.98), we can express the expectation value of the number operator as

$$\langle n_{\vec{k}} \rangle = \frac{1}{e^{8\pi\omega G_{NM}} - 1} = \frac{(e^{-4\pi\omega G_{NM}})^2}{1 - (e^{-4\pi\omega G_{NM}})^2} = \frac{\tanh^2 r_k}{1 - \tanh^2 r_k} = \sinh^2 r_k. \quad (5.99)$$

Wien's law states that

$$\lambda_{\max} T = 2.898 \times 10^{-3} K.m, \quad (5.100)$$

where the black hole temperature is  $T = \frac{1}{8\pi G_{NM}}$ . At the maximum of the Planck spectrum, we find that  $r_k \approx 0.25$ . This corresponds to  $\langle n_{\vec{k}} \rangle \approx 0.06$ .

Let us suppose that space is finite, i.e. the black hole is in a box. This allows us to write  $\Psi = \prod_{\vec{k}} \psi_{\vec{k}}$ , where

$$\psi_{\vec{k}} \propto \exp[-k \coth(2\pi k G_{NM} + ikt) |\phi(k)|^2]. \quad (5.101)$$

We can express this differently, by rewriting the hyperbolic cotangent as

$$\coth(2\pi k G_{NM} + ikt) = \frac{1 + e^{-4\pi k G_{NM} + ikt}}{1 - e^{-4\pi k G_{NM} + ikt}} = \frac{1 + e^{2i\varphi_k} \tanh r_k}{1 - e^{2i\varphi_k} \tanh r_k}, \quad (5.102)$$

where  $\varphi_k = -kt$  is the squeezing angle. Now we have

$$\psi_{\vec{k}} \propto \exp\left[-k \frac{1 + e^{2i\varphi_k} \tanh r_k}{1 - e^{2i\varphi_k} \tanh r_k} |\phi(k)|^2\right] \equiv \exp[-(\Omega_R + i\Omega_I) |\phi(k)|^2]. \quad (5.103)$$

The Wigner function for every mode is

$$W(\phi, p) = \frac{1}{\pi} \exp\left[-\frac{2(p + \Omega_I)^2}{\Omega_R} - 2\Omega_R \phi^2\right], \quad (5.104)$$

where  $\phi$  and  $p$  denote a single mode of the field and its momentum, respectively. In phase space, the contour of the Wigner function explicitly shows both the direction and the amount of squeezing for a given squeezed state.  $p$  is peaked around its classical value,  $p_{\text{cl}} = -\Omega_I$ , with a width of  $\sqrt{\Omega_R}$ . The field mode  $\phi$  is peaked around zero, with a width of  $\frac{1}{\sqrt{\Omega_R}}$ .

The time-dependent form of  $\Omega_R$  is given by [50]

$$\Omega_R(t) = k \frac{1 - e^{-8\pi\omega G_{NM}}}{1 + e^{-8\pi\omega G_{NM}} - 2e^{-4\pi\omega G_{NM}} \cos(2kt)}. \quad (5.105)$$

At  $t = 0$ , we have

$$\begin{aligned}
\Omega_R(0) &= k \frac{1 - e^{-8\pi\omega G_N M}}{1 - 2e^{-4\pi\omega G_N M} + e^{-8\pi\omega G_N M}} \\
&= k \frac{1 - (e^{-4\pi\omega G_N M})^2}{(1 - e^{-4\pi\omega G_N M})^2} \\
&= k \frac{1 + e^{-4\pi\omega G_N M}}{1 - e^{-4\pi\omega G_N M}} \\
&= k \frac{1 + \tanh r_k}{1 - \tanh r_k} \\
&> k.
\end{aligned} \tag{5.106}$$

At  $t = \frac{\pi}{2k}$ , we have

$$\begin{aligned}
\Omega_R\left(\frac{\pi}{2k}\right) &= k \frac{1 - e^{-8\pi\omega G_N M}}{1 + 2e^{-4\pi\omega G_N M} + e^{-8\pi\omega G_N M}} \\
&= k \frac{1 - e^{-4\pi\omega G_N M}}{1 + e^{-4\pi\omega G_N M}} \\
&< k.
\end{aligned} \tag{5.107}$$

In the ground state, where  $r_k = 0$ , we have  $\Omega_R = k$ . Upon comparing a state to the ground state, we deduce that for  $\Omega_R(0) > k$ , the state is squeezed in  $\phi$ . For  $\Omega_R\left(\frac{\pi}{2k}\right) < k$ , the state is squeezed in the  $p$ -direction. Upon calculating the ratio, we find

$$\frac{\Omega_R\left(\frac{\pi}{2k}\right)}{\Omega_R(0)} = \tanh^2(2\pi\omega G_N M) \approx 0.37. \tag{5.108}$$

The typical time scale of the exchange of squeezing between  $\phi$  and  $p$  is  $t_k = \frac{\pi}{2k} \approx 14G_N M$ . Since  $t_k$  is much smaller than typical observation times, we can perform a coarse-graining with respect to the squeezing angle. The squeezing angle is quickly rotating. Since squeezed states are highly sensitive to interactions with environmental degrees of freedom, we find that this interaction leads to the reduced density matrix, in the occupation number basis, becoming approximately diagonal. Consequently, the local entropy is maximised. This corresponds to the Wigner ellipse being coarse-grained into a circle. The entropy is given by

$$S_k = (1 + n_k) \ln(1 + n_k) - n_k \ln n_k \rightarrow 2r_k. \tag{5.109}$$

If we integrate over all modes, we get  $S = \left(\frac{2\pi^2}{45}\right) T_H V$ , which is the entropy corresponding to the Hawking radiation. We deduce that we cannot distinguish between the pure squeezed state and a canonical ensemble with temperature  $T_H = \frac{1}{8\pi G_N M}$ . It's interesting to point out that the state remains a pure state.

The discussion above refers to hypersurfaces which remain outside the black hole horizon. The author shows in [50] that the above arguments should also hold for hypersurfaces which

enter the black hole horizon. In the above argument, a mixed state never occurs. There is no pure state to mixed state evolution. This suggests that unitarity is conserved during the entire black hole evolution, so we can conclude that no information is lost.

Recall that the AdS/CFT correspondence asserts that quantum gravity in the AdS bulk is dual to a conformal field theory on the AdS boundary [13]. The conformal field theory on the boundary does not allow for pure to mixed state evolution. In other words, unitarity is manifest in the conformal field theory. Using the AdS/CFT “dictionary”, we can conclude that pure to mixed state evolution is not possible in the gravitational theory. This includes the formation and evaporation of black holes. It is interesting to note that two very different approaches to the black hole information paradox lead to the same conclusion: no information is lost. Despite these conclusions, this does not mean that the black hole information paradox has been resolved.

In this section, we studied aspects of the black hole entropy in a more general sense. Much of what was discussed may have applications in cosmology. For instance, in [47], the author makes several references to cosmic inflation. The squeezing of the initial vacuum state occurs mostly during the process of cosmic inflation, which was a very brief period in the very early universe [51]. We shall not discuss cosmological models here. However, by studying the squeezed vacuum at the black hole horizon, and integrating over all the modes, it was shown in [50] that the expression for the entropy corresponds to the entropy associated with Hawking radiation.

## 6 Conclusion

We began this dissertation by talking about the thermodynamic properties of black holes. We showed that black holes have a finite, and quite large, entropy. We also saw that a semi-classical analysis of black holes demonstrates that black holes radiate energy, Hawking radiation.

We went through the derivation of Hawking radiation for a star that collapses. In Minkowski space, black holes eventually evaporate away. For this reason, it is often useful to study black holes in AdS space, where the black holes come to equilibrium with their Hawking radiation. We studied some of the properties of AdS space and black holes in this spacetime. By introducing the AdS/CFT correspondence, we were able to discuss more precisely what it means for a black hole to reach equilibrium in AdS space.

The following section discussed aspects of quantum information theory, primarily with the goal of trying to apply these concepts to black holes. Entropy was discussed and formulated within the framework of quantum information theory. In this sense, entropy is a measure of uncertainty. We also discussed quantum entanglement and the idea of quantum cloning. The link between quantum information and black holes is the black hole information paradox, where there is an inconsistency in trying to reconcile quantum theory with general relativity. We introduced the idea of quantum typicality and Levy's lemma, which allows us to quantify typicality. Quantum typicality allows us to make generalisations about an entire ensemble merely by studying some of the states within the ensemble. Conversely, having knowledge about the entire ensemble can allow us to draw conclusions about the underlying microstates.

In the fourth section, we embarked on a study of several quantum models. We found that for the models considered in sections 4.1.1 and 4.1.2, it is very difficult, if not downright impossible, to distinguish microstates. For the Morse potential, the quantum model failed to exhibit typicality. We hypothesised that this is due to the fact that the wave function consists of orthogonal functions. These calculations were done within the framework of the microcanonical formalism. We used Levy's lemma and Chebyshev's inequality to quantify our results. (It is important to note that Levy's lemma does *not* apply to the canonical formalism, since the states cannot be interpreted as being uniformly distributed over the surface of a  $d$ -dimensional sphere, due to the fact that not all microstates have the same probability of occurring). However, by virtue of the thermodynamic limit, these results extend to the canonical formalism as well. In the canonical formalism, we studied an interesting example in which it was shown that black hole radiation and black body radiation are indistinguishable in the thermodynamic limit.

The final section tackled the idea of decoherence. Before we could study decoherence, we had to introduce coherent states and squeezed states. We studied the coherent states and squeezed states for a particle in an infinite potential well. The main idea was to try to see if we could relate some ideas from the entropy of the squeezed states of a simple quantum model, and the entropy of black holes. We found expressions for the wave functions of a

class of coherent states, and squeezed coherent states, for the particle in an infinite potential well. We then deduced that the von Neumann entropy is larger for these wave functions than for the ordinary wave functions. Furthermore, we argued that our inability to distinguish among the microstates would still be true, even though the wave functions have been altered. This means that squeezed states and coherent states do not make it any easier to distinguish microstates within an ensemble.

Finally, we looked at a simple quantum model which demonstrated how decoherence comes about from fluctuating boundaries. These fluctuating boundaries are analogous to spacetime fluctuations. We briefly discussed how fluctuations in the spacetime geometry can cause decoherence in quantum systems. We then studied how Hawking radiation can be interpreted as an effect of decoherence. Interestingly, it was found that no information is lost.

# A The Morse Potential

## A.1 The Energy Levels

We consider a potential of the form

$$V(r) = D_e (1 - e^{-ar})^2. \quad (\text{A.1})$$

The Schrödinger equation for this system can be written as

$$\frac{d^2\psi}{dr^2}(r) - \frac{2mD_e}{\hbar^2} (1 - e^{-ar})^2 \psi(r) + \frac{2mE}{\hbar^2} \psi(r) = 0. \quad (\text{A.2})$$

To solve this equation, we are going to have to make a number of substitutions. We'll start with the dimensionless parameter  $y = ar$ , then we can rewrite the Schrödinger equation as

$$\frac{d^2\psi}{dy^2}(y) - \frac{2mD_e}{a^2\hbar^2} (1 - e^{-y})^2 \psi(y) + \frac{2mE}{a^2\hbar^2} \psi(y) = 0, \quad (\text{A.3})$$

where  $\psi$  is now expressed as a function of  $y$ .

We need a few more substitutions. Let  $\varepsilon = \frac{E}{D_e}$  and  $\lambda = \frac{\sqrt{2mD_e}}{a\hbar}$ , then equation (A.3) becomes

$$\frac{d^2\psi}{dy^2}(y) - \lambda^2 (1 - e^{-y})^2 \psi(y) + \lambda^2 \varepsilon \psi(y) = 0. \quad (\text{A.4})$$

We need to perform one more substitution. Let  $x = 2\lambda e^{-y}$ , then we can write equation (A.4) as

$$\frac{d^2\psi}{dx^2} + \frac{1}{x} \frac{d\psi}{dx} - \frac{1}{x^2} \lambda^2 (1 - \varepsilon) \psi - \left( \frac{1}{4} - \frac{\lambda}{x} \right) \psi = 0. \quad (\text{A.5})$$

We define the following dimensionless quantity  $\beta^2 = \lambda^2(1 - \varepsilon)$ , and write equation (A.5) as

$$\frac{d^2\psi}{dx^2} + \frac{1}{x} \frac{d\psi}{dx} - \frac{\beta^2}{x^2} \psi - \left( \frac{1}{4} - \frac{\lambda}{x} \right) \psi = 0. \quad (\text{A.6})$$

As  $x \rightarrow \infty$ , the terms with a  $\frac{1}{x}$  and  $\frac{1}{x^2}$  dependence vanish. So we are left with

$$\frac{d^2\psi}{dx^2} - \frac{1}{4} \psi = 0. \quad (\text{A.7})$$

Solving this equation, we find that  $\psi \propto e^{\pm x/2}$ . We want our wave function to be finite as  $x \rightarrow \infty$ , which corresponds to  $r \rightarrow 0$ . Thus,  $\psi \propto e^{-x/2}$ .

Now let  $\psi(x) = w(x)e^{-x/2}$ . Then

$$\frac{d\psi}{dx} = \left( w' - \frac{1}{2}w \right) e^{-x/2}, \quad \text{and} \quad (\text{A.8})$$

$$\frac{d^2\psi}{dx^2} = \left( w'' - w' + \frac{1}{4}w \right) e^{-x/2}. \quad (\text{A.9})$$

Our plan is to now express equation (A.6) in terms of  $w(x)$ . We get

$$w'' + \left(\frac{1}{x} - 1\right) w' + \left[-\frac{\beta^2}{x^2} + \left(\lambda - \frac{1}{2}\right) \frac{1}{x}\right] w = 0. \quad (\text{A.10})$$

To solve this equation, we will use the method of Frobenius. Let  $w(x) = x^\gamma (c_0 + c_1x + c_2x^2 + \dots) = \sum_{k=0}^{\infty} c_k x^{k+\gamma}$ , then

$$w'(x) = \sum_{k=0}^{\infty} (k + \gamma) c_k x^{k+\gamma-1}, \quad \text{and} \quad (\text{A.11})$$

$$w''(x) = \sum_{k=0}^{\infty} (k + \gamma)(k + \gamma - 1) c_k x^{k+\gamma-2}. \quad (\text{A.12})$$

Now equation (A.10) becomes

$$\begin{aligned} & \sum_{k=0}^{\infty} (k + \gamma)(k + \gamma - 1) c_k x^{k+\gamma-2} + \sum_{k=0}^{\infty} (k + \gamma) c_k x^{k+\gamma-2} - \\ & - \sum_{k=0}^{\infty} (k + \gamma) c_k x^{k+\gamma-1} - \beta^2 \sum_{k=0}^{\infty} c_k x^{k+\gamma-2} + \left(\lambda - \frac{1}{2}\right) \sum_{k=0}^{\infty} c_k x^{k+\gamma-1} = 0. \end{aligned} \quad (\text{A.13})$$

The polynomial on the LHS must be zero. This means that the coefficient preceding every power of  $x$  must disappear individually.

Consider the lowest power of  $x$ , namely  $n + \gamma - 2$ :

$$(\gamma + k)(\gamma + k - 1) c_k + (\gamma + k) c_k - \beta^2 c_k = 0. \quad (\text{A.14})$$

Setting  $k = 0$  yields

$$\gamma(\gamma - 1) + \gamma - \beta^2 = \gamma^2 - \beta^2 = 0, \quad (\text{A.15})$$

and therefore

$$\gamma = \beta = \pm \lambda \sqrt{1 - \varepsilon}. \quad (\text{A.16})$$

By demanding that  $w \rightarrow 0$  as  $x \rightarrow 0$  (which is  $r \rightarrow \infty$ ), we must have that  $\gamma = \lambda \sqrt{1 - \varepsilon}$ . We shift our summation bounds so that all the coefficients are multiples of  $x^{\gamma+n-1}$ :

$$\begin{aligned} & \sum_{k=0}^{\infty} (k + \gamma)(k + \gamma + 1) c_{k+1} x^{k+\gamma-1} + \sum_{k=0}^{\infty} (k + \gamma + 1) c_{k+1} x^{k+\gamma-1} - \\ & - \sum_{k=0}^{\infty} (k + \gamma) c_k x^{k+\gamma-1} - \beta^2 \sum_{k=0}^{\infty} c_{k+1} x^{k+\gamma-1} + \left(\lambda - \frac{1}{2}\right) \sum_{k=0}^{\infty} c_k x^{k+\gamma-1} = 0 \\ \Rightarrow & (k + \gamma)(k + \gamma + 1) c_{k+1} + (k + \gamma + 1) c_{k+1} - (k + \gamma) c_k - \beta^2 c_{k+1} + \left(\lambda - \frac{1}{2}\right) c_k = 0 \\ \Rightarrow & [(k + \gamma)(k + \gamma + 1) + (k + \gamma + 1) - \beta^2] c_{k+1} - \left[(k + \gamma) - \left(\lambda - \frac{1}{2}\right)\right] c_k = 0 \end{aligned}$$

We get the following recurrence relation ,

$$c_{k+1} = \frac{\gamma + k - \lambda + 1/2}{(\gamma + k + 1)^2 - \beta^2} c_k. \quad (\text{A.17})$$

Since our system is bounded, there exists a  $k = n$  such that  $c_{k+1} = 0$ . Thus, setting the numerator to zero, we get

$$\gamma + n - \lambda + 1/2 = 0. \quad (\text{A.18})$$

Thus, we have

$$\gamma = \lambda - n - \frac{1}{2}. \quad (\text{A.19})$$

From this equation, we get

$$\begin{aligned} \gamma^2 &= \lambda^2 - 2\lambda \left(n + \frac{1}{2}\right) + \left(n + \frac{1}{2}\right)^2 \\ \Rightarrow \lambda^2(1 - \varepsilon) &= \lambda^2 - 2\lambda \left(n + \frac{1}{2}\right) + \left(n + \frac{1}{2}\right)^2 \\ \Rightarrow \lambda^2 \varepsilon &= 2n\lambda + \lambda - \left(n + \frac{1}{2}\right)^2 \\ \Rightarrow \frac{2mE_n}{a^2 \hbar^2} &= 2n\lambda + \lambda - \left(n + \frac{1}{2}\right)^2 \\ \Rightarrow E_n &= \frac{a^2 \hbar^2}{2m} \left[ 2n\lambda + \lambda - \left(n + \frac{1}{2}\right)^2 \right] \\ \Rightarrow E_n &= \frac{1}{2} \hbar \left( a \sqrt{\frac{2D_e}{m}} \right) \left( \frac{a \hbar}{\sqrt{2mD_e}} \right) \left[ 2n\lambda + \lambda - \left(n + \frac{1}{2}\right)^2 \right] \\ \Rightarrow E_n &= \hbar \left( a \sqrt{\frac{2D_e}{m}} \right) \left( \frac{a \hbar}{\sqrt{2mD_e}} \right) \left[ \lambda \left(n + \frac{1}{2}\right) - \frac{1}{2} \left(n + \frac{1}{2}\right)^2 \right] \end{aligned}$$

By defining

$$\omega = a \sqrt{\frac{2D_e}{m}}, \quad (\text{A.20})$$

and noting that

$$\frac{1}{\lambda} = \frac{a \hbar}{\sqrt{2mD_e}}, \quad (\text{A.21})$$

we have

$$E_n = \left[ -\frac{1}{2\lambda} \left(n + \frac{1}{2}\right)^2 + \left(n + \frac{1}{2}\right) \right] \hbar \omega. \quad (\text{A.22})$$

By considering the spacing between adjacent energy levels, we find that

$$E_{n+1} - E_n = \hbar \omega \left[ 1 - \frac{1}{\lambda} (n + 1) \right] \quad (\text{A.23})$$

As  $n$  increases, the spacing between adjacent energy levels decreases. The energy converges to the value of the dissociation energy,  $D_e$ . Once it reaches that energy, the system is no longer bounded.

We may express our expression for the energy as a quadratic equation, i.e.

$$E_n = \left[ -\frac{1}{2\lambda}n^2 + \left(1 - \frac{1}{2\lambda}\right)n + \frac{1}{2} \left(1 - \frac{1}{4\lambda}\right) \right] \hbar\omega. \quad (\text{A.24})$$

We know that the lowest energy state is the ground state, i.e.  $n = 0$ . This allows us to compute the ground state energy,  $E_0$ . The ground state energy is

$$E_0 = \frac{4\lambda - 1}{8\lambda} \hbar\omega. \quad (\text{A.25})$$

Using equation (A.24), we can express  $n$  as a function of  $E$ . This is

$$n(E) = \lambda \left[ 1 - \frac{1}{2\lambda} - \sqrt{1 - \frac{2}{\lambda\hbar\omega}E} \right]. \quad (\text{A.26})$$

From equation (A.26), it follows that  $1 - \frac{2}{\lambda\hbar\omega}E \geq 0$ . This implies that  $E \leq \frac{\lambda\hbar\omega}{2}$ . Thus,  $E_{\max} = \frac{\lambda\hbar\omega}{2}$ . Plugging the value for  $E_{\max}$  into equation (A.26) gives us a value for  $n_{\max}$ , which is  $n_{\max} = \lambda - 1/2$ . (Note:  $n$  is an integer, so  $n_{\max}$  is the greatest integer  $\leq \lambda - 1/2$ ).

## A.2 The Wave Function

Now we would like to determine the wave function. We expressed the wave function as

$$\psi(x) = e^{-x/2}w(x), \quad (\text{A.27})$$

where  $w(x) = x^\gamma \sum_{k=0}^{\infty} c_k x^k$ . From equation (A.19), we can write

$$w(x) = x^{\lambda-n-1/2} \sum_{k=0}^{\infty} c_k x^k. \quad (\text{A.28})$$

From the recurrence relation of the coefficients (equation (A.30)), we see

$$\begin{aligned} c_{k+1} &= \frac{\gamma + k - \lambda + 1/2}{(\gamma + k + 1)^2 - \gamma^2} c_k \\ \Rightarrow c_{k+1} &= \frac{k - (\lambda - \gamma - 1/2)}{(\gamma + 1)(\gamma + 2\gamma + 1)} c_k \\ \Rightarrow c_{k+1} &= \frac{k - n}{(\gamma + 1)(\gamma + 2\gamma + 1)} c_k. \end{aligned}$$

By defining

$$\alpha := 2\gamma = 2\lambda - 2n - 1, \quad (\text{A.29})$$

we have

$$c_{k+1} = \frac{k - n}{(\gamma + 1)(\gamma + \alpha + 1)} c_k. \quad (\text{A.30})$$

This is the recurrence relation for the coefficients of the associated Laguerre polynomials [52]. Thus,

$$w(x) = L_n^{2\lambda-2n-1}(x) = L_n^{(\alpha)}(x). \quad (\text{A.31})$$

We can express our wave function as

$$\psi(x) = N x^{\alpha/2} e^{-x/2} L_n^{(\alpha)}(x), \quad (\text{A.32})$$

where  $N$  is the normalisation constant which has yet to be determined. For the wave function to be normalised, we require

$$\int_{-\infty}^{\infty} |\psi(y)|^2 dy = 1. \quad (\text{A.33})$$

But we have expressed the wave function in terms of  $x = 2\lambda e^{-y}$ . As  $y \rightarrow -\infty$ ,  $x \rightarrow \infty$ ; and as  $y \rightarrow +\infty$ ,  $x \rightarrow 0$ . We also note that  $dy = -\frac{e^y}{2\lambda} dx = -\frac{dx}{x}$ . In terms of  $x$ , the normalisation condition becomes

$$\int_0^{\infty} \frac{1}{x} |\psi(x)|^2 dx = N^2 \int_0^{\infty} x^{\alpha-1} e^{-x} [L_n^{(\alpha)}(x)]^2 dx = 1. \quad (\text{A.34})$$

Upon evaluating the above integral, we find that the normalisation constant is given by [38]

$$N(\lambda, n) = \left[ \frac{(2\lambda - 2n - 1)\Gamma(n + 1)}{\Gamma(2\lambda - n)} \right]^{1/2}, \quad (\text{A.35})$$

In terms of  $\alpha$ , we can express the normalisation constant as

$$N(\alpha, n) = \left[ \frac{\alpha\Gamma(n + 1)}{\Gamma(n + \alpha + 1)} \right]^{1/2}. \quad (\text{A.36})$$

The associated Laguerre polynomials are orthogonal with respect to the weighting function  $x^\alpha e^{-x}$ . They satisfy the following orthogonality relation,

$$\int_0^{\infty} x^\alpha e^{-x} L_n^{(\alpha)}(x) L_m^{(\alpha)}(x) dx = \frac{\Gamma(n + \alpha + 1)}{n!} \delta_{nm}. \quad (\text{A.37})$$

We also have this important identity, [53]

$$\int_0^{\infty} x^{\alpha+1} e^{-x} L_n^{(\alpha)}(x) L_m^{(\alpha)}(x) dx = \frac{\Gamma(n + \alpha + 1)}{n!} (2n + \alpha + 1) \delta_{nm}. \quad (\text{A.38})$$

Another important identity is [53]

$$\int_0^{\infty} x^{\alpha} e^{-x} dx = \Gamma(\alpha + 1). \quad (\text{A.39})$$

The associated Laguerre polynomials can be determined using the Rodrigues formula,

$$L_n^{(\alpha)}(x) = \frac{x^{-\alpha} e^x}{n!} \frac{d^n}{dx^n} (e^{-x} x^{n+\alpha}). \quad (\text{A.40})$$

## B The Wigner Distribution

We mentioned the Wigner distribution in section 5. It might be useful to briefly explain what the Wigner function is. A quantum state described by a density operator yields the Wigner phase space distribution,

$$W(x, p) \equiv \frac{1}{2\pi\hbar} \int_{-\infty}^{+\infty} e^{-ipz/\hbar} \left\langle x + \frac{1}{2}z \left| \hat{\rho} \right| x - \frac{1}{2}z \right\rangle dz. \quad (\text{B.1})$$

Let us motivate this [53] by considering the motion of a particle from position  $x_1$  to  $x_2$ . We shall consider a quantum jump from  $x_1$  to  $x_2$ , i.e. a quantum jump over the distance  $z \equiv |x_2 - x_1|$ . The matrix element  $\langle x_2 | \hat{\rho} | x_1 \rangle$  describes this quantum jump from the position eigenstate  $|x_1\rangle$  to  $|x_2\rangle$ . The centre of the jump can be defined as  $x \equiv \frac{x_1+x_2}{2}$ . We introduce the coordinates  $x_1 = x - \frac{1}{2}z$  and  $x_2 = x + \frac{1}{2}z$ . Thus, we have

$$\left\langle x + \frac{1}{2}z \left| \hat{\rho} \right| x - \frac{1}{2}z \right\rangle \quad (\text{B.2})$$

for our quantum jump. (In physical terms, an example of a “quantum jump” is the transition of an electron from one energy level to another).

After performing a Fourier transform with respect to (B.2), we get the Wigner function. Thus, the Wigner function is a Fourier transform of the density operator  $\rho(x_2, x_1) \equiv \langle x_2 | \rho | x_1 \rangle$  in the position representation. (However, we express the position in the variables  $x \equiv \frac{x_1+x_2}{2}$  and  $z \equiv |x_2 - x_1|$ , which correspond to the centre of the jump and the distance of the jump, respectively).

For a pure state  $|\psi\rangle$ , where  $\hat{\rho} = |\psi\rangle \langle\psi|$ , we have

$$W(x, p) = \frac{1}{2\pi\hbar} \int_{-\infty}^{+\infty} e^{-ipz/\hbar} \psi^* \left( x - \frac{1}{2}z \right) \psi \left( x + \frac{1}{2}z \right) dz, \quad (\text{B.3})$$

where the position representation of the state  $|\psi\rangle$  is  $\psi(x) \equiv \langle x | \psi \rangle$ .

There are many properties of the Wigner function which we can prove. For instance, if we integrate over momentum  $p$ , we get the probability distribution  $W(x)$ , for the position, i.e.

$$\begin{aligned} \int_{-\infty}^{+\infty} W(x, p) dp &= \int_{-\infty}^{+\infty} \left\langle x + \frac{1}{2}z \left| \hat{\rho} \right| x - \frac{1}{2}z \right\rangle dz \frac{1}{2\pi\hbar} \int_{-\infty}^{+\infty} e^{-ipz/\hbar} dp \\ &= \int_{-\infty}^{+\infty} \left\langle x + \frac{1}{2}z \left| \hat{\rho} \right| x - \frac{1}{2}z \right\rangle dz \delta(z) \\ &= \langle x | \hat{\rho} | x \rangle \\ &\equiv W(x). \end{aligned}$$

The reader is invited to consult [53] for more information about the Wigner function. We shall merely point out that the Wigner function is *not* a probability distribution. This is

because it is sometimes negative, which is uncharacteristic for probability distributions. The Wigner function is a phase space distribution function. Phase space plays a very important role in classical mechanics and statistical mechanics. The classical notion of phase space is not useful in quantum mechanics, due to the Heisenberg uncertainty principle. This makes the Wigner function very useful in semiclassical systems. Sometimes we find it convenient to study the Wigner function instead of the wave function.

## References

- [1] Vijay Balasubramanian, Donald Marolf, & Moshe Rozali, *Information Recovery from Black Holes*, Gen Relativ Gravit (2006) 38:15291536
- [2] Nima Lashkari & Joan Simón, *From state distinguishability to effective bulk locality*, J. High Energ. Phys. (2014) 38.
- [3] P. C. W. Davies, *Thermodynamics of Black Holes*, (Rep. Prog. Phys., Vol. 41, 1978)
- [4] Larry Smarr, *Mass Formula for Kerr Black Holes*, (Phys. Rev. Lett. Vol. 30 No. 2, 1973)
- [5] S. W. Hawking, *Black Holes in General Relativity*, Comm. Math. Phys. 25, 152 (1972); *The Four Laws of Black Hole Mechanics*, Comm. Math. Phys. 31, 161 (1973)
- [6] Robert M. Wald, *Gravitational Collapse and Cosmic Censorship*, (1997), arXiv:gr-qc/9710068v3
- [7] K. Binder & A. P. Young, *Spin glasses: Experimental facts, theoretical concepts, and open questions*, (Rev. Mod. Phys. **58**, 801, 1986)
- [8] Leonard Parker & David Toms, *Quantum Field Theory in Curved Spacetime: Quantized Fields and Gravity*, (Cambridge University Press, 2009)
- [9] Ted Jacobson, *Black holes and Hawking radiation in spacetime and its analogues*, Lect.Notes Phys. 870 (2013) 1-29
- [10] S. W. Hawking, *Particle Creation by Black Holes*, Comm. Math. Phys. 43, 199 (1975)
- [11] Maulik K. Parikh and Frank Wilczek, *Hawking Radiation As Tunneling*, Phys. Rev. Lett. 85, 5042,(2001)
- [12] Peng Zhao, *Black Holes in Anti-de Sitter Spacetime*, Lent term Part III Seminar Series, Essay, (2008)
- [13] Alfonso V. Ramallo, *Introduction to the AdS/CFT correspondence*, Physics Today 69, 8, 56, (2016)
- [14] C. A. Ballón Bayona & Nelson R. F. Braga, *Anti-de Sitter boundary in Poincaré coordinates*, Gen.Rel.Grav.39:1367-1379, (2007)
- [15] Philippe Francesco, Pierre Mathieu, & David Sénéchal, *Conformal Field Theory*, (Springer-Verlag New York, 1997)
- [16] David Tong, *Lectures on String Theory*, (2012), arXiv:0908.0333v3[hep-th]
- [17] Makoto Natsuume, *AdS/CFT Duality User Guide*, (2015), arXiv:1409.3575v3 [hep-th]
- [18] Edward Witten, *Anti De Sitter Space And Holography*, Adv. Theor. Math. Phys. 2

- (1998) 253-291
- [19] Juan Maldacena, *The Large N Limit of Superconformal Field Theories and Supergravity*, Adv.Theor.Math.Phys. 2 (1998) 231-252
  - [20] Thomas Hartman, *Lectures on Quantum Gravity and Black Holes*, (2015), Lecture Notes
  - [21] Juan Maldacena, *Eternal Black Holes in AdS*, Journal of High Energy Physics. (2003)
  - [22] Michael A. Nielsen & Isaac L. Chuang, *Quantum Computation and Quantum Information*, (Cambridge University Press, 2010)
  - [23] Benjamin Schumacher & Michael Westmoreland, *Quantum Processes, Systems, & Information*, (Cambridge University Press, 2010)
  - [24] J.J Sakurai & Jim Napolitano, *Modern Quantum Mechanics - Second Edition*, (Addison-Wesley, 2011)
  - [25] Michael A. Nielsen & Dénes Petz, *A simple proof of the strong subadditivity inequality*, (2005), arXiv:quant-ph/0408130v3
  - [26] Su-Kuan Chu, Chen-Te Ma, Rong-Xiu Miao, & Chih-Hung Wu, *Maximally Entangled State and Bell's Inequality in Qubits*, (2017), arXiv:1711.04415v1[quant-ph]
  - [27] Leonard Susskind & James Lindesay, *An Introduction to Black Holes, Information and the String Theory Revolution: The Holographic Universe*, (World Scientific Publishing Co. Pte. Ltd.), (2005)
  - [28] Samir D. Mathur, *The information paradox: A pedagogical introduction*, Class.Quant.Grav.26:224001, (2009)
  - [29] John D. Norton, *Einstein for Everyone*, (Nullarbor Press, 2007)
  - [30] Samir D. Mathur, *Remnants, Fuzzballs, or Wormholes?*, Int.J.Mod.Phys. D23 (2014), no.12, 1442024
  - [31] Samir D. Mathur, *Fuzzballs and black hole thermodynamics*, (2014), arXiv:1401.4097v1[hep-ph]
  - [32] Juan Maldacena & Leonard Susskind, *Cool Horizons for Entangled Black Holes*, Fortsch.Phys. 61 (2013) 781-811
  - [33] Paolo Facchi, Saverio Pascazio, & Francesco V. Pepe, *Quantum Typicality and Initial Conditions*, The Royal Swedish Academy of Sciences, Physica Scripta, Volume 90, Number 7, (2015)
  - [34] Manuel Gerken, *Measure concentration: Levys Lemma Lecture notes for Talk 6, on Selected topics in Mathematical Physics: Quantum Information [3]*, (2013)

- [35] John A. Rice, *Mathematical Statistics and Data Analysis - Third Edition*, (Thomson Brooks/Cole 2007)
- [36] S. Popescu, A.J. Short, & A. Winter, *The foundations of statistical mechanics from entanglement : Individual states vs. averages*, quant-ph/0511225.
- [37] Vijay Balasubramanian, Bartłomiej Czech, Veronika E Hubeny, Klaus Larjo, Mukund Rangamani, & Joan Simón, *Typicality versus thermality: An analytic distinction*, Gen Relativ Gravit (2008) 40: 1863.
- [38] J. P. Dahl & M. Springborg, *The Morse oscillator in position space, momentum space, and phase space*, Journal of Chemical Physics 88 (7) (1988)
- [39] F. Stern, *Self-Consistent Results for n-Type Si Inversion Layers*, Physical Review B, vol. 5, no. 12, pp. 4891 - 4899, (1972)
- [40] D. N. Page, *Average entropy of a subsystem*, Phys. Rev. Lett. 71 (1993) 1291
- [41] Vijay Balasubramanian, Jan de Boer, Vishnu Jejjala, & Joan Simón, *The Library of Babel: On the origin of gravitational thermodynamics*, Journal of High Energy Physics, Volume 2005, JHEP12 (2005)
- [42] Seth Lloyd, *Black Holes, Demons, and the Loss of Coherence: How complex systems get information and what they do with it*, (1988), arXiv:1307.0378v1[quant-ph]
- [43] T. D. Lee, *Are Black Holes Black Bodies?*, Nucl. Phys. B **264**, 437 (1985)
- [44] Marlan O. Scully & M. Suhail Zubairy, *Quantum Optics*, Cambridge University Press, (1997)
- [45] H. R. Jalali & M. K. Tavassoly, *On the ladder operators and nonclassicality of generalised coherent states associated with a particle in an infinite square well*, Optics Communications 298-299: 161-167 (2013)
- [46] R. de Lima Rodrigues, *The Quantum Mechanics SUSY Algebra: An Introductory Review*, (2002), arXiv:hep-th/0205017
- [47] Tomislav Prokopec, *Entropy of the Squeezed Vacuum*, Class. Quantum Grav. **10** 2295-2306 (1993)
- [48] V. A. De Lorenci & L. H. Ford, *Decoherence induced by fluctuating boundaries*, (2012), arXiv:1205.2348v1[quant-ph]
- [49] V. A. De Lorenci & L. H. Ford, *Decoherence induced by long wavelength gravitons*, Phys. Rev. D 91, 044038 (2015)
- [50] Claus Kiefer, *Hawking Radiation from Decoherence*, Class.Quant.Grav.18:L151, (2001)
- [51] John A. Peacock, *Cosmological Physics*, (Cambridge University Press, 1999)

- [52] N. N. Lebedev, *Special Functions and Their Applications*, translated and edited by Richard A. Silverman, Dover Publications, Inc. New York (1972)
- [53] H. M. Srivastava, H. A. Mavromatis, & R. S. Alassar, *Remarks on Some Associated Laguerre Integral Results*, Applied Mathematics Letters (16), (2003)
- [54] Wolfgang P. Schleich, *Quantum Optics in Phase Space*, WILEY-VCH, (2007)